UNIVERSITY OF NAIROBI

MODELLING GREEN GRAM PRODUCTION IN KENYA UNDER THE CURRENT AND FUTURE CLIMATES

BY

MUGO, JANE WANGUI

I80/52673/2018

A Research Thesis Submitted in Fulfilment of the Requirements for the Degree of Doctor of Philosophy in Meteorology, University of Nairobi, Kenya

2021

DECLARATION

I declare that this dissertation/thesis is my original work and has not been submitted elsewhere for examination, award of degree or publication. Where other people's work or my own work has been used, this has properly been acknowledged and referenced in accordance with University of Nairobi's requirements.

Signature ..... Date 1/9/2021

Mugo Jane Wangui

I80/52673/2018

Department of Meteorology

School of Physical Sciences

University of Nairobi

This dissertation/thesis is submitted for examination with our approval as research supervisors:

	Signature	Date
Dr. Franklin J. Opijah Department of Meteorology University of Nairobi fopija@uonbi.ac.ke, or fopijah@gmail.com		1/9/2021
Dr. Joshua Ngaina Department of Meteorology University of Nairobi jngaina@gmail.com		02/09/2021
Prof. Faith Karanja Department of Geospatial and Space Technology University of Nairobi faithkaranja@uonbi.ac.ke		1/9/2021

for Prof. Mary Mburu 1/9/2021

Department of Agriculture

South Eastern Kenya University

mmburu@seku.ac.ke; mwambui2011@gmail.com

DEDICATION

In loving memory of my father James Mugo Thuo who always wanted his children to succeed in education, my dear mother Susan Wangui Mugo who always encourages and supports my studies, and to rest of my family and friends for their love.

ACKNOWLEDGMENTS

I am grateful to GOD ALMIGHTY for without His graces and blessings this study would not have been possible.

I am grateful to my supervisors, Dr. Franklin Opijah, Dr. Joshua Ngaina, Prof. Faith Karanja, and Prof. Mary Mburu for their encouragement, insightful comments, and hard questions. I could not have imagined having better mentors for my Ph.D. study. I am also grateful to the University of Nairobi (UoN) and all the staff of the Department of Meteorology for creating an enabling environment during the entire period of this study. I express my appreciation to the German Academic Exchange Service (DAAD) scholarship for financing my studies.

I acknowledge the sources of data used as provided by the Kenya Meteorological Department, Climate Research Unit (CRU), and Coordinated Regional Downscaling Experiment (CORDEX). I thank South Eastern Kenya University for providing me with a piece of land in their institution to carry out field experiments. I acknowledge Mr. Aston Nyongesa of the Institute of Atmospheric Physics (IAP), University of Chinese Academy of Sciences for his help.

Last but not least, I wish to appreciate most sincerely the patience and moral support from my mother, Mrs. Susan Wangui Mugo; my sister Judy; my brothers Nahashon and Gibson; My nephews Nolan, Jason, and Nate and all my friends especially Lewis, Nick, Mercy, Peggy, and Keziah. Thank you for your understanding, love, and support.

ABSTRACT

Green gram is one of the legumes considered suitable for cultivation in the Arid and Semi-Arid Lands (ASALs) of Kenya. However, the area that is currently suitable remains small due to inadequate knowledge on the variation of climatic elements in space and time in the ASALs. The changing climate may have an effect on the areas presently suitable for green gram production. This study purposed to model the suitability of green grams in Kenya under the current and projected future climates.

The CORDEX RCA4 models' ability to simulate the observed rainfall and temperature from Climate Research Unit (CRU) datasets were assessed using statistical measures of bias and normalised root mean square error (NRMSE). The bias in rainfall was reduced by using an ensemble of the models adjusted using the scaling method. The temporal analysis of temperature and rainfall were assessed using the Mann Kendall test to determine whether there was an increasing or decreasing trend in the datasets. Mapping for different levels of green gram suitability in Kenya was done through the use of a weighted overlay of climate, soil, and topography parameters. The APSIM model was calibrated for four varieties of green gram, namely Biashara, Tosha, N26, and KS20 varieties to evaluate the impact of climate change on green gram yield, biomass and days to maturity in a highly suitable region.

Although the CORDEX models and their ensemble did not replicate the spatial and temporal variability of rainfall during the MAM and OND season very well, the models and their ensemble captured the temperature pattern well. The rainfall ensemble, despite performing better than the individual CORDEX models, still showed notable biases, necessitating bias adjustment before further use in green gram crop modelling. The bias-corrected ensemble of rainfall and the ensemble of temperature were then used to study the space and time variability of rainfall under baseline (1971 to 2000) and future RCP 4.5 and RCP 8.5 scenarios (2021 to 2050) and their effect on green gram production.

The temporal trend of rainfall has been increasing at most stations under the baseline scenario and the trend is projected to continue under the RCP 4.5 and 8.5 scenarios for the MAM and OND seasons with statistical significance for some stations at a P-Value of 0.05. The temporal trend of maximum temperature during the MAM season has been increasing and statistical significance is noted at most stations under the baseline, RCP 4.5, and 8.5 scenarios at a P-Value of 0.05. The temporal trend of minimum temperature shows that minimum temperature has been increasing at all stations under the baseline, RCP 4.5 and 8.5 scenarios

for the MAM and OND seasons with statistical significance at most stations at a P-Value of 0.05. The increase in temperature is attributed to global warming due to a rise in the level of greenhouse gases.

Most of Kenya was found moderately suitable for green gram production during the MAM and OND seasons under the baseline, RCP 4.5 and RCP 8.5 scenarios. During the MAM season, the area currently highly suitable for green gram production (67842.6 km^2) is projected to increase slightly to 68600.4 km^2 (1.1%) under the RCP 4.5 scenario and reduce to 61307.8 km^2 (-9.6%) under the RCP 8.5 scenario. This decrease could be attributed to unfavourable temperature and rainfall above the threshold suitable for green gram production. During the OND season the area currently highly suitable (49633.4 km^2) will increase under both RCP 4.5 (22.2%) and RCP 8.5 (58.5%) scenarios. This increase is attributed to good rainfall and temperature conditions in the future which are favourable for green gram production.

The calibrated green gram model captured the observed yield, biomass and days to maturity of the four varieties of green gram shown by a coefficient of determination (CoD) which ranged between 87.0% and 99.0%; bias values which ranged between 1.3 and 25.3 and levels of NRMSE which ranged between 4.7% and 45.5%. During the MAM and OND seasons, a decline in yield, biomass, and days to maturity is expected under both the RCP 4.5 and RCP 8.5 scenarios. The increase in rainfall amount under both the RCP 4.5 and RCP 8.5 scenarios will translate to a lower yield and increased biomass. The increase in temperature will result in reduction of the days to maturity for green gram in Kitui County.

The maps of green gram suitability indicate that the area suitable for green gram production will increase in the future. There is, however, a net decrease in yield of the four green gram varieties modelled. Kenya, currently, only produces 460kg/ha of green grams. The study found that despite the decrease in yield, potential production under the future climate scenarios was still above 460kg/ha. There is, thus, potential to expand on the current production of green grams. Therefore, despite the decrease in the future, green gram is still a lucrative crop since farmers still stand to increase their current production.

Policymakers can refer to the developed green gram suitability maps under past and future climate scenarios, to determine how suitable their region will be for green gram production. Policymakers should also make use of the four green gram varieties developed under the APSIM model to mitigate against the possible impacts of climate change on green gram

yield. Given that the government aims to revive farming in the ASALs by promoting climate smart agriculture through planting drought resistance crops, there is need to develop green gram varieties which are more tolerant to the expected increase in rainfall and temperature to increase yield and in turn benefit farmers, the society and the country at large.

TABLE OF CONTENTS

LIST OF TABLES

LIST OF FIGURES

ACRONYMS

AHP	Analytical Hierarchy Process
AIM	Asia-pacific Integrated Model
APSIM	Agricultural Production Systems sIMulator
ASALs	Arid and Semi-Arid Lands
C	Celsius
CCCma	Canadian Center for Climate modelling and analysis
CCSM4	Community Climate System Model, version 4
CEC	Cation Exchange Capacity
CERES	Crop Environment Resource Synthesis
CI	Consistency Index
CMIP5	Fifth Phase of the Coupled Model Intercomparison Project
CNRM-CMS	Centre National de Recherches Météorologiques Coupled global Climate Model, version 3
CORDEX	Coordinated Regional Downscaling Experiment
CR	Consistency Ratio
CRU	Climate Research Unit
CROPsyst	Cropping Systems Simulation Model
DAISY	Danish Simulation Model
DEM	Digital Elevation Model
DJF	December January February
DSSAT	Decision Support System for Agrotechnology Transfer
ECHAM	European Centre Hamburg Model
ECMWF	European Centre for Medium-Range Weather Forecasts
ENSO	El Niño–Southern Oscillation
EPIC	Environmental Policy Integrated Climate
ERA	Economic Review of Agriculture
FarmSim	Farming Simulator
Fasse	Farm ASSEssment Tool
GHA	Great Horn of Africa
GHG	Greenhouse gas
GIS	Geographic Information System
GCM	General Circulation Models

GLAM	General Large-Area Model
GPCC	Global Precipitation Climatology Centre
HadGEM2-ES	Hadley Centre Global Environment Model 2 - Earth System
HERMES	High-Elective Resolution Modelling Emission System
ICHEC	Irish Centre for High-End Computing
IIASA	International Institute for Applied Systems Analysis
IMAGE	Integrated Model to Assess the Global Environment
IOD	Indian Ocean Dipole
IPCC	Intergovernmental Panel on Climate Change
ITCZ	Inter Tropical Convergence Zone
JJA	June July August
MAM	March April May
MaxENT	Maximum Entropy
MCDA	Multi-Criteria Decision Analysis
ME	Modelling Efficiency
MESSAGE	Model of Energy Supply Systems and their General Environmental Impact
MIROC	Model for Interdisciplinary Research on Climate
MOHC	Met Office Hadley Centre
MPI-M	Max Planck Institute for Meteorology
NDVI	Normalized Difference Vegetation Index
NCC	Norwegian Climate Centre
NIB	National Irrigation Board
NOAA-GFDL	National Oceanic and Atmospheric Administration- Geophysical Fluid Dynamics Laboratory
NorESM1-M	Norwegian Earth System Model
NRMSE	Normalised Root Mean Square Error
OND	October November December
PBL	Planbureau voor de Leefomgeving
RCA4	Fourth edition of the Rossby Centre Regional Climate model
RCP	Representative Concentration Pathway
RI	Random Inconsistency Index
RMSD	Root Mean Square Deviation
RMSE	Root Mean Square Error

RCM	Regional Climate Model
RSM	Regional Spectral Model
SASOL	Sahelian Solution Foundation
SRES	Special Report on Emissions Scenarios
SEKU	South Eastern Kenya University
SST	Sea Surface Temperature
STICS	Simulateur mulTIdisciplinaire pour les Cultures Standard
SUCROS	Simple and Universal Crop Growth Simulator
SWAP	Soil, Water, Atmosphere and Plant
UN	United Nations
USGS	United States Geological Survey
WMO	World Meteorological Organisation
WOFOST	World Food Studies

CHAPTER 1: INTRODUCTION

1.1 Background Information

Natural resources are the key drivers of economic development and livelihoods in Kenya. This dependency means that extremes in climate, particularly in temperature and rainfall, may unfavourably affect the physical, biological, and socio-economical arrangements ensuing in adversities such as crop failure and loss of livestock in the agricultural sector.

Upward of 80% of Kenya's land mass is classified as Arid and Semi-Arid Lands (ASALs) and is home to close to 10 million people whose dependence on rain-fed agriculture makes them most disposed to climate change (Omoyo *et al.,* 2015; Bobadoye *et al.,* 2016). It is expected that the vast land in the ASALs has the potential to contribute to Kenya's economy through agriculture. However, conflicts, droughts, and food insecurity are the most common occurrences. One of the solutions to food insecurity in the ASALs is for the Kenyan government to introduce farming in these areas. Practising climate-smart agriculture, either by supplementing the available rainfall with irrigation or by growing drought-resistant crops, can help the country increase income, create employment opportunities and attain food security (NIB, 2014).

Climatic conditions are changing, and the agricultural sector is likely to be one of the sectors most severely affected under future climates. Globally, an increase of the earth's surface temperature by 0.8 °C has been observed in the last hundred years and by 0.6°C in the last thirty years (Hansen *et al.,* 2003). The continued rise in greenhouse gas concentration has been projected to increase the average worldwide temperatures by between 1.4 °C and 5.8 °C by the time the 21st Century ends (IPCC, 2007) making precipitation amount and distribution unpredictable. During the 20th Century a warming trend of roughly 0.7 °C was observed in most parts of the African continent, causing increased rainfall over the southeast part of Africa and decreased rainfall over the Sahel; this warming trend is projected to continue, possibly leading to a sea-level rise and more recurrent extreme weather events (Thornton *et al.,* 2006).

Subsistence farming in the tropical region is expected to be the most susceptible to the changing climate, as smallholder farmers lack enough resources to acclimatize to the changing climate conditions (Eriksen *et al.,* 2007). Increased frequency in droughts, which is anticipated with the changing climate will worsen the state of food insecurity and deepen

poverty in the ASALs of Kenya (Omoyo *et al.,* 2015; Bobadoye *et al.,* 2016). Drought is the most destructive natural hazard to people living in Kenya and Africa (Bobadoye *et al.,* 2016).

Opiyo *et al.* (2015) have reported possible short term and long term strategies that may be adapted for mitigating against the adverse effects of climate variability and change. Some adaptation approaches in the short term include water harvesting, development of early warning systems and infrastructure, encouraging cooperative societies, and table banking. Long term approaches include building schools, child education and livestock diversification (Bobadoye *et al.,* 2016). Agriculture is important to the livelihoods of rural communities who practice crop and animal production. The coping mechanisms employed by communities towards climate shocks inform us of their ability to deal with future variability (Kates, 2000). The models used by the Intergovernmental Panel on Climate Change (IPCC), have projected that the level of dryness and water stress in the arid regions will intensify; therefore, there is need to implement the adaptation policies that cater to the expected changes (El-Beltagy and Madkour, 2012).

Green gram (*Vigna radiata L.*) has been reported to do well in the arid lands of Kenya and has the capacity to lessen poverty and improve food security (SASOL, 2015). Green gram is grown for sale to the local and export markets with good returns. Through value addition, the seeds are processed into flour, bread, and noodles (Morton *et al.,* 1982). Green gram has better returns based on input and output and price per kilogram compared to popular crops like maize and beans (ERA, 2013).

The sub-Saharan Africa region is categorised by high levels of poverty with most farmers relying on rain-fed agriculture to produce crops (Cooper *et al.,* 2008) including Kenya. Green gram is a short season crop that is well adapted to the warmer and drier conditions of the sub-tropics and tropics (Morton *et al.,* 1982). Green gram will grow in the range of temperature of about 20 to 40 °C (Morton *et al.,* 1982). Since green gram is observed to perform well under dry conditions, with this dryness anticipated to continue, the green gram crop may be a better crop for farmers to survive the projected conditions. This study shall model which zones in the ASAL regions of Kenya would be most suitable for green gram production and estimate what the expected yields in the high impact areas would be.

1.2 Statement of the Problem

Green gram is a legume fit for agriculture in the ASALs of Kenya due to its capacity to do well under the dry soil conditions in the semi-arid regions. The production of green gram in

Kenya remains low due to inadequate knowledge on the variation of climatic elements in space and time in the ASALs and its rich nutritional value is unknown making it difficult to exploit its agricultural potential. Mugo *et al*. (2016) identified some areas in Kitui County, an ASAL county in Kenya, as suitable for green gram production in terms of climate, soil and topography. There is, however a gap in knowledge on whether there are presently other ASAL regions in Kenya suitable for green gram production, and how the projected changes in climate will affect these suitable regions.

The temporal and spatial variability of climate variables is one of the key aspects responsible for the agricultural production in an area. A shift in climate variables may have an impact on both the high potential and ASAL regions of Kenya making current agricultural practices unsuitable. There is, therefore, a need to determine how suitable green gram will be in Kenya under future climate conditions. The impact of increased temperature, and changing rainfall intensity and pattern has led to reduced agricultural production globally (Adhikari *et al.*, 2015).

To develop agricultural policies in the long-term, planners should recognise the possible influence that the changing climate may have on the suitability zones of agriculture (Holzkämper *et al.,* 2011). Planners need to understand the spatial and temporal changes in climatic suitability for the development of appropriate adaptation strategies (Holzkämper *et al*., 2011).

1.3 Objectives

The overall objective of this study was to model the suitability of green gram production under the current and projected future climates in Kenya.

The specific objectives were, namely, to:

i. Determine the temporal and spatial variability of climate parameters in Kenya.
ii. Identify present and future suitability for green gram production in Kenya.
iii. Simulate the effects of climate change on green gram yield in Kenya.

1.4 Research Questions

The research questions in this study are:

i. What is the nature of the current and future variability of climate elements in space and time over Kenya?

ii. Which areas are currently suitable for green gram production in Kenya, and will the areas that are currently suitable still be fit for its production in the future?
iii. How will modified climate elements affect green gram production in Kenya in the future?

1.5 Justification and Significance of the Study

Second to maize, legumes are the most preferred grain crop in Kenya (Muthomi *et al.*, 2007). Legumes are commonly planted together with cereals such as sorghum, maize, millet and cassava, where the cereals are the majority crops (Hauggaard-Nielsen *et al.*, 2007). Most farmers located in the ASALs prefer to intercrop maize with beans, with drought resistant crops such as green gram, finger millet and sorghum not being as preferable (Yvonne *et al.*, 2016). Green gram is a potential food and cash crop that has been reported to do well as opposed to maize which is characterised by frequent crop failure in the arid regions of Kenya (SASOL, 2014).

Green gram has the ability to improve nutrition, enhance soil fertility and benefit the economy. Green gram is not only an affordable source of plant protein but also of minerals, carbohydrates, and vitamins. It plays an important role in easing undernourishment in resource-poor homes who cannot afford animal protein (Tharanathan and Mahadevamma, 2003; Hanumantharao *et al*., 2016). Green gram can improve the soil structure and leave a residual of between 33 and 37 Kg N/ha for the subsequent crop after sustaining its own need; fulfilling nearly 25% of the nitrogen required by the succeeding crop (Ali and Gupta, 2012; Kaur *et al*., 2015; Hanumantharao *et al*., 2016). By adding nitrogen, into the soil green gram can increase agricultural production in soils which are limited by lack of supply of Nitrogen fertilizer (Raza *et al.*, 2012).

Land classified as ASALs in Kenya is considered as most disposed to the effects of varying and changing climate (Opiyo, 2014). The ASAL regions of Kenya which are characterised by low rainfall that varies highly in time and space, are also prone to lengthy dry seasons with high evapotranspiration amounts (Opiyo, 2014). Given that the temperature and rainfall in the ASALs has been postulated to change (IPCC, 2007), it is essential to recognize the degree to which these climate elements could change in space and time at a local level.

Lack of knowledge on climate variability means farmers are not aware of the crops that would perform best in their area. Planting green gram in the most suitable area will generate

more income to farmers, increase food production, and enhance food security (Kihoro *et al.*, 2013). Elimination of hunger, improvement of nutrition, and food security, and promotion of sustainable agriculture are some of the Sustainable Development Goals (UN, 2015). In order to improve the production of green gram, it is essential to develop a land suitability map. Analysis of the suitability of crops helps define which regions are presently appropriate for the crops and whether those regions will remain suitable in the future, which is important when developing policies regarding the future.

While the valuation of the effects of climate change on green gram production in space is important for the identification of areas suitable for its cultivation, it is also essential to simulate the potential effects of changing climate on green gram yield in the future. Decision support tools such as Agricultural Production Systems sIMulator (APSIM), which have the ability to predict yield based on various agronomic scenarios, can be trained to model climate change effects on green gram yield. This will help develop policies that improve adaptive capabilities of farmers in the future.

CHAPTER 2: LITERATURE REVIEW

2.1 The Spatial and Temporal Variability of Climate Variables in East Africa

The spatial variability of climate variables, especially rainfall over various regions, exhibits high variability in space and time (Indeje *et al.*, 2001; Ongoma and Chen, 2016). Interest is growing in studies on rainfall over East Africa following observations that the main seasonal rainfall is decreasing (Ongoma and Chen, 2016), and that climate change by the end of the 21st century period shall adversely affect crop yields, especially due to temperature change (Adhikari *et al.*, 2015).

Shisanya *et al.* (2011) analysed the variability in rainfall in the ASAL regions of Kenya and the impact it had on the normalized difference vegetation index (NDVI). The study found climate variability was persistent and had an effect on the production of crops. Correlation analysis between rainfall (1961-2003) and NDVI (1981-2003) showed that the March-May (MAM) season was not as dependable as the October-December (OND) season. They also found that the La Niña and El Niño occurrences in southeast Kenya showed temporal and spatial variations, with the El Niño variation intensity being higher.

Omoyo *et al.* (2015) analysed the influence of varying climate on the yield of maize in the ASALs of Counties located in lower eastern Kenya. They found maize yield had been decreasing with the highest levels observed in Machakos, Kitui, Mwingi and Makueni Counties in that order. They also found a rainfall decline of close to 3 mm per annum in four out of the six weather stations analysed. An upward warming of 0.03 °C per annum was also observed. The study concluded that indeed climate variability had an impact on maize yield in lower eastern Kenya which in turn impacts food security.

Ongoma *et al.* (2015) analysed the climate variability in East Africa during the 2010-2011 drought experienced over Kenya. During that year most parts of the country experienced drought because of the low-level divergence identified in the majority of areas in the eastern and western portions of Kenya.

Ochieng *et al.* (2016) using a fixed household model estimated the effect that varying and changing climate had on the income generated from all crops, tea, and maize. Temperature had a positive impact on tea and a negative one on maize incomes; rainfall had a negative

effect on tea. They found that climate change would unfavourably affect agriculture in the years 2020, 2030 and 2040 and the tea production would bear the greatest impact.

Sabiiti *et al.* (2018) determined the future suitability of growing bananas in Uganda under a changing climate. The approach involved the identification of the climate thresholds within which banana thrives and the development of suitability levels for the production of bananas for the four Representative Concentration Pathway (RCP) scenarios and the two Special Report on Emissions Scenarios (SRES) scenarios. The results showed that RCPs 2.6 and 6.5 were inclined to result in higher production of bananas than the RCPs 4.5 and 8.5. Further, the expected temperature rise under SRES A1B would support banana growth, while the anticipated increases in temperatures under SRES A2 would lead to moisture deficits leading to reduced banana growth.

Ouma *et al.* (2018) investigated the trend and magnitude of rainfall and temperature extremes as pointers of varying and changing climate in the ASALs of Kenya using the gridded climate proxy datasets and in-situ measurements and evaluated the trend using the Mann-Kendall and Gaussian-Kernel statistics. The results showed that the minimum and maximum temperatures are rising, especially during the night. On average the change the in mean minimum and maximum seasonal surface air temperature was 0.60 °C and 0.74 °C, correspondingly between the periods from 1961 to 1990 and 1991 to 2013. A decreasing statistically insignificant trend in seasonal rainfall was also observed, with the highest decrease being observed in the MAM rainfall season.

Owiti and Zhu (2012) analysed the geographical changes of rainfall seasonality during the period of 1962-2006 over East Africa using pentad rainfall data at 36 stations. Understanding the spatial variation of climate parameters, especially rainfall, and their relationship with important crops can help increase the welfare of smallholder farmers by cultivating their knowledge on the management of natural assets for improved agricultural production (Kisaka *et al.,* 2015).

2.1.1 Factors Affecting Spatial Variation of Rainfall

The East African seasonal rainfall patterns are regulated by several factors, some of which are discussed below.

The Inter-Tropical Convergence Zone (ITCZ) is a low pressure region near the equator and the convergence zone for the northeast and southeast trade winds (Okoola, 1999). The

North-South movement of the ITCZ is the main cause of the seasonality of rainfall in Kenya where rainfall occurs during the March April May (MAM) and October November December (OND) season (Asnani, 2005).

The Madden Julian oscillation causes amplified rainfall during MAM and suppressed rainfall in the OND season over the East Africa region (Omeny, 2008). Indeje *et al.* (2000) found there was a strong significant correlation between rainfall over some parts of East Africa and the equatorial stratospheric lower zonal wind. Okoola and Camberlin (2008) found the presence of intra-seasonal oscillations with a periodicity of 40-50 days which move across East Africa.

A monsoon is a seasonal shift in the course of the usual, or strongest, winds of an area. Monsoons blow from cold to warm areas and are caused by the annual temperature trends over land and sea. They originate from oceans in summer and from land in winter. Kenya experiences the Northeast monsoons which transport dry air into the country during the December January February (DJF) season and Southeast monsoon which carry cool moist air into Kenya during the June July August (JJA) season (Okoola, 1999).

El-Niño is the cycle of warming and cooling of the eastern and central equatorial Pacific Ocean as indicated by Sea Surface Temperature (SST) (Muhati *et al.*, 2007). The changes in SST affect climate and weather globally and impact food security, water availability, health and energy.

2.1.2 Climate Studies using Climate Models

Opijah *et al*. (2017) assessed the ability of the Regional Spectral Model (RSM) to downscale the European Centre Hamburg Model (ECHAM) simulations between 1970 and 1999 in Kenya. The results disclosed that the model had poor skill in demonstrating the spatial and annual cycle of rainfall and convection in Kenya. The Regional Climate Model (RCM) had better certainty of seasonal rainfall over the OND season relative to the MAM season. However, seasonal temperature prediction was better during the MAM season than the OND season. During the JJA season the RCM predicted rainfall better than temperature. They concluded that improving the development of convective systems (through sensitivity analysis) that control precipitation in the tropical region may help improve the performance of the model.

Endris *et al*. (2013) investigated the skill of ten RCMs from the Coordinated Regional Downscaling Experiment (CORDEX) to mimic rainfall characteristics over eastern Africa. The study assessed the skill of the RCMs in replicating rainfall climatology and in capturing inter-annual rainfall variability and teleconnection signals (El Niño–Southern Oscillation (ENSO) and Indian Ocean Dipole (IOD)). The study considered two gauge-based observed datasets, the Global Precipitation Climatology Centre (GPCC) and Climate Research Unit (CRU) datasets. The GPCC was chosen since in addition to having a long time series it also has the same resolution as the CORDEX RCMs. Results indicated most RCMs adequately reproduced the key characteristics of rainfall climatology as well as the documented ENSO and IOD forcing. It was also noted that individual models exhibited biases based on the sub-region and season; the ensemble was a better representative of the observed rainfall. They concluded that the ensemble adequately simulated rainfall over eastern Africa and could subsequently be used to future climate studies over the region.

Mutayoba and Kashaigili (2017) assessed the ability of four CORDEX RCMs to reproduce the patterns of rainfall patterns in the Mbarali river catchment area in Rufiji basin, Tanzania from 1979 to 2005 using the observed Era Interim dataset. The individual models although fairly representing the inter-annual and annual cycle of rainfall were not as good as the ensemble. They concluded that the ensemble average could thus be used for hydrological studies over the Mbarali river catchment areas. In addition to this, bias correction is essential since it would enhance the results of the impact studies.

Ogega *et al*. (2016) sought to determine if smallholder farmers in coastal Kenya were aware of the change in climate and experienced its impacts, and if they had taken any adaptation measures against climate change. This involved first assessing historical trends in climate parameters over the study area. Rainfall in the study area showed a negative trend for the period 1961 to 2010. Future rainfall using the Fourth edition of the Rossby Centre (RCA4) RCM driven by 8 CORDEX Global Climate Models (GCMs) with special attention on the Canadian Center for Climate Modelling and Analysis (CCCma), Norwegian Climate Centre (NCC) and Ensemble models showed that rainfall was expected to increase for the period 2015 to 2045 under both RCP 4.5 and 8.5 scenarios. Many farmers were either unaware or unable to implement effective adaptation options. Adaptation measures that linked indigenous and scientific knowledge were proposed based on the climate study and responses of farmers.

Mukhala *et al*. (2017) analysed the historical, current and future temporal and spatial trends in temperature and rainfall in East Africa using the CORDEX RCA4 models. Majority of the models were not consistent in their representation of the distribution of rainfall over East Africa; the ensemble, however, had a better representation. Temperature was, however, well represented by both the individual models and the ensemble of the models. Generally, the ensemble was generally a better representation of rainfall and temperature in the study area. They concluded a warming trend was expected under both RCP 4.5 and 8.5 scenarios, and this would lead to small rainfall gains due to the increased evaporation and in turn moisture gains in the atmosphere.

George *et al*. (2018) assessed the skill of the European Centre for Medium-Range Weather Forecasts (ECMWF) to replicate annual rainfall, inter-annual rainfall variability and seasonal mean cycles over the Greater Horn of Africa. The gridded observational datasets were the CRU and GPCC. The models had better certainty of mean rainfall during the OND relative to the MAM season. The model, however, failed to adequately reproduce the double rainfall peak over the equatorial region. The model adequately replicated rainfall in the years associated with the ENSO events despite overestimation and underestimation of the rainfall peak. The model showed poor skill in the highland regions of the Great Horn of Africa (GHA). It was concluded that the ECMWF model would be adequate in providing realistic climate information over the GHA when its physics and model dynamics are turned.

Akhter *et al*. (2017) evaluated the ability of the Fifth Phase of the Coupled Model Intercomparison Project (CMIP5) models' to replicate the spatial pattern of rainfall for seven homogenous zones in India. The results showed that most of the models had poor skill in reproducing rainfall over the chosen zones. Therefore, four bias adjustment techniques were used, to improve the skill of the GCMs, i.e. Standardized Reconstruction, scaling, Gamma Quantile Mapping, and Empirical Quantile Mapping. The scaling method was found to have better skill in reproducing the pattern of rainfall when compared to the other three methods.

Ezéchiel *et al*. (2016) assessed the ability of seven bias adjustment methods to reduce bias in rainfall in three RCMs (SMHI-RCA4, DMI-HIRHAM5, and MPI-REMO) from the CORDEX Africa project at the Mekrou catchment, Benin, West Africa using observed data from available rain gauges. Three of the seven methods showed satisfactory results, i.e., the scaling, Adjusted Quantile Mapping methods, and the Empirical Quantile Mapping. The results confirmed that most of the bias correction methods have great difficulty in correcting

rainfall in time and space due to its high variability. The models were then used for future climatic studies after bias correction where an increase in annual precipitation was noted under the RCP 8.5 condition.

Ayugi *et al.* (2020) used quantile mapping to adjust the bias in five RCMs of the CORDEX RCA4 models over Kenya using various statistical measures of skill. The results show that despite the quantile mapping methods performing variously among the models, reasonable improvement was noted at seasonal and annual timescales. The bias corrected data performed better against the observed CRU data compared to the uncorrected RCM outputs. They concluded that the corrected models could now be used in future climate studies.

2.1.3 Data Quality Control

Data quality control is an important step taken before data analysis; it consists of several checks. Limit checks ensure the physical limits of each parameter are not exceeded. For example, under limit checks negative values of precipitation cannot exist (Steinacker *et al*., 2011; Musa *et al*., 2003; Feng *et al*., 2004).

Temporal consistency checks determine whether the readings displayed in instruments are likely compared to the expected climatological time series (Steinacker *et al*., 2011; Musa *et al*., 2003). Internal consistency checks investigate whether the expected relationship between two weather parameters, e.g. cloud cover and sunshine, exists without much contradiction (Musa *et al*., 2003). Spatial consistency checks confirm that values of the same parameters measured at the nearby station do not differ much from each other (Musa *et al.*, 2003; Feng *et al.*, 2004).

2.2 Cropland Suitability Analysis

Cropland suitability describes the capacity of the land to consent to the production of crops in a sustainable mode (Halder, 2013). Land suitability process examines the productivity of land. The process involves evaluating different criteria ranging from climate, socio-economic, infrastructure and market, to soil and terrain for the suitability of a certain type of land use (Bunruamkaew and Murayam, 2011).

Ahamed *et al.* (2000) endorsed determining crop suitability based on the different levels of climate, soil, and terrain of the land. Decision makers can be engaged to choose which parameters they consider the most influential for crop suitability analysis using Multiple Criteria Decision Analysis (MCDA) methods; the results are then used in a Geographic

Information System (GIS) as weights for the suitability analysis. The Analytical Hierarchy Process (AHP) is the most popular method of developing weights for the factors the decision makers consider most significant for suitability analysis (Kihoro *et al.*, 2013).

2.2.1 Past Studies on the Suitability Analysis Process

Kogo *et al*. (2019) determined the present and future land suitable for rainfed maize production in Kenya using the maximum entropy (MaxENT) model. The study used data from two GCMs (Community Climate System Model, version 4 (CCSM4) and Hadley Centre Global Environment Model 2 - Earth System (HadGEM2-ES)) for the RCP 4.5 and 8.5 scenarios from the worldclim database, and maize occurrence location data. Simulation results indicated a reduction of the moderately suitable areas by 14.6 to 17.5% and an increase of unsuitable lands by 1.9 to 3.9%. Accordingly, the highly suitable areas will increase by 9.6% and the suitable areas by 17 to 20%. The study was important to the future of maize production in Kenya especially in the development of appropriate adaptation strategies.

Jayasinghe *et al*. (2019) determined the land suitable for tea production in Sri Lanka using climate, soil, and topography as the main factors influencing tea production. The factors were given weights using the AHP and used to a generate suitability map. Most of Sri Lanka was unsuitable for production. They concluded the study was important in ensuring better management of land and tea production in Sri Lanka.

Wanyama *et al*. (2019) used the GIS-based AHP to define the land most suitable for maize production in Kenya using variables of climate, soil, and topography. The study found most of the land (55.6%) was only marginally suitable. The observed change in the rainfall pattern was associated with reduced maize yield in the country. Appropriate timing of rainfall, crop diversification, better seeds usage, and soil fertility restoration and retention were found as the most practical adaptation strategies.

Mugo *et al*. (2016) identified areas suitable for the cultivation of green gram in Kitui County, Kenya using the GIS-based AHP technique. The first step was a review of the literature to develop a suitability table for green gram growth. The maps of climate, soil, and topography were divided into four classes of suitability and overlaid on a GIS environment using the weights obtained from the AHP.

Kamau *et al*. (2015) identified the land suitable for potato production in Nyandarua County, Kenya using the GIS-based AHP technique. Three parameters i.e. climate (rainfall, temperature), soil (texture, pH, drainage, and depth) and topography were rated using the AHP technique and overlaid over each other in a GIS environment. Results show that the area currently under potato farming in Nyandarua is currently low and can be expanded into the highly suitable lands.

Kihoro *et al*. (2013) generated a rice suitability map using the climatic and physical factors affecting rice production using the AHP and GIS approach in central Kenya. A review of literature was first conducted to determine the levels of suitability for rice production based on climate, soil and topography. The results showed that the area under rice cultivation in the Counties is currently low and can be expanded.

2.2.2 Land Suitability Based on the Agro-climatic Zones of Kenya

Kenya has two main rainy seasons, the long rains which occur in MAM, and the short rains of OND (Sombroek *et al.,* 1982). By the use of a moisture index, Kenya is alienated into seven agro-climatic zones. The moisture index is calculated by dividing the annual rainfall with potential evaporation and expressing it as a percentage (Sombroek *et al.,* 1982) (Figure 2-1and Table 2-1).

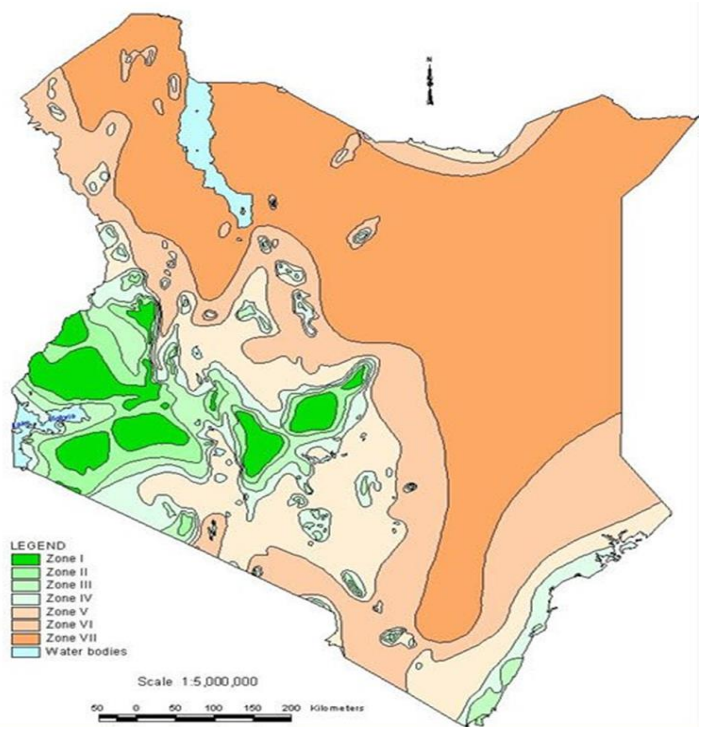

Figure 2-1: Agro-climatic zones of Kenya where Zone I through to Zone VII represent the Humid, Sub-Humid, Semi-Humid, Semi-Humid to Semi-Arid, Semi-Arid, Arid and Very Arid areas in Kenya respectively (Source: Sombroek *et al*., 1982)

In Figure 2-1, the agricultural climatic zones I–III represent regions of high to medium potential land with annual rainfall of above 1100 mm, at least 50% moisture index and mean annual temperatures below 18 °C, sustainable agriculture under rain-fed environments is only considered probable in these agro-climatic zones. The agricultural climatic zones IV-VII represent semi-humid to arid lands with an annual total rainfall below 1100 mm, a moisture index below 50 % relative humidity, and mean yearly temperatures between 22 °C and 40 °C (Table 2-1).

Table 2-1: Agricultural Climatic Zones of Kenya

Zone	Classification	Mean yearly rainfall (mm)	Vegetation	Eo, mean yearly potential evaporation (mm)	R/Eo (%)
I	Humid	1,100- 2,700	Moist forest	1,200-2,000	>80
II	Sub-humid	1,000-1,600	Moist and dry	1,300-2,100	65-80
III	Semi-humid	800-1,400	Forest	1,450-2,200	50-65

Zone	Classification	Mean yearly rainfall (mm)	Vegetation	Eo, mean yearly potential evaporation (mm)	R/Eo (%)
IV	Semi-humid to semi-arid	600-1,100	Dry forest and	1,550-2,200	40-50
V	Semi-arid	450 – 900	Moist	1,650-2,300	25-40
VI	Arid	300 – 550	woodland	1,900-2,400	15-25
VII	Very arid	150 – 350	Dry woodland	2,100-2,500	<15

(Source: Sombroek *et al*., 1982)

2.2.3 Information on Green Gram for Use in Determining Suitability

The first step in land suitability is to determine the thresholds within which the crop performs best and worst. Sufficient literature review is important in achieving this.

2.2.3.1 History of Domestication and Cultivation

Green gram is a fast-maturing (65-90 days) legume (Nair *et al.*, 2012) cultivated on more than 6 million hectares globally in the warm regions (Malik, 2006). Green gram originated from the Indian subcontinent (HanumanthaRao *et al.*, 2016), but it is also cultivated in the dry and hot regions of Eastern Africa, Southern United States, and Southern Europe (SASOL, 2015; Infonet, 2018). It spread early into northern Africa and other Asian countries. India produces and consumes majority of the green gram produced in the world, accounting for 54 and 65% of the global consumption and acreage respectively. Green gram is a common legume in most subtropical and tropical areas (SASOL, 2015).

2.2.3.2 Climate and Soil Requirements

Green gram has a rainfall requirement of between 350 and 700 mm per annum (SASOL, 2015; Infonet, 2018). Heavy rainfall reduces the pod setting and increases vegetative growth (SASOL, 2015). Water stress reduces the rate of nutrients uptake, leaf area change, flowering, and photosynthesis affecting yield (Malik, 2006). Excess rainfall and high humidity late in the green gram season can lead to crop diseases and harvest losses caused by delayed pod setting (Mogosti, 2006; Oplinger *et al*., 1990).

The growth and development of green gram are associated with temperature requirements at different growth stages, i.e. growing degree days (Robertson *et al*., 2002). The APSIM green gram model uses degree days to drive phenological growth and canopy extension. APSIM model uses 7.5 °C base temperature, 30 °C optimal temperatures, and 40 °C extreme

temperatures as the key values in the calculation of degree days (Carberry, 2007; Chauhan *et al*., 2010).

Although green gram is a tropical crop and performs best in the ASAL areas, heat is an important environmental control obstructing crop production in terms of growth and yield (El-Lateff*et al.*, 2018). A temperature of 28 to 30 °C is found ideal for seed germination and plant growth (Mogosti, 2006; Morton *et al*., 1982; Kaur *et al*., 2015) and the temperatures should always be above 15 °C (Mogosti, 2006). Green gram bears 10 to 20 flowers. Under normal conditions, the green gram plan will shed a large number of flowers. Shedding is worsened under high temperatures leading to substantial loss of potential pods (Kaur *et al*., 2015). High temperatures at the reproductive stages decrease photosynthetic rates, by inducing chlorophyll loss and reduced carbon assimilation and fixation (El-Lateff *et al*., 2018), reduce pod weights and final yield when compared to an ambient temperature of 27 °C (Islam, 2015; El-Lateff*et al*., 2018; Luo, 2011; Hatfield and Prueger, 2015). A change in temperature by 8-10°C from the optimum resulted in shorter phenological periods especially the vegetative phase leading to earlier maturity (Luo, 2011; Hatfield and Prueger, 2015). Low temperatures delay and reduce the germination of green gram and lead to very slow plant growth (Hanumantharao *et al*., 2016).

Green gram performs best at a height of 0-1600 m above sea level (SASOL, 2015) and not exceeding 2,000 m elevation (SASOL, 2015). Grealish *et al*., (2008) found green gram is highly suitable at a slope of 0-10%, moderately suitable at 11-20%, marginally suitable at 21 to 35% and not suitable at slope above that percentage.

Green gram is suitable for most soil textures but prefers fertile, deep, well-drained loams or sandy loams (Oplinger *et al*., 1990; Morton *et al*., 1982; SASOL, 2015; Infonet, 2018, Meena, 2013). The legumes are most suitable to clayey soils (SASOL, 2015) but don't do well on heavy clay soils with poor drainage and are somewhat tolerant of saline soils (Grealish *et al*., 2008, Oplinger *et al*., 1990). For green gram cultivation sandy soils require good fertilizer and water supply and organic soils need drainage and raised beds since their water tables occur at or near the soil surface (Grealish *et al*., 2008).

Green gram is well adapted to a pH range of 5 to 8 (Grealish *et al*., 2008; SASOL, 2015; Infonet, 2018, Meena, 2013; Hanumantharao *et al*., 2016). The performance of green gram is best when the soil has a pH of between 6.2 and 7.2. Otherwise, the plants depict serious iron

chlorosis signs and micronutrient deficits on alkaline soils (Morton *et al*., 1982; Oplinger *et al*., 1990). They require slightly acid soil for the best growth (Morton *et al*., 1982).

The soil Cation Exchange Capacity (CEC) has an impact on the acidity and availability of nutrients in the soil. Generally, soils with a high CEC do not require much liming as compared to those soils with low CEC. However, when high CEC soils become acidic, higher lime rates are required to achieve optimum pH (Moore and Blackwell, 1998). Soils with CEC greater than 10 meq/100g in general experience little cation leaching making application of nitrogen and potassium fertilizer more realistic during the rainy season. Soils with a low CEC less than 5 meq/100g are prone to deficits of magnesium, potassium, and other cations (CUCE, 2007).

Green gram can tolerate more saline conditions compared to other legumes. However, high salinity levels around the root zone in the ASALs where evaporation exceeds precipitation can affect green gram production by causing osmotic stress, ion toxicity and reduced nodulation by rhizobia (Hanumantharao *et al*., 2016). Green gram is most affected by moisture stress during the poding and seed development stage. The effect is least during the stage from emergence to flowering. Increased moisture increases branch development (Raza *et al.*, 2012). However, green gram needs less water compared to other legumes for growth (Hanumantharao *et al*., 2016).

Robertson *et al*. (2002) conducted field experiments at various locations in tropical and subtropical Australia. The simulated grain yield accounted for 77% of the variance for the green gram. Biomass at maturity was simulated less precisely, accounting for 64% of the variance.

2.2.3.3 Food Value of Green Gram

Green gram, like most legumes, can improve soil fertility via nitrogen fixation (HanumanthaRao *et al.,* 2016; Malik, 2006) in synergy with *Rhizobium* green gram fixes atmospheric nitrogen (58-109 kg/ha), which is enough to meet its needs and those of crops to be planted later (Ali and Gupta, 2012). Green grams, provide a less expensive source of protein; the stocks and husks are useful as fodder and green manure (Malik, 2006, Meena, 2013). Its seeds contain 58% carbohydrate, 24% protein and 36% minerals (Nadeem, 2004; Malik, 2006).

2.2.3.4 Agronomic Aspects

Green gram is a straight thick plant which attains a height of between 30 and 120 cm. It has a green colour, but it can also establish in shacks of yellow and black. The pods are linear, at times hairy and curved (Baldev, 1988; SASOL, 2015). Only a few of the many flowers produced by the crop are developed into pods; the rest fall off (Sengupta, 2011). Flowering normally starts 50 to 60 days after sowing and continues for a few weeks. Finally, the leaves dry up, but may not drop off completely. Flowers are also self-fertile and self-pollinated. The weight of green gram seeds varies from 15 to 85 milligrams (Baldev, 1988). Pods normally mature approximately 20 days after flowering (Sengupta, 2011).

2.2.3.5 Green Gram Pests

Green gram is affected by several pests such as thrips, aphids, pod borers, whiteflies, foliage beetles, and weevils. Thrips attack the plant petioles and leaves leaving tiny holes encircled by discoursed areas. Thrips have a preference for flowers and feed on pollen decreasing pollination and seed set (SASOL, 2015, Infonet, 2018). Aphids feed on the young plants, stems, leaflets, and pods; the attacked young leaves normally appear twisted. Further, the emission of honeydew by aphids results in the growth of sooty mould (SASOL, 2015; Infonet, 2018).

Pod borers feed by scrapping the tissues of leaves while their young caterpillars dig holes into the pods in order to feed on the interior of seeds and can lead to a serious economic loss (SASOL, 2015; Infonet, 2018). Whiteflies attack leaves causing them to shrink and suck plant sap leading to retarded growth (SASOL, 2015; Infonet, 2018). Foliage beetles are a threat when in large numbers and like to feed on young plants (SASOL, 2015; Infonet, 2018). Weevils are very common insect pests in grains that are stored, attacking pods in the field and seeds in storage when they are nearly mature and dry (SASOL, 2015; Infonet, 2018).

2.2.3.6 Green Gram Diseases

Green gram is affected by several diseases such as powdery mildew, rust, and bean blight. Powdery mildew is white blotches on leaves which later turns leaves dull after infection (SASOL, 2015; Infonet, 2018). Rust is round reddish-brown blisters which commonly develop on or underneath the leaves, less plentiful on pods and thinly on stems (Infonet, 2018). Bacterial blight (bean blight) appears as small patches of water-soaked or light-green areas on leaves, which later dry up and turn brown. The spots caused by bean blight may affect the leaf surface, ultimately killing the affected leaf (Infonet, 2018).

2.2.3.7 Seed Varieties in the Kenyan Market

There are two popular varieties of green gram in Kenya, KS20 and N26 (SASOL, 2015; Infonet, 2018). The KS20 variety also known as Uncle, KVR 2 and N 22 takes 60 to 65 to flower, 80 to 90 days to mature and has a yield potential of 1.0-1.3 t/ha. The improved variety N26 also known as Nylon, K26, KVR 26 takes 40 to 45 days to produce flowers, 60 to 65 days to mature and has a yield potential of 0.3-1.5 t/ha. The KS20 seeds are big, dull and housed in brown pods while the N26 seeds are small, shiny and housed in dark pods.

The Kenya Agricultural and Livestock Research Organisation (KALRO) developed and released three new varieties in April 2017. The three new varieties mature earlier and produce higher yields. Table 2-2 presents a summary of these varieties and their features.

Table 2-2: The New Green gram Varieties

Green Gram Variety	Characteristics
KAT 00301 (Ndengu Tosha)	Early maturity (60-70 days) Potential yield of 1800 to 2300 kg/ha Large pod and grain size enabling easier harvest Seed weight of 6 to 7 g/100 seeds Non-stony seeds
KAT 00308 (Biashara)	Early maturity (65-75 days) Potential yield range 1800 – 2100 kg/ha Large pod and grain size enabling easier harvest Seed weight of 8 to 10 g/100 seeds Non-stony seeds
KAT 00309 (Karembo)	Early maturity (65-75 days) Potential yield of 1800 to 2100 kg/ha Large pod and grain size enabling easier harvest Seed weight of 8 to 10 g/100 seeds Grain has shiny green Non-stony seeds

Source (KALRO, 2017)

2.2.4 Status of Green Gram in Kenya

Green gram in Kenya is mostly produced in Makueni and Tharaka Nithi, but it is also grown in Kitui, Nairobi, Mombasa, Machakos, Uasin Gishu, and Nakuru counties (Kilimo Trust, 2017). There is a preference to grow local varieties such as Nylon which are characterised by long maturity periods (3 to 4 months) and low yields (less than 500kg/ha). Kenya has the potential to produce 3MT/ha, but only produces 0.46MT/ha thus there is potential to expand on green gram production and a suitability map can help identify these areas. The price of green grams can go up to USD 116/MT in Nairobi Kenya (Kilimo Trust, 2017). About 70% of the green gram produced in Kenya is marketed and not consumed by farmers. However,

domestic trade is highly informal and middlemen play the biggest role in linking exporters to farmers hence benefit more than the farmers (Kilimo Trust, 2017).

Green grams are consumed in Kenya, but are not as popular as other legumes, for instance, common beans and peas (Kilimo Trust, 2017). The most marketed varieties in Kenya comprise the N26-Nylon and the local variety (Kilimo Trust, 2017; SASOL, 2015; KALRO, 2017). Some of the challenges facing green gram farming in Kenya include: high variability of climate variables, the local variety grown is considered low quality in the export market since it has small and stony seeds, poor roads in areas where green gram is produced making it hard to market, lack of linkage between producers, traders and exporters, lack of support for agricultural value chains from financial institutions, and preference for other legumes such as beans (Kilimo Trust, 2017; KALRO, 2017).

2.3 Climate Change and Crop Production

Climate models predict that the level of dryness will rise in the future, with the variability in rainfall and temperature intensifying in the ASALs (IPCC, 2007). Green gram due to its low moisture requirements has the potential to perform well despite the expected climatic changes in the ASALs (Yvonne *et al.*, 2016). Crop models offer a way to measure how different soils, climate conditions, and management practices, affect agricultural production output (Nain and Kersebaum, 2007).

2.3.1 Past Studies on Simulation of Crop Production

Crop simulation tools can work without field trials and are thus cheaper and more time-saving research tools (Pathak *et al.*, 2005). Nain and Kersebaum (2007) simulated the production of barley and wheat with the Crop Environment Resource Synthesis (CERES) model in Germany.

Nyang'au *et al.* (2014) studied the impact of weather changes such as atmospheric CO_2 concentration, solar radiation and temperature on the yield of grains of the Basmati IR 2793-80-1 and 370 in Mwea and Western Kenya irrigation schemes using the Ceres rice model

Delve *et al.* (2009) simulated the responses of Phosphorus on maize and beans in Kenya on different soil types using the APSIM- model. An average coefficient of determination of 0.69 and 0.79 were reported for biomass and grain yield. The model predicted the growth of maize and beans under different Phosphorous treatments as well.

Agesa (2014) using the APSIM determined the impact of changing climate on sorghum biomass and grain yields in Yatta sub-county, Eastern Kenya. The data showed that changing climate in terms of reduced rainfall and increased temperatures had a harmful consequence on sorghum biomass and yields.

2.3.2 Crop Models

A mathematical *model* represents processes in an intricate system using a set of equations (Kasampalis *et al*., 2018; Gowda, 2013; Chakrabarti, 2013). In mathematical modelling, it is assumed that any complex process can be presented using mathematical statements (Chakrabarti, 2013).

Mathematical c*rop models* mimic how crops associate with their environment; they capture the crop's physiological growth to estimate the expected yield at maturity (Kasampalis *et al*., 2018). The model mimics the growth of a real plant by estimating the time needed to develop its components, for example grains, leaves, and roots. Crop models, in addition to quantifying yield, also give quantifiable information on the major progressions involved in plant development (Gowda, 2013).

Growth is the increase in volume and size which cannot be reversed and is caused by the differentiation and distribution happening in the plant (Gowda, 2013).

2.3.2.1 Categories of Crop Growth Models

Statistical or correlative models are a type of empirical models conveyed as regression equations. They require fewer data compared to dynamic crop models (Kasampalis *et al*., 2018). Experiments are used to develop equations that explain the behaviour of the system. However, since crop behaviour changes under different weather, soil and crop practices, large deviations emerge under different weather patterns between years making predictions difficult (Gowda, 2013). Empirical models may not be able to simulate the outcome of future climates on crop production where other controllers of crop yield are projected to alter in ways different from what is observed in the past (Kasampalis *et al*., 2018).

Dynamic models use differential equations to model crop growth and development. Dynamic models require more data compared to the statistical models and require physiological data on crops to parameterise and calibrate the model (Kasampalis *et al*., 2018). Crop growth processes such as leaf expansion are normally quantified as a function of environmental aspects such as soil properties, temperature, water accessibility and radiation, which give the

status of the crop (Gowda, 2013). Unlike empirical models, dynamic models can be used to explore crop development under diverse management practices and future climates (Kasampalis *et al*., 2018). Popular crop simulation models are presented in Table 2-3.

Table 2-3: Common Crop Simulation Models. The Acronyms have been Defined in the List of Acronyms

Crop Model	Characteristics/ application of the model	References
APSIM	A suite of modules simulating various animal, plant, management, climate and soil interactions	McCown *et al.*, 1996
AgrometShell	Software toolbox for assessing the impact of climatic conditions on crops, analysing climate risks and performing regional crop forecasting using statistical and crop modelling approaches.	Di Paola *et al.*, 2016
Aqua crop	Particularly well suited for environments in which water restricts crop growth.	Steduto *et al.*, 2009
CERES-wheat	Simulates the yield of wheat under diverse management, weather and soil conditions.	(Lobell and Burke, 2010)
CROPGRO-Soybean	Simulates the yield of Soybean under diverse management, weather and soil conditions.	Batchelor *et al.*, 2002
Cropsyst	Simulates the growth of a variety of crops under diverse management, weather and soil conditions.	Stöckle *et al.*, 2003
DAISY	It can follow the fate of energy, water, nitrogen, pesticides, and carbon, both below and above the ground. It can calculate crop production and environmental impact in terms of change in soil quality and leaching over time.	Palosuo *et al.*, 2011
DSSAT	Able to simulate the growth of over 28 crops under different climate, management and soil conditions	Jones *et al.*,2003
EPIC	Developed to evaluate crop productivity as affected by soil erosion.	Di Paola *et al.*, 2016
Fasse	Estimates the impact of changes in prices, subsidies, regulations, and management on different indicators of farm sustainability such as farm profitability, energy consumption, nitrogen losses, and greenhouse gas emissions.	Palosuo *et al.*, 2011
GLAM	It simulates the development of crops and also the impact variable and changing climate may have on the crops.	Challinor *et al.*, 2004
HERMES	Describes crop development and nitrogen and water interactions in the soil-crop system.	Palosuo *et al.*, 2011
ORYZAv3	Simulates rice development under nitrogen-deficient and drought conditions.	Li *et al.*, 2017
STICS	Simulates growth of crops, soil nitrogen and water balances as driven by climatic data.	Palosuo *et al.*, 2011
WOFOST	Simulates the growth of annual field crops	Palosuo *et al.*, 2011

The least amount of data essential to run a crop growth model is presented in Table 2-4.

Table 2-4: Minimum Input Data Required to Successfully Run a Crop Model

Site	- Elevation, latitude, and longitude -Aspect and slope -Mean annual temperature
Weather	- Minimum and maximum temperatures, precipitation and solar radiation
Soils	- pH, Organic carbon, soil nitrogen -Soil depth, bulk density, root growth factor -Soil type
Initial conditions	-Water, nitrates, and ammonium by layer of soil -Crop previously grown, amount of root nodule
Management	-The cultivar, planting date, depth, row spacing, and crop population, water management and irrigation (dates, amounts, and methods) - Residue applications(organic fertilizer) (nutrient levels, depth of incorporation and amount) -Fertilizer (inorganic) applications -Chemical (pesticide) applications (amount, material) -Tillage - Harvesting calendar

Source: Kasampalis *et al*., 2018

2.3.2.2 Crop Growth Model Uses

Crop growth models are important tools to evaluate weather threats, to determine optimal planting dates, and to calculate the performance of crops where they have not been cultivated before (Chakrabarti, 2013). Models are developed to help us understand how crops interact with climate in processes such as photosynthesis and water flow and to find gaps in knowledge (Jame and Cutforth, 1996). Models are able to represent the relationship between crop development, genetic constraints and the environment thus, may be used to assist in plant breeding efforts (Yin *et al.*, 2004).

2.4 Study Assumptions

In carrying out this study, it was necessary to make certain assumptions. The following assumptions were made:

- When making a suitability map for green gram production, the variation in suitability is only accredited to climate parameters under past and future scenarios.
- Land use persists in the future since the model precedes the prevalent land use structures.
- The physical and chemical properties of the soil remain constant in the future. In reality soil is affected by many factors such as fertilizer application, irrigation practices, liming and erosion, among others.

- The topography of the area remains constant in the future. Ecological and geographical activities such as afforestation, landslides and earthquakes among other major alterations may change the applicability of this study's results.
- This study seeks to show that green gram can be a suitable option for protein supply in the ASALs of Kenya. However, the location chosen for further analysis of projected yield using APSIM-Green gram model was the most suitable for green gram production. Although only the most suitable area for green gram growth was chosen for use in the APSIM model, the results would be applicable in other ASAL areas as well where the climate and soil patterns are similar.
- The model applied in this study was ad hoc, having been calibrated to give the best results on green gram suitability. Users need to recalibrate the model to suit their area of interest before using the findings of this study.

2.5 Conceptual Framework

This study set out to determine the suitability for green gram production in Kenya under a changing climate.

Literature shows there is insufficient material on the effects of variable and changing climate on green gram growth stages, and land suitability for green gram production. Mugo *et al.* (2016) determined the suitability of green gram production in Kitui County; however, they did not quantify how much yield is expected or how climate change will affect future production. Robertson *et al.* (2002) successfully created a model that can simulate the growth of green grams; however, the study is yet to be done in Kenya.

Figure 2-2 shows an illustration of the conceptual framework. The first part of the study involved understanding how climate variables behave in time and space in Kenya. The second step identified land that is suitable for green gram production presently and in the future. Lastly, the study simulated the effect the changing climate would have on green gram yield using the APSIM model.

The specific details on research design including variables, materials (data, tools and climate models) selected and analysis methods adopted to achieve the specific objectives are presented in Chapter Three under materials and methods.

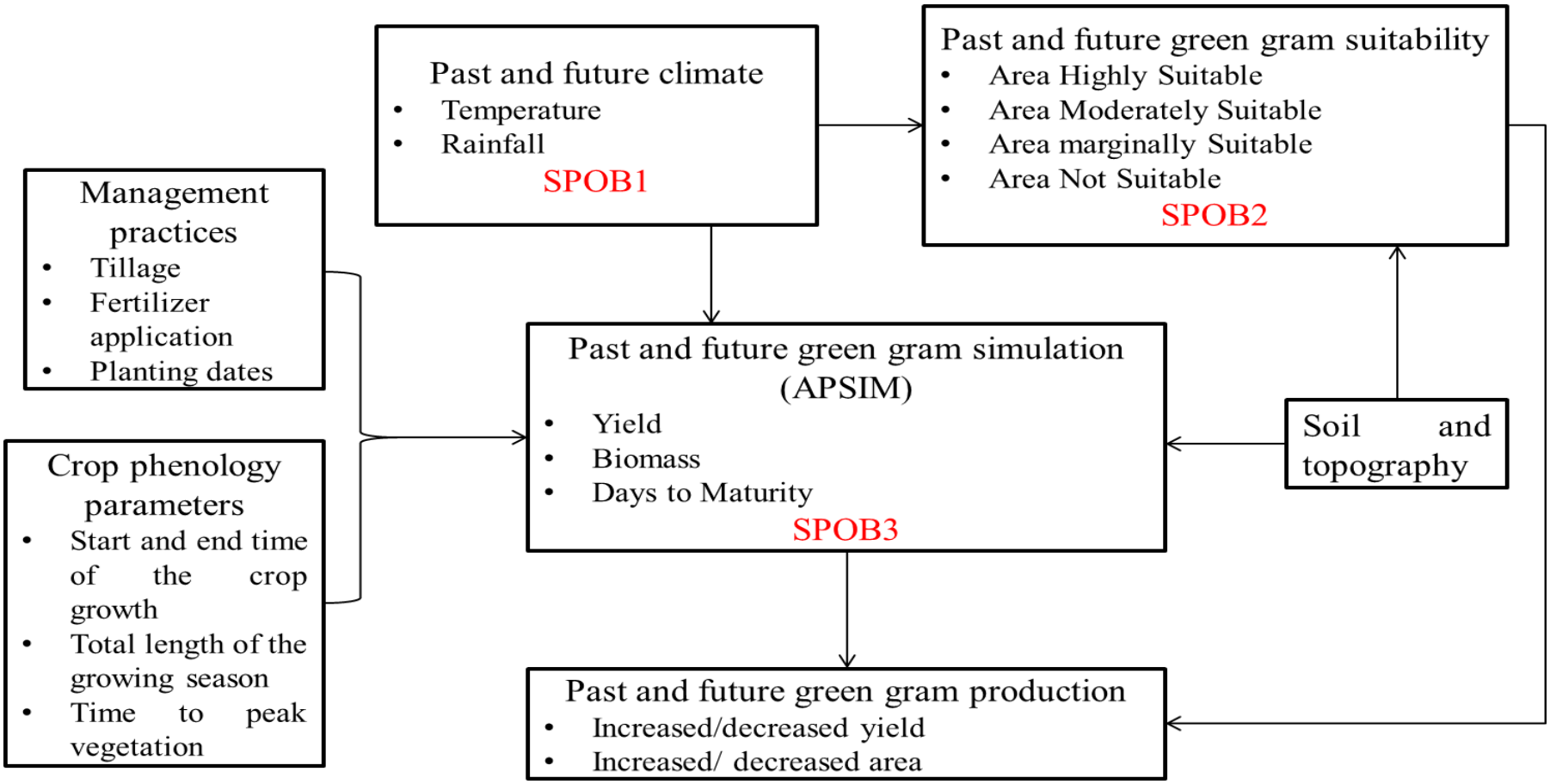

Figure 2-2: Conceptual framework of the study. Where SPOB1, SPOB2, and SPOB3 stand for specific objectives one (1), two (2), and three (3) respectively

CHAPTER 3: MATERIALS AND METHODS

3.1 Study Area

Kenya (Figure 3-1) is a country in East Africa lying approximately between longitudes 34°E and 42°E and latitudes 5°N and 5°S and has a land area of roughly 584,000 km^2.

Kenya receives rainfall in a bimodal pattern that coincides with the movement of the ITCZ. The existence of high mountains, plains, valleys, vegetation, soil types, urbanisation and large water bodies, among others, also influence the climatic patterns in the country. Climate is highly correlated to topography with the high elevation parts receiving more rainfall than the low elevation areas (Herrero *et al.,* 2010). Rainfall is highly variable in Kenya, with the ASALs experiencing the highest variability in space and time.

The ASALS, which constitute in excess of 80% of Kenya's land quantity, are home to nearly 38% of Kenya's population. The ASALs are endowed with vast resources. These regions are home to more than 90% of the wildlife in the country and support tourism, generating 12% of Kenya's Gross Domestic Product (GDP) (GoK, 2012). Approximately 70% of Kenya's livestock resource is also found in the ASALS and are estimated at a value of Ksh.70 billion. Further, they have great potential for renewable energy especially solar and wind power (GoK, 2012). Despite all these resources the inhabitants in the ASALs endure poor infrastructure, high poverty levels, human conflicts, low illiteracy levels, and land degradation (GoK, 2012). The ASALs are also disposed to floods and droughts. Drought occurrence in Kenya is still a challenge to predict and this has an undesirable effect on crop production in the ASALs. Periods of high rainfall, which cause floods, follow the droughts resulting in the loss of life and property (Herrero *et al.,* 2010).

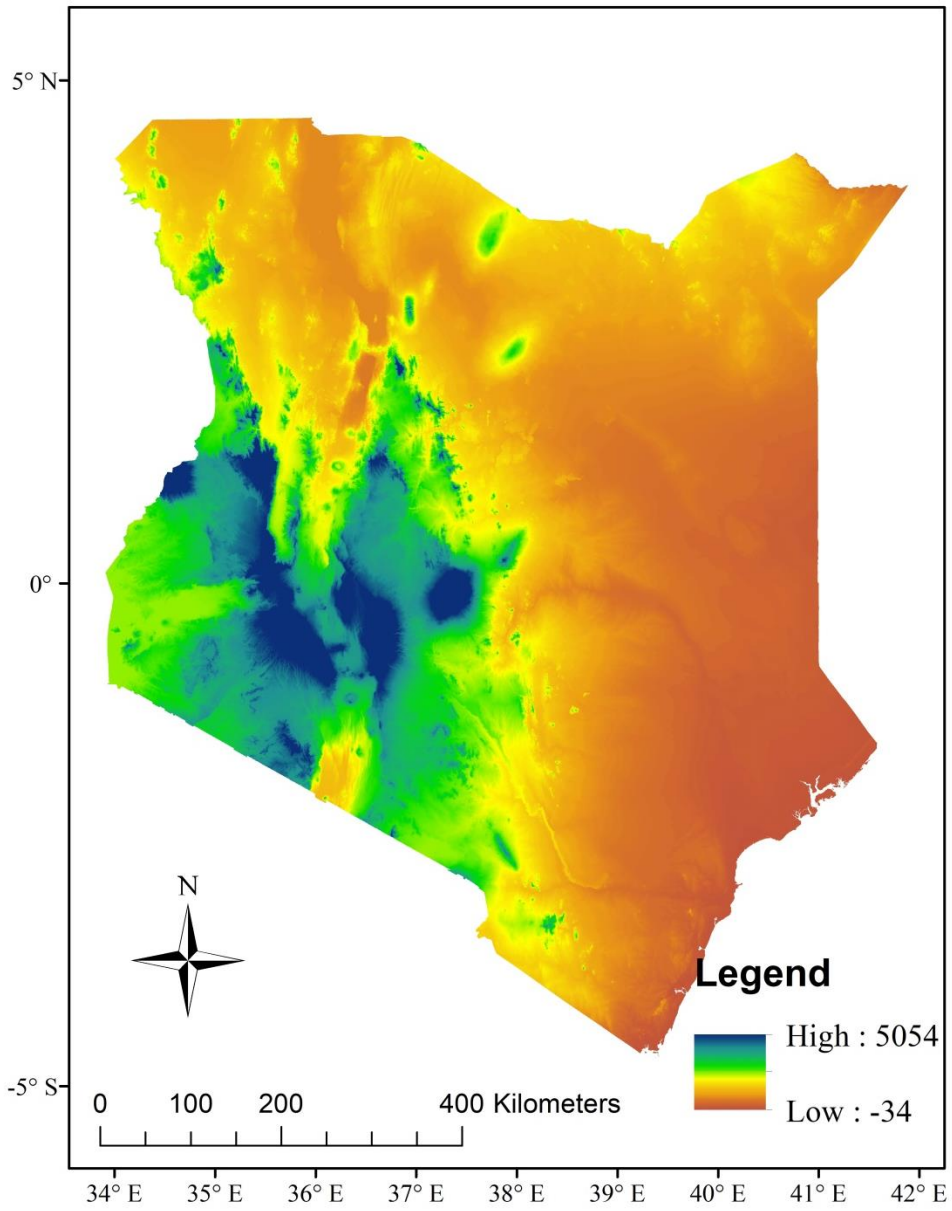

Figure 3-1: Topography of the Study Area (in meters). The brown regions show areas of low elevation increasing through to the blue regions. Source (Mugo *et al.*, 2020)**.**

3.2 Materials

The datasets utilised in this study were climate data and non-climate data on soils, topography and green gram phenological data.

3.2.1 Climatic Data

This subsection presents the climate data used in this study which includes the historical station-based data, CRU datasets and the CORDEX datasets.

3.2.1.1 Historical Station-based Climate Data

The station data utilized in the study was 47 years of monthly rainfall, and 47 years of monthly temperature data from 1970 to 2016 of the homogenous zones in Kenya (Table 3-1) obtained from the Kenya Meteorological department. The stations chosen for analysis are based on the homogenous zones for the MAM and OND seasons as shown in Figure 3-2a and Figure 3-2b.

In addition to this, daily rainfall, solar radiation, and maximum and minimum temperature data were collected from the South Eastern Kenya University (SEKU) meteorological station in Kitui County, Kenya for the years 2018 and 2019 when the green gram production experiments were conducted. SEKU is located in the ASALs region of Kenya and it falls in the homogenous zone 7 in MAM (Voi station) and the homogenous zone 7 in OND (Dagoretti station).

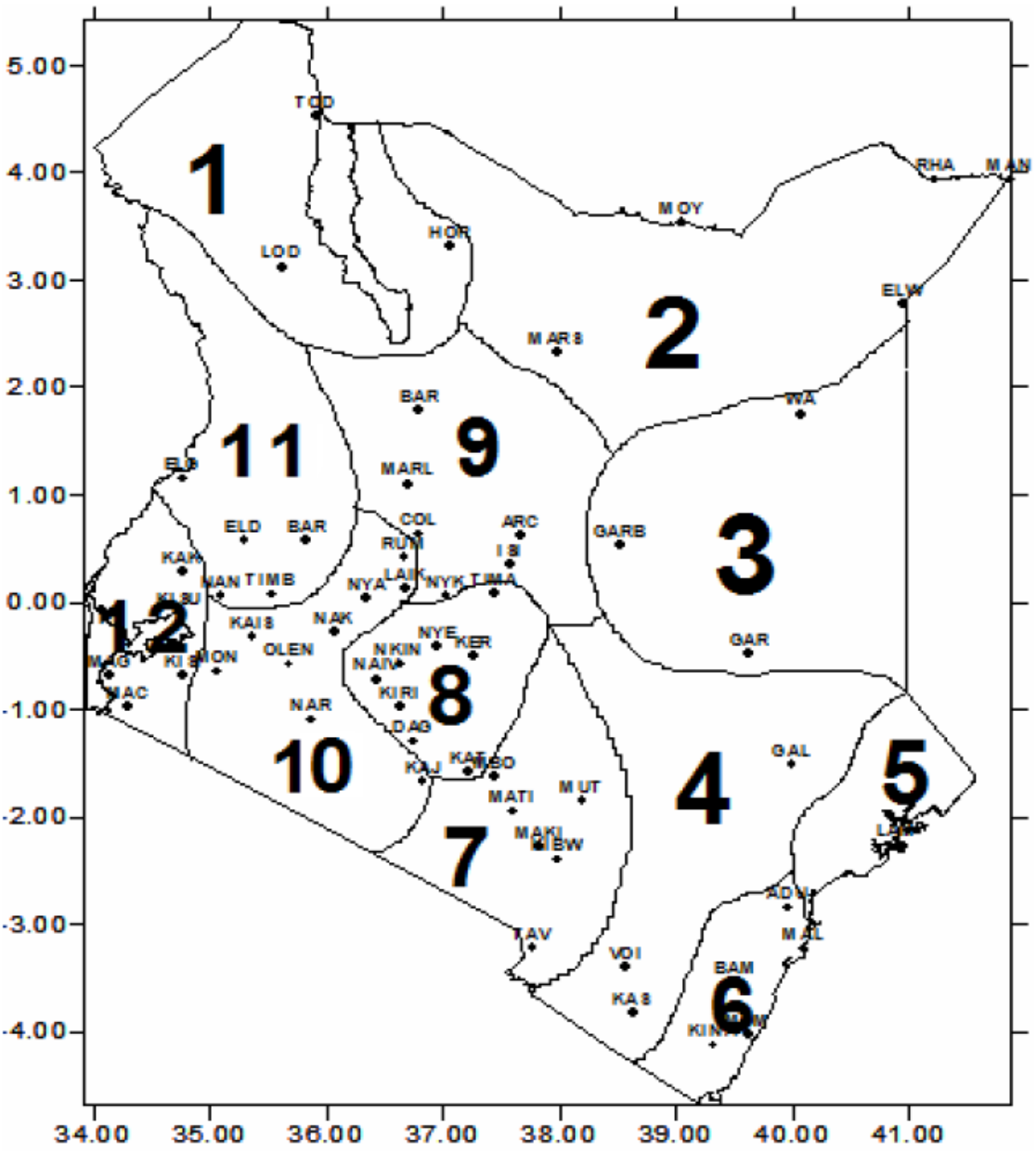

Figure 3-2a: Homogenous rainfall stations in Kenya during the MAM season. The stations located in each homogenous zone can be used to represent the entire zone. Source (Indeje *et al*., 2000)

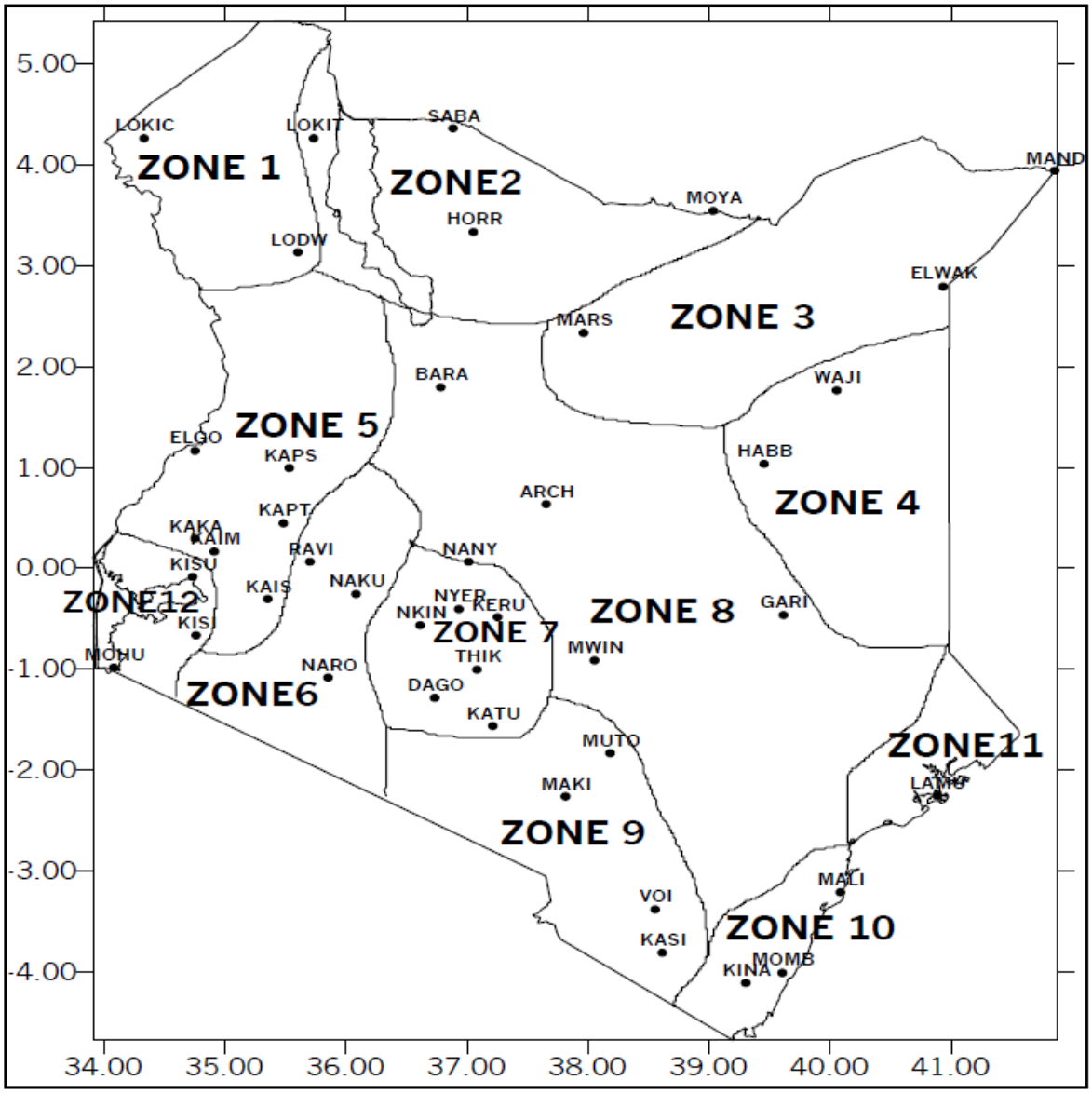

Figure 3-3b: Homogenous rainfall stations in Kenya during the OND season. The stations located in each homogenous zone can be used to represent the entire zone. Source (Indeje *et al*., 2000)

Table 3-1: Names of Meteorological Stations Utilized in the Study, Showing their Elevations, Geo-location (where E, N, and represent East, North and South, Respectively), and Homogenous Zones during the MAM and OND Seasons

				Homogenous zone	
Station Name	**Latitude (°)**	**Longitude (°)**	**Elevation (m)**	**MAM**	**OND**
Dagoretti	36.8 E	1.3 S	1798	8	7
Garissa	39.6 E	0.5 S	147	4	8
Kakamega	34.8 E	0.3 N	2133	-	5
Kisumu	34.8 E	0.1 S	1146	12	12
Lamu	40.9 E	2.3 S	30	5	11
Mandera	41.9 E	3.9 N	230	-	3
Marsabit	38 E	2.3 N	1345	11	-
Mombasa	39.6 E	4.1 S	55	6	10
Moyale	39.1 E	3.5 N	1097	2	2
Nakuru	36.1 E	0.3 S	1901	-	6
Nanyuki	37 E	0.1 N	1905	9	-
Narok	35.9 E	1.1 S	1890	10	-
Voi	38.6 E	3.4 S	597	7	9
Wajir	40.1 E	1.7 N	244	3	4
Lodwar	35.6 E	3.1 N	523	1	1

3.2.1.1 Coordinated Downscaling Experiment Data

Coordinated Downscaling Experiment (CORDEX) is an international project instituted by the World Climate Research Programme. CORDEX is a coordinator for the global efforts in downscaling datasets from Global Climate Models to scales of regional scope (Gutowski *et al.*, 2016).

Table 3-2 shows the 9 GCMs downscaled by the RCA4 RCM for Africa which have been used in this study. The Africa-CORDEX ensemble (9 GCMs downscaled) and the Euro-CORDEX ensemble (9 GCMs downscaled), are the largest ensembles of transitory (1951-2100) regional climate simulations ever made by one regional model determined by different CMIP5 GCMs under both the RCP 8.5 and RCP 4.5 scenarios.

Table 3-2: Global Climate Models Downscaled in the CORDEX Africa Project (Source: (Endris *et al.*, 2013))

	Institute Name	GCM Name	Country	Calendar Days
1	Canadian Center for Climate Modelling and Analysis (CCCma)	CanESM2	Canada	365 days
2	Centre National de Recherches Météorologiques (CNRM-CERFACS)	CNRM-CM5	France	Standard
3	Commonwealth Scientific and Industrial Research Organisation (CSIRO)	QCCCE-CSIRO-Mk3-6-0	Australian	365 days
4	Institut Pierre Simon Laplace (IPSL)	CM5A-MR	France	365 days
5	Max Planck Institute for Meteorology (MPI-M)	MPI-ESM-LR	Germany	Standard
6	Met Office Hadley Centre (MOHC)	HadGEM2-ES	United Kingdom	360 days
7	Model for Interdisciplinary Research on Climate (MIROC)	MIROC5	Japan	365 days
8	National Oceanic and Atmospheric Administration- Geophysical Fluid Dynamics Laboratory (NOAA-GFDL)	GFDL-ESM2M	USA	365 days
9	Norwegian Climate Centre (NCC)	NorESM1-M	Norway	365 days

The data from the CORDEX the Fourth edition of the Rossby Centre (RCA4) RCM was used to determine the future changes in climate variables over Kenya under the RCP 4.5 scenarios which assume that there is business as usual, and the RCP 8.5 scenario, which is the worst case scenario. The period of time considered for the future climate was between 2021 and 2050, which is the period for implementation of Kenya's vision 2030 goals.

3.2.1.2 Projection of Future Climate under Various RCP Scenarios

The Representative Concentration Pathways (RCPs) are courses of greenhouse gas (GHG) levels agreed upon in the fifth Assessment Report of the IPCC (2014). The RCPs succeeded the SRES projections issued in 2000. The RCPs are named in accordance with the radiative forcing target level for 2100.

The RCP 2.6 scenario represents conditions leading to very low GHG concentration levels. During the RCP 2.6 Scenario the radiative forcing level will peak to 3.1 W/m^2 by the mid-century and then drop to 2.6 W/m^2 by the year 2100. The scenario was developed at the Planbureau voor de Leefomgeving (PBL) Netherlands Environmental Assessment Agency by the Integrated Model to Assess the Global Environment (IMAGE) modelling team.

The RCP 4.5 scenario represents conditions where the level of greenhouse gases will stabilize to 4.5 W/m^2 by the year 2100 (Wise *et al.*, 2009). The RCP 4.5 scenario was developed in the

United States at the Pacific Northwest National Laboratory's Joint Global Change Research Institute (JGCRI) by the GCAM modelling group (Clarke *et al.,* 2007; Smith and Wigley 2006; Wise *et al.,* 2009).

The RCP 6.0 scenario represents conditions where the level of greenhouse gases will stabilize to 6.0 W/m^2 by the year 2100. The RCP 6.0 scenario was established in Japan at the National Institute for Environmental Studies (NIES) by the Asia-pacific Integrated Model (AIM) modelling team (Fujino *et al.,* 2006; Hijioka *et al.,* 2008).

The RCP 8.5 scenario represents cases in literature where GHGs increase over time, leading to high GHG concentrations. The RCP 8.5 scenario was established in Austria using the Model of Energy Supply Systems and their General Environmental Impact (MESSAGE) model together with the Integrated Assessment Framework of the International Institute for Applied Systems Analysis (IIASA) (Van Vuuren *et al.,* 2011).

3.2.2 Non Climatic Data

Data on topography was obtained from the United States Geological Survey (USGS) digital elevation model (DEM) and soil data from the Kenya Soil Survey (KSS).

Primary data was also collected on green gram phenology for four different varieties on an experiment set up in Kitui at the SEKU farm.

3.2.3 Quality Control of Climate Data

The purpose of data quality control is to identify errors and missing data, and where possible correct them to ensure the highest level of accuracy when using the data (Steinacker *et al.,* 2011).

Correlation and regression methods were used to determine approximate values of missing data. The first step was to determine the station with the highest correlation with the station with missing data. A regression equation between the two stations was developed for the period of time where data was available. Provided that not more that 10% of the data in a time series is missing, the World Meteorological Organisation recommends the use of this method.

Consistency tests help to ascertain that the variability in the data is climatological and not due to other factors such as change of instrument over time, change in observers, instrument

malfunction, or change in exposure condition of the site. The single mass curve was used to check for the data consistency.

Other homogeneity tests conducted included the Pettitt test, Buishand range test and the Standard Normal homogeneity test. These methods tested at the 0.05 level of significance that there is no unwarranted change in the data meaning it is homogenous. These tests were conducted using the available trend package in the R software (Pohlert, 2018).

3.2.3.1 Pettit's Test

The Pettitt (1979) test was used to identify whether there was a significant change in the mean of the time series when the precise time of change is unknown. According to Pettitt's test, if $x_1, x_2, x_3,\ldots, x_n$ is a time series of observed data which has a change at time *t* such that $x_1, x_2,\ldots, x_t$ has a distribution function $F_1(x)$ which is different from the distribution function $F_2(x)$ of the second part of the time series $x_{t+1}, x_{t+2}, x_{t+3},\ldots, x_n$ then the test statistics U_t for the Pettitt test may be computed as presented in Equation 3.1, and defined in Equation 3.2.

$$U_t = \sum_{i=1}^{t} \sum_{j=t+1}^{n} sgn(x_t - x_j) \tag{3.1}$$

$$sgn(x_t - x_j) = \begin{cases} +1 \; if(x_j - x_i) > 0 \\ 0 \; if(x_j - x_i) = 0 \\ -1 \; if(x_j - x_i) < 0 \end{cases} \tag{3.2}$$

The test statistic *K* and the allied confidence level (ρ) for the sample length (*n*) may be defined as in Equation 3.3 and Equation 3.4, respectively.

$$K = Max|U_t| \tag{3.3}$$

$$\rho = exp\left(\frac{-K}{n^2 + n^3}\right) \tag{3.4}$$

When ρ is less than the confidence interval level, the null hypothesis is rejected. The approximate significance probability (*p*) for a change-point is defined as shown in Equation 3.5.

$$p = 1 - \rho \tag{3.5}$$

3.2.3.2 Buishand Range Test

In the Buishand range test (Buishand, 1982) the adjusted partial sum (S_k), that is the cumulative deviation from the mean for the k^{th} observation of a time series $x_1, x_2, x_3,\ldots, x_k,\ldots, x_n$ which has a mean ($\bar{x}$) can be calculated using Equation 3.6:

$$S_k = \sum_{i=1}^{k} x_i - \bar{x} \tag{3.6}$$

A time series is assumed to be homogenous, that is without any change point, if $S_k = 0$. This is because in a random series the deviation from the mean will be distributed on both sides of the mean of the series. The significance of the change can be assessed by calculating the rescales adjusted range (R) as shown in Equation 3.7.

$$R = \frac{Max(S_k) - Min(S_k)}{\bar{x}} \tag{3.7}$$

The calculated value of $R/\sqrt{n}$, where n is sample size, is likened with the critical values given by Buishand (1982).

3.2.3.3 Standard Normal Homogeneity Test

In the standard normal homogeneity test (Khaliq and Ouarda, 2007), the test statistic (T_k) is used to compare the mean of the first n observations with the mean of the remaining (n-k) observations with n data points as shown in Equation 3.8.

$$T_k = kZ_1^2 + (n-k)kZ_2^2 \tag{3.8}$$

Z_1 and Z_2 can be computed as shown in Equation 3.9 and Equation 3.10, respectively

$$Z_1 = \frac{1}{k}\sum_{i=1}^{k}\frac{(x_i - \bar{x})}{\sigma} \tag{3.9}$$

$$Z_2 = \frac{1}{n-k}\sum_{i=k+1}^{n}\frac{(x_i - \bar{x})}{\sigma} \tag{3.10}$$

In Equation 3.10, $\bar{x}$ and σ are the mean and the standard deviation of the time series. The year k is the change point and contains a break where the value of T_k achieves the maximum value. In order to reject the null hypothesis, the test statistic should be larger than the critical value, which is contingent on the sample size (n).

3.3 Methodology

This subsection presents the methodologies used to determine the temporal and spatial variability of climate variables in Kenya, the analysis of land suitability for green gram production, and the simulation of the effects of climate change on green gram yield in Kenya.

3.3.1 Temporal and Spatial Variation of Climate Elements in Kenya

This subsection presents the methodologies on trend analysis, error analysis and bias correction.

3.3.1.1 Trend Analysis

Both parametric and non-parametric methods can be used to detect trend in a time series. Parametric methods make the assumption that the data is free from outliers and are thus normally distributed; non-parametric methods do not have such assumptions.

The Mann-Kendall method, proposed by Mann (1945), is one commonly applied non-parametric method for identifying trend in a time series. Several recent studies have used the Mann-Kendall test to identify trends in time series (Taxak *et al.*, 2014; de Carvalho *et al.*, 2014; Mallya *et al.*, 2016). The Mann-Kendall method is often preferred for trend analysis, because it can work with missing data, non-normality, seasonality and outliers in a time series (Oloruntade *et al.*, 2016).

a) Mann- Kendall Test

The Mann-Kendall test (S) (Equation 3.11) was used to determine whether there was a trend in the rainfall and temperature, annually and in the MAM and OND seasons.

$$S = \sum_{i=1}^{n-1} \sum_{j=i+1}^{n} sgn(x_j - x_i) \tag{3.11}$$

In Equation 3.12 x_j represents the successive values and *n* represents the number of data points in a set.

$$sgn(x_j - x_i) = \begin{cases} +1 \; if(x_j - x_i) > 0 \\ 0 \; if(x_j - x_i) = 0 \\ -1 \; if(x_j - x_i) < 0 \end{cases} \tag{3.12}$$

According to Equation 3.12 if a data variable from a previous time (x_j) is larger than one from a later time (x_i), the value (S) is increased by 1, and vice versa.

The variance statistic, Var (S), is given by Equation (3.13):

$$Var\ (S) = \frac{n(n-1)(2n+5) - \sum_{p=1}^{r} t_p(t_p-1)(2t_p+5)}{18} \quad (3.13)$$

In Equation 3.13, *r* represents the number of tied clusters (i.e., sample data with equal value), and t_p are the data points in the p^{th} tied cluster. The values of *S* and *Var(S)* are then used to determine the test *Z* value as shown in Equation 3.14:

$$Z = \begin{cases} \frac{S-1}{\sqrt{Var(S)}}\ if\ S > 0 \\ 0\ if\ s = 0 \\ \frac{S+1}{\sqrt{Var(S)}}\ if\ S < 0 \end{cases} \quad (3.14)$$

From Equation 3.14, an increasing trend is reported if *Z* is positive and, in addition, the calculated value is larger than the significance level. A decreasing trend is reported if *Z* is negative and the calculated value is greater than the significance level. If the calculated value of *Z* is smaller than the significance level then the trend is not significant. A significance level of 5% was applied.

b) The Sen's Slope Estimator Test for the Magnitude of Trend

The magnitude of trend was estimated using the Sen's slope test. Here, the slope (T_i) of all pairs of data is calculated as shown in Equation 3.15 (Sen, 1968).

$$T_i = \frac{x_j - x_k}{j-k} \qquad \text{For i=1, 2, …, n} \quad (3.15)$$

In Equation 3.15 parameters x_j and x_k are the values of data at period *j* and *k* where *j* is greater than *k*. The mean of the *n* values of T_i is symbolized as the Sen's estimator of slope and computed using Equation 3.16.

$$Q_i = \begin{cases} T_{\frac{n+1}{2}} & if\ n\ is\ odd \\ \frac{1}{2}\left(T_{\frac{n}{2}} + T_{\frac{n+2}{2}}\right) & if\ n\ is\ even \end{cases} \quad (3.16)$$

Positive values of Q_i indicate an increasing trend while negative values of Q_i indicate a decreasing trend in the time series.

3.3.1.2 Spatial Analysis and the Performance of CORDEX in Simulating Historical Climate

The data from 1971 to 2000 was used as the baseline for the verification of CORDEX models. The performance of CORDEX RCMs in mimicking climate conditions in various places has been studied by a number of authors (Endris *et al.,* 2013; Mascaro *et al.,* 2015; Luhunga *et al.*, 2016; Mutayoba and Kashaigili, 2017). The skill of an RCM to mimic the climate of an area has been shown using diverse techniques, but no specific system is considered better than another. The collective use of many methods is what brings an all-inclusive impression of the model presentation (Flato *et al.*, 2013).

The CORDEX model outputs were assessed against the observed data using statistical measures of bias (Equation 3.17) and the normalised root mean square (NRMSE) (Equation 3.18) which was calculated using the root mean square error (RMSE) (Equation 3.19); the World Meteorological Organisation recommends these measures (Luhunga *et al*., 2016).

$$Bias = \frac{1}{N}\sum_{i=1}^{N}(P_i - O_i) \tag{3.17}$$

$$NRMSE = \frac{RMSE}{Mean_{Obs}} \times 100 \tag{3.18}$$

$$RMSE = \sqrt{\frac{1}{N}\sum_{i=1}^{N}(P_i - O_i)^2} \tag{3.19}$$

In Equations 3.17 and 3.19, *O* is the observed value, *P* the simulated value and *N* the total number of these pairs (Luhunga *et al.*, 2016).

The Normalised Root Mean Square Error (*NRMSE)* (Equation 3.18) measures the absolute error of the RCM in simulating observed climate. Smaller values of *NRMSE* indicate that the RCM simulated the observed climate well; large values show model deficiency in simulating the observed climate.

3.3.1.3 Bias Correction

Bias correction is done to reduce the error of the models in overestimating or underestimating future climate. There are four popular bias correction methods which include the Standardization-Reconstruction, Scaling, Gamma Quantile Mapping, and Empirical Quantile

Mapping methods (Akhter *et al.*, 2017). This study used the Scaling method also called the change factor method (Equation 3.20). The choice was based on its simplicity and extensive usage in literary works (Wetterhall *et al.*, 2012).

The scaling method involves adjusting the model data using the multiplicative (quotient) or additive (difference) factor between the observed and model data. The multiplicative approach is best suited to variables with a lower bound, (e.g. precipitation), and the additive approach to boundless variables, (e.g. temperature) (Akhter *et al.*, 2017). For rainfall which was corrected for bias, the formula was expressed as shown in Equation 3.20.

$$P_{C,i} = P_{O,i} \times \frac{\Delta_p}{\Delta_r} \tag{3.20}$$

Here $P_{C,i}$ and $P_{O,i}$ are the corrected and uncorrected model outputs, respectively; Δ_p and Δ_r are the average observed and GCM precipitation during the reference period. The equation for the addictive approach involves changing the quotient (multiplicative) sign to the difference (additive) sign.

3.3.2 Land Suitability Analysis

The analysis of the suitability of land involved the determination of the thresholds from literature within which green gram performs best and worst. The data on climatic, soil and topographical conditions suitable for green gram was first categorized into two classes; these were the suitable class and not suitable class. The two classes were additionally alienated into four classes namely, Highly suitable (S1), Moderately suitable (S2), Marginally suitable (S3) and not suitable (N) as directed by Table 3-3.

Table 3-3: Land Suitability Classification Structure

Order	Class	Explanation
S	**S1**	Land with no major limits to sustain a particular continued use, or whose limitations are only minor and cannot reduce production and benefits and will not require inputs above a level which is not acceptable.
	S2	Land whose limits are only moderately severe to the sustenance of a particular use; the limitations thus would affect production and benefits and increase the required inputs to a level where the final benefit gained, although still good, is substantially lower to that anticipated in the S1 class.
	S3	Land whose limits are severe to the sustenance of a particular use and thus would lower production and benefits, and increase the inputs required, such that the final benefit is only marginally justifiable.

Order	Class	Description
N	N1	Land whose limits may be overcome with time but cannot be corrected using the current information at a tolerable cost; the limitation is so severe to support the sustained use of land in the suggested way.
	N2	Land that has limits so severe that they exceed any chance to support the sustained use of land in the suggested manner.

Source: FAO (1976)

3.3.2.1 Green Gram Suitability Table

Table 3-4 shows four classes of the suitability of green gram production under different soil, climate and topography summarized as the Highly suitable class (S1), Moderately suitable class (S2), Marginally suitable class (S3) and not suitable class (N).

Table 3-4: Green gram Suitability Table for Factors used in Developing Suitable Areas for Green gram Production in Kenya, Where, S1, S2, S3 and N are the Highly suitable class, Moderately suitable class, Marginally suitable class, and not suitable class (N) Respectively.

Parameter	S1	S2	S3	N	Source
Rainfall	250-350 mm	150-250 mm 350-600 mm	75-150 mm >600	<75 mm	(Gaiser *et al.* 2001)
Temperature	30-21°C	18-21 °C	15-18 °C	<15 °C >30 °C	(Al-Mashreki *et al.*, 2011)
Soil pH	6.2-7.2	5-6.2	7.2-8.0	>8.0 <5.0	(Mugo *et al.*, 2016; Ogunwale *et al.*, 2009)
Drainage	Well-drained	Imperfectly drained	Poorly drained, Rapidly drained	Very poorly drained	(Mugo *et al.*, 2016; Yohannes and Soromessa, 2018)
Texture	Loam Sandy Loam	Clayey	Very clayey Extremely sandy	-	(Mugo *et al.*, 2016; Yohannes and Soromessa, 2018)
CEC	>10meq/100g	5-10 meq/100g	0-5 meq/100g	-	(Mugo *et al.*, 2016; Ogunwale *et al.*, 2009)
Depth	>50cm	30-50cm	<30cm		(Mugo *et al.*, 2016; Yohannes and Soromessa, 2018)
Altitude	0-1600	1600-2000	2000-3000	<0 >3000	(Mugo *et al.*, 2016; Ogunwale *et al.*, 2009)

3.3.2.2 Pairwise Comparison Matrix

Saaty's (2008) scale of values from 1 to 9 (Table 3-5) was used to compare and assign weights to factors under climate (rainfall and temperature), soil (pH, texture, depth, drainage and CEC) and altitude.

Table 3-5: Scale of Relative Importance between any Two Factors which Affect Green Gram Production e.g. Rainfall vs. Drainage

Definition of Importance	**Scale**
Equally ranked factors	1
One factor's rank is weaker than the other	3
One factor's rank is much stronger than the other	5
One factor's importance is more than the other	7
One factor has absolute rank over the other	9
Values used when a factor's rank is between odd numbers	2,4,6,8

3.3.2.3 Criteria Weights Assignment

A Consistency Ratio (CR) as presented in Equation 3.21 was calculated and for the weights to be adopted, the ratio was required to be less than 10% to avoid bias (Halder, 2013).

$$CR = \frac{\mathrm{CI}}{\mathrm{RI}} \tag{3.21}$$

$$CI = \frac{(\lambda\mathrm{max} - \mathrm{n})}{(\mathrm{n} - 1)} \tag{3.22}$$

In Equation 3.22 *CI* denotes the Consistency Index; *λmax* Denotes the maximum Eigen value of the pairwise comparisons; *N* is the number of parameters being related; *CR* is the Consistency Ratio and *RI* stands for the Random Inconsistency Index which depends on the number of factors being related as shown in (Table 3-6).

Table 3-6: Random Inconsistency Index (RI) for N=I, II..., XI

N	I	II	III	IV	V	VI	VII	VII	IX	X	XI
RI	0.00	0.00	0.58	0.90	1.12	1.24	1.32	1.41	1.45	1.49	1.51

Source: Saaty (2008)

3.3.2.4 Model Inputs Preparation

Secondary data were attained from a number of sources as presented in (Table 3-7). The secondary databases were maps of soil parameters obtained from the Kenya Soil Survey map, present and future temperature and rainfall data from CORDEX and altitude extracted from the Digital Elevation model (DEM) of the United States Geological Survey (USGS). The secondary layers were used as inputs to the ArcGIS weighted overlay model.

Table 3-7: Description of Secondary Data Sources used as Map Layers in Delineating Areas Suitable for Green gram Production

Data layer	Source	Scale/ Resolution	Data Format
Climate: Temperature and rainfall	CORDEX	0.44 degrees/ 50km	Raster format
Soil: pH, CEC, depth, drainage and texture	KSS		Vector format
Topography/ DEM: Slope	USGS	30m	Raster format

3.3.2.5 Soil Data of the Study Area

The five vector layers of interest for this analysis (pH, depth, drainage, texture, and CEC) were extracted and converted into a raster format. The 5 raster layers were then reclassified into 4 classes of suitability (Highly suitable class, Moderately suitable class, Marginally suitable class and not suitable class).

3.3.2.6 Altitude of the Study Area

The altitude of the area was obtained in raster format from the DEM of the area. The altitude was reclassified into 4 classes of suitability (Highly suitable class, Moderately suitable class, Marginally suitable class and not suitable class).

3.3.2.7 Climate of the Study Area

The current and future seasonal total precipitation during the MAM and OND seasons and the seasonal mean temperature for these seasons were calculated from the normal average ensemble of the nine RCA4 RCM model. The temperature and rainfall was then reclassified into 4 classes of suitability as presented earlier in Table 3-4.

3.3.2.8 Green Gram Suitability Map

After rating and reclassifying the maps of climate, soil and altitude parameters, each was given a percentage stake (weight). These weights were obtained through the Analytical Hierarchy Process (AHP) (Mugo *et al.,* 2016; Kihoro *et al.,* 2013; Kamau *et al.,* 2015). The

maps were then overlaid to generate a green gram suitability map under current and future climates.

3.3.3 Simulation of the Impact of Changing Climate on Green Gram Production

From the green gram suitability maps, a highly suitable area in Kitui County was identified for further study to simulate what would be the actual yield of such an area under various agronomic scenarios. This involved planting four main green gram varieties at the SEKU farm under various agronomic scenarios and collecting the phenology, biomass, days to maturity and seed yield data upon harvesting.

3.3.3.1 APSIM Model Calibration

The APSIM module can simulate nine cultivars of the green gram crop. The varieties calibrated in APSIM include: Satin, a dull green seed resembling KS20; Celera, a small seeded, shiny green seed with hard seed levels resembling N26, and Berken and Emerald, medium-large and shiny green seeds resembling Tosha and Biashara varieties respectively (Gentry and Gordon, 2010). The calibrated Biashara, Tosha, KS20 and N26 were used to simulate the effect of changing climate on the yield, biomass and days to physiological maturity of green gram.

The Agricultural Production Systems sIMulator (APSIM) mimics the development of a crop by pooling management and biophysical modules (Mohanty, 2012). The modules mimic crop growth upon input of certain data, for instance, crop management data, weather data and soil data which have been described in more detail in the subsections below.

a) Crop Management data

Green gram was planted at a distribution of four to six kilograms per hectare, spacing of 15 cm and 45 cm between plants and rows, respectively, and a depth of three to five centimetres. Weeding was done two weeks after the emergence of seeds and before flowering. Pesticides were applied twice during the growth of green grams; at the budding stage and at the podding stage. Fertiliser was applied before the crop flowered and during fruiting to increase yields (SASOL, 2015).

b) Weather data

The APSIM weather module requires daily data on rainfall, solar radiation, minimum temperature, and maximum temperature. The APSIM model requires the data to be input as one file of daily weather parameters arranged in columns in chronological order. The data was saved as a **.prn** file under excel and this was converted to **.met** using the Tav_Amp program written in FOTRAN language. The **.met** is then read into the APSIM weather module.

Daily data on rainfall, solar radiation, minimum temperature, and maximum temperature were collected from the SEKU weather station which is located in Kitui County, Kenya during the year, 2018 and 2019 in the seasons when green gram experiments were conducted for use in model initialization and validation. Data on the number of rainy days in each month when green gram was planted was also collected to help understand the distribution of rainfall. A rainy day was described as a day when rainfall was more than or equal to 0.85 mm (Barron *et al.*, 2003).

Daily data on rainfall and temperature from the CORDEX RCA4 model ensemble under the baseline scenario (1971 to 2000), and the future RCP 4.5 and 8.5 scenarios (2021 to 2050) were also used as inputs in the green gram weather module to study the effect of climate change on green gram yield.

c) Sampling of Soil Parameters

Samples of soils were obtained using a soil auger at various depths (0-15 m, 15-30 m, and 30-45 m) sampled at different points in the experimental site using a zigzag pattern. The soils' subsamples were placed in three buckets based on the different depths (0-15 m, 15-30 m, and 30-45 m) and thoroughly mixed. A final sample of 1 kg from each bucket was obtained and placed in three collection bags labelled according to the soil depths. The three samples were then transported on the same day to the National Agricultural Research Laboratory (NARL) in Kabete, Kenya for physical and chemical analysis. Table 3-8 shows the physical and chemical soil parameters tested and the methods used.

Table 3-8 Soil Parameters Required by APSIM and the Analysis Method Used

Parameter	Units	Analytical method
Field capacity	(g/cm^3)	Initial Drainage Curve (IDC) (Klute, 1986)
Saturated water content	(mm/mm)	Initial Drainage Curve (IDC) (Klute, 1986)
Labile Phosphorus	(mg/kg)	Olsen method (Olsen and Sommers, 1982)
Bulk Density	(g/cm^3)	Oven dried (105^oC) to constant weight, after Blake and Hartge (1986)
Organic Carbon	(g/kg)	Walkley and Black process (Nelson and Sommers, 1996)
Total Nitrogen	mg/L	Kjeldahl process, (Bremner and Mulvaney, 1982)
Cation Exchange Capacity	Cmol+/kg	Ammonium-acetate process (Schollenberger and simon, 1945)
pH	1:5 water	1:2.5 soil (KCl I1M), by a standardized pH meter
Potassium	Cmol+/kg	Ammonium-acetate process (Schollenberger and simon, 1945)
Sodium	Cmol+/kg	Ammonium-acetate process (Schollenberger and simon, 1945)
Texture (Particle size of clay, sand)		Soil texture class and size classification conferring to USDA system (Gee *et al*.,1986)

3.3.3.2 Validation of the APSIM Green gram Model

The APSIM model was investigated for its ability to simulate the yield, biomass, and days to maturity of the green gram experimental data collected during the years 2018 and 2019.

a) Statistical Evaluation of the Green Gram Model Performance

The ability of the of the APSIM green gram model to simulate the observed green gram yield, biomass, and days to maturity were evaluated using the Bias and NRMSE tests (Section 3.3.1.2).

b) Future Green Gram Suitability

The effect that climate change will have on green gram yield under RCP 4.5 and RCP 8.5 scenarios from CORDEX was investigated using the validated green gram module. The period of consideration for the future climate was between 2021 and 2050 which is the implementation period for Kenya's vision 2030 objectives.

CHAPTER 4: RESULTS AND DISCUSSIONS

This Chapter presents the results and discussions of modelling green gram production in Kenya under current and future climates. It specifically presents the results and discussions on data quality control, spatial and temporal variability of climate, suitability of land to green gram production, and the simulated yield of green gram under the changing climate.

4.1 Data Quality Control

Missing data were estimated using the correlation and regression method as described in Section 3.2.3 provided that not more than 10% of the total data was missing.

Figure 4-1 presents the results of the single mass curve for all stations which generally displays no major shifts from the general trend during the period from 1970 to 2016.

Table 4-1 presents the results of homogeneity tests conducted using the Pettit, Buishand range and standard normal tests (Taxak *et al.*, 2014; Andang'o *et al.*, 2016) at a significance level of 0.05. There is no station where all the tests showed a statistically significant change in the homogeneity of the data. The year when a break occurred in the time series is also presented. For example a break is noted in the Dagoretti station forty years after 1970, in the year 2010. Andang'o *et al.* (2016) recorded similar results where they found 12 rainfall stations in Kenya were homogenous and thus useful for further analysis.

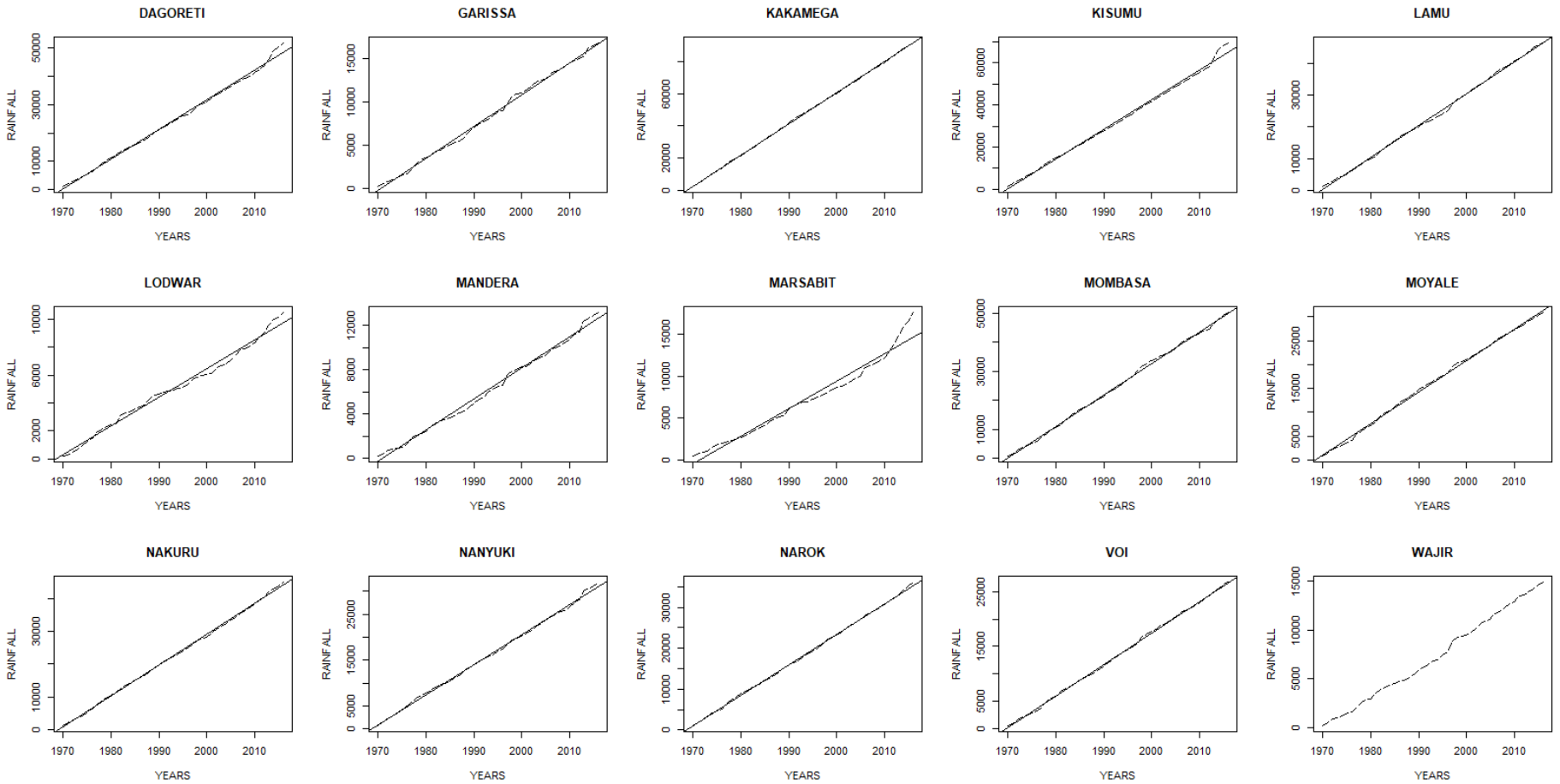

Figure 4-1 Singe mass curves of annual rainfall of stations in Kenya. The results generally show no major shifts from the general trend during the period 1970 to 2016

Table 4-1: Homogeneity Tests Showing the Year between 1970 and 2016 when a Break Occurred in the Time Series of Rainfall e.g. 40 Years After 1970 a Break is noted in the Dagoretti Station, in the Year 2010; S Denotes Significant and NS Not Significant Using a P-Value Of 0.05

Station	Pettitt (Break)	Buishland range (Break)	Standard normal (Break)	Verdict
Dagoretti	NS (40)	NS (40)	S (42)	Good
Garissa	NS (18)	NS (18)	NS (7)	Good
Kakamega	NS (22)	NS (22)	NS (22)	Good
Kisumu	NS (24)	NS (40)	S (43)	Good
Lamu	NS (27)	NS (27)	NS (27)	Good
Lodwar	NS (32)	NS (32)	NS (41)	Good
Mandera	NS (19)	NS (19)	NS (43)	Good
Marsabit	S (32)	S (36)	NS (41)	Good
Mombasa	NS (7)	NS (7)	NS (43)	Good
Moyale	NS (21)	NS (29)	NS (29)	Good
Nakuru	NS (31)	NS (31)	NS (40)	Good
Nanyuki	NS (9)	NS (40)	NS (41)	Good
Narok	NS (40)	NS (40)	NS (44)	Good
Voi	NS (7)	NS (7)	NS (47)	Good
Wajir	NS (19)	S (42)	NS (20)	Good

4.2 Spatial and Temporal Variability of Climate Parameters in Kenya

This subsection presents results on the spatial and temporal variability of climate variables in Kenya. In this section the CORDEX RCA4 models are assessed on their ability to replicate the observed rainfall and temperature. The bias corrected ensemble of rainfall and the ensemble of temperature are then used to study the temporal and spatial variability.

4.2.1 Performance of the CORDEX RCA4 Models in Simulating the Observed Temporal Distribution of Rainfall and Temperature Climatology in Kenya

This subsection presents results on the ability of the CORDEX RCA4 model to replicate the annual cycle of rainfall and temperature in Kenya.

4.2.1.1 Performance of the CORDEX RCA4 Models in Simulation the Observed Temporal Distribution of Rainfall

Figure 4-2 shows the distinct bimodal pattern of total mean annual rainfall in Kenya for some homogeneous stations. The models and the ensemble replicate the bimodal pattern of annual rainfall, but have notable biases. The CORDEX models and their ensemble underestimate rainfall during the MAM season and overestimate the rainfall during the OND season. The propensity of the CMPI models to underestimate the rainfall during the MAM season and overestimate the rainfall in the OND season over East Africa has also been observed by others (Ongoma *et al*., 2019; Yang *et al*., 2015). MAM is considered the main rainy season

due to its large spatial coverage and amount, especially along the coast and the Lake Victoria regions, while the OND season is the main season in the lower eastern and central regions (Ayugi *et al*., 2016). Kenya's rainfall patterns are mainly dependent on the movement of the ITCZ during the MAM season as it moves North and the OND season as the ITCZ moves south. During the JJA season rainfall in Kenya is controlled by the Southeast monsoon which brings moist air to the western and coastal portions of Kenya, the moist Congo air mass from the west, and the northward displacement of the ITCZ which bring moist air to the northern part of the country (Opijah *et al.*, 2017).

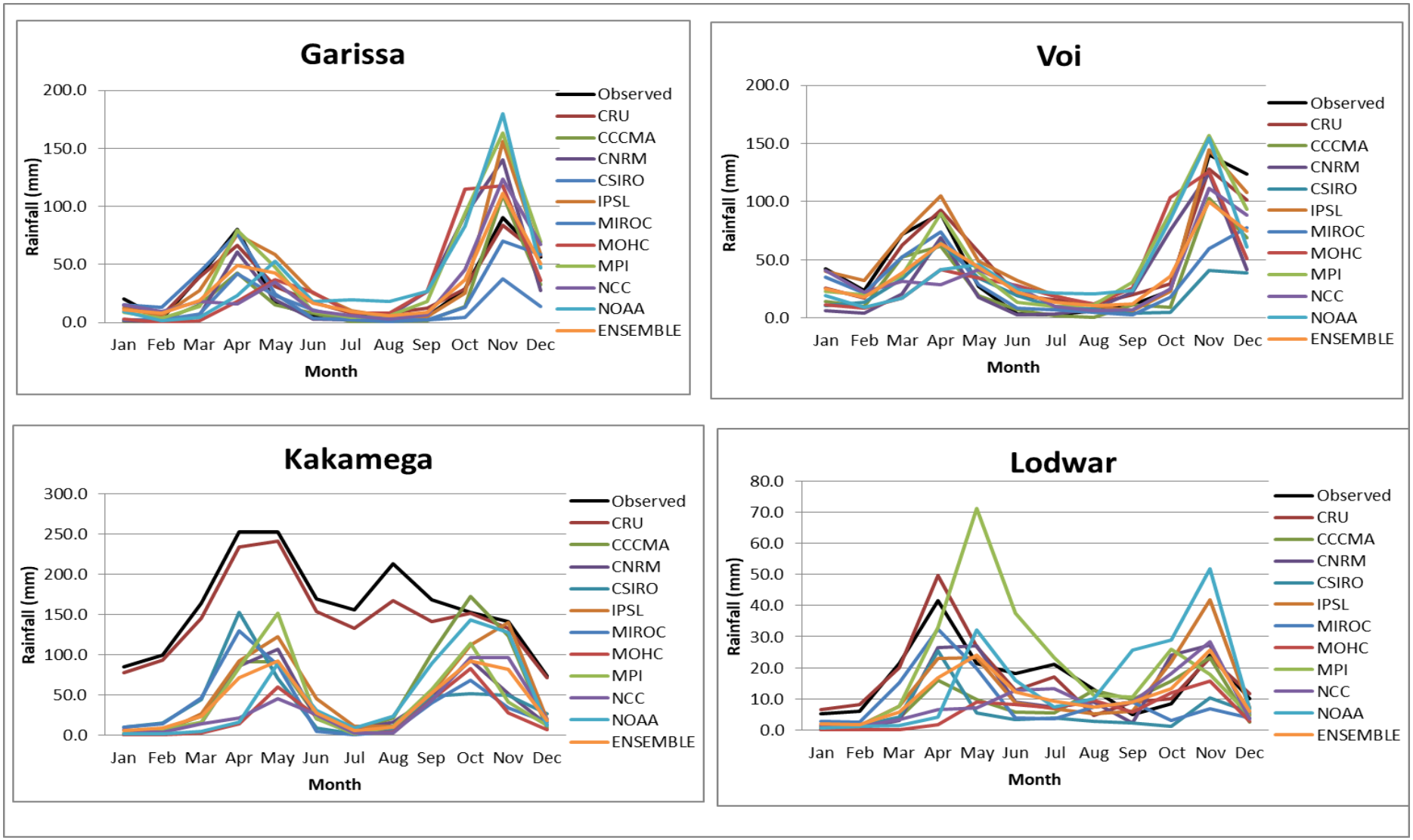

Figure 4-2: Average monthly observed and model rainfall (mm) patterns for stations in Kenya during the 1971 to 2000 period

4.2.1.2 Performance of the CORDEX RCA4 Models in Simulation the Observed Temporal Distribution of Temperature

Figure 4-3 and Figure 4-4 illustrate the pattern of the mean annual maximum and mean annual minimum temperature, respectively. Maximum and minimum temperature as presented in Figures 4-3 and 4-4 show small variability throughout the year with a decrease in temperature taking place during the MAM and OND rainy seasons because of the influence of cloud cover, and during the JJA season when there is advection of cold air from the South (Opijah *et al.*, 2017).

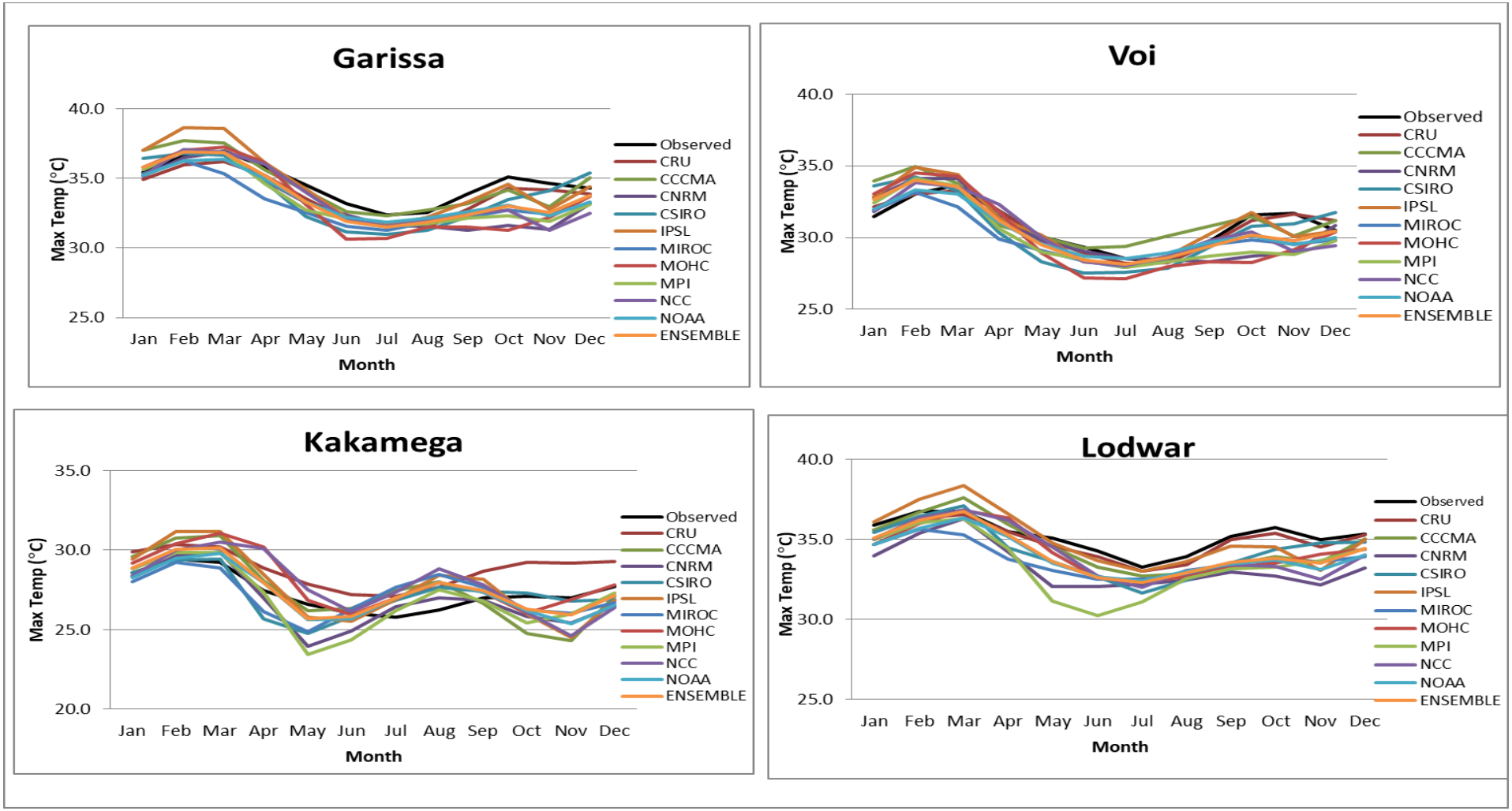

Figure 4-3: Average monthly observed and model maximum temperature patterns for stations in Kenya during the 1971 to 2000 period

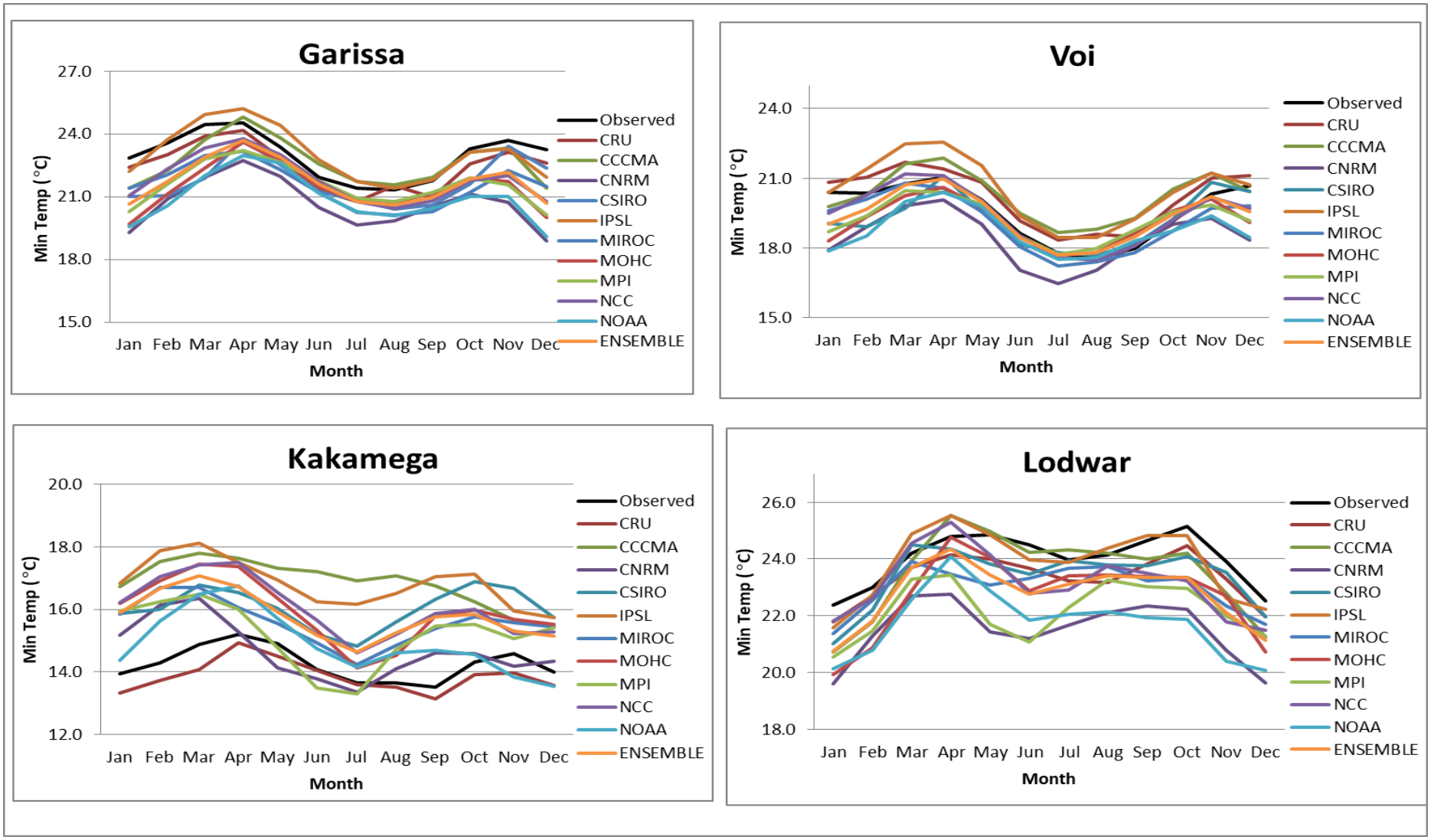

Figure 4-4: Average monthly observed and model minimum temperature patterns for stations in Kenya during the 1971 to 2000 period

4.2.2 Performance of the CORDEX RCA4 Models in Simulating the Spatial Pattern of Observed Rainfall Climatology in Kenya

This subsection presents the results on the ability of the CORDEX models to simulate the MAM and OND seasonal rainfall which are the main planting seasons in Kenya.

4.2.2.1 Climatology of Observed and Simulated Rainfall over Kenya

The spatial plots of the rainfall climatology of the MAM and OND seasons for the observed (Climate Research Unit (CRU)) and nine models is displayed in Figures 4-5 and 4-6 respectively. In Figure 4-5, the observed distribution shows that much of the rainfall is concentrated in the central, western, and coastal regions of Kenya. The rainfall pattern could be attributed to the influence of the meso-scale systems around the regions and the apparent position of the ITCZ which is around the equator. All the nine models and their ensemble overestimate the rainfall over the Mt. Kenya and Mt. Kilimanjaro regions since the values of total rainfall are larger than that of the CRU dataset. The results agree with other studies that indicate that models tend to have poor accuracy in high altitude areas (Endris *et al.*, 2013; Mukhala *et al.*, 2017; Kisembe *et al.*, 2019; Warnatzsch and Reay, 2019).

The distribution of the observed OND rainfall climatology differs slightly from that of MAM rainfall climatology. The models and their ensemble also overestimate rainfall peaks around Mt. Kenya and Mt. Kilimanjaro regions as shown in Figure 4-6. Generally the ensemble which is a normal average of the nine CORDEX models (Endris *et al.*, 2013) is a better representation than the individual models during both the MAM and OND seasons. The better representation by the ensemble can be attributed to its ability to cancel opposite signed biases across individual models. Individual models can sometimes be unreliable since they give good results in one region and poor results in another region over the same time period. The ensemble, although potentially biased, simulated rainfall better compared to individual models; model ensembles have previously been used for future climate studies (Endris *et al.*, 2013; Buontempo *et al.*, 2015; Ogega *et al.*, 2016; Mukhala *et al.*, 2017; Mutayoba and Kashaigili, 2017; Gibba *et al.*, 2019; Kisembe *et al.*, 2019).

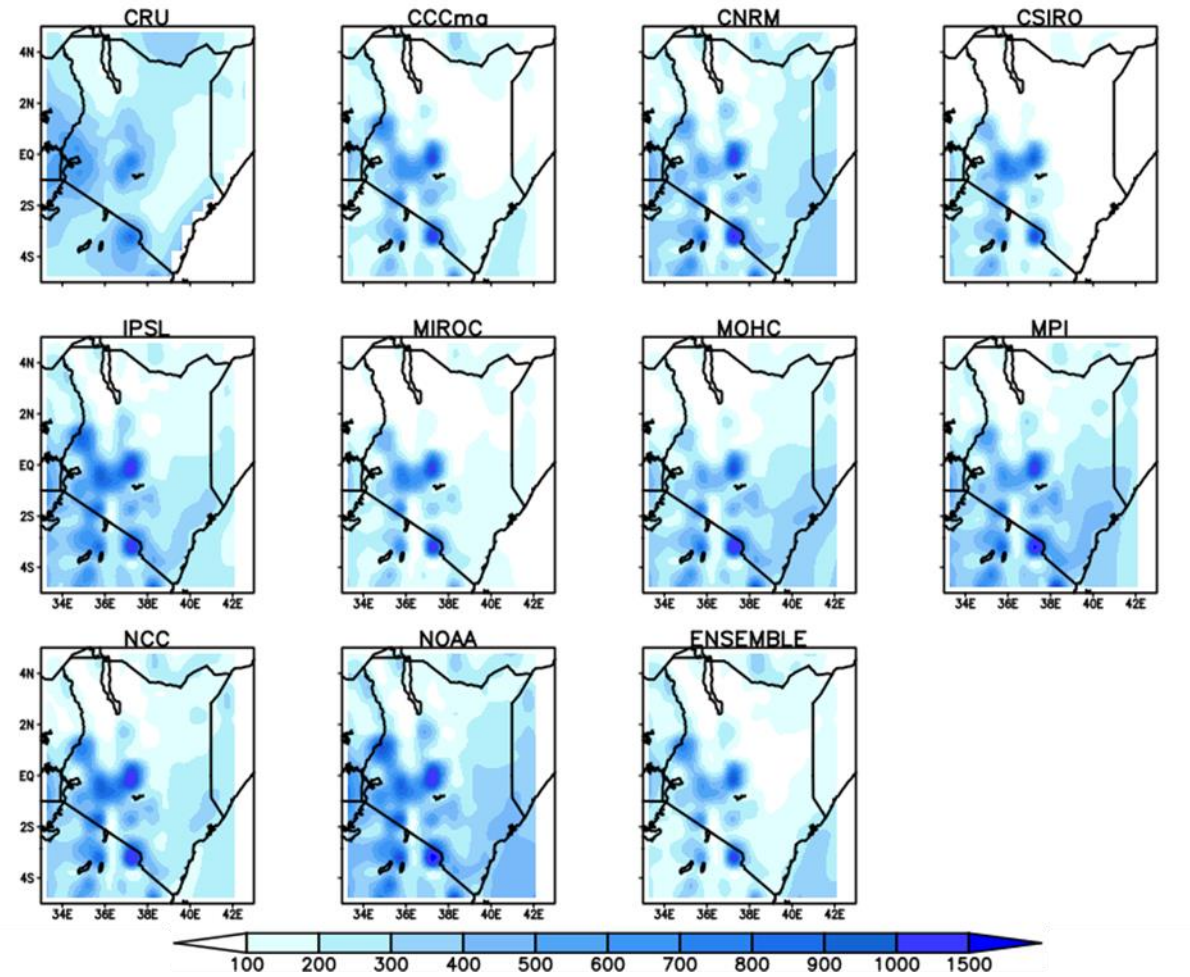

Figure 4-5: Performance of CORDEX models in simulating the observed MAM rainfall total (in mm) over Kenya for 1971-2000. Rainfall amount increases from the white shaded areas through to the blue shaded areas.

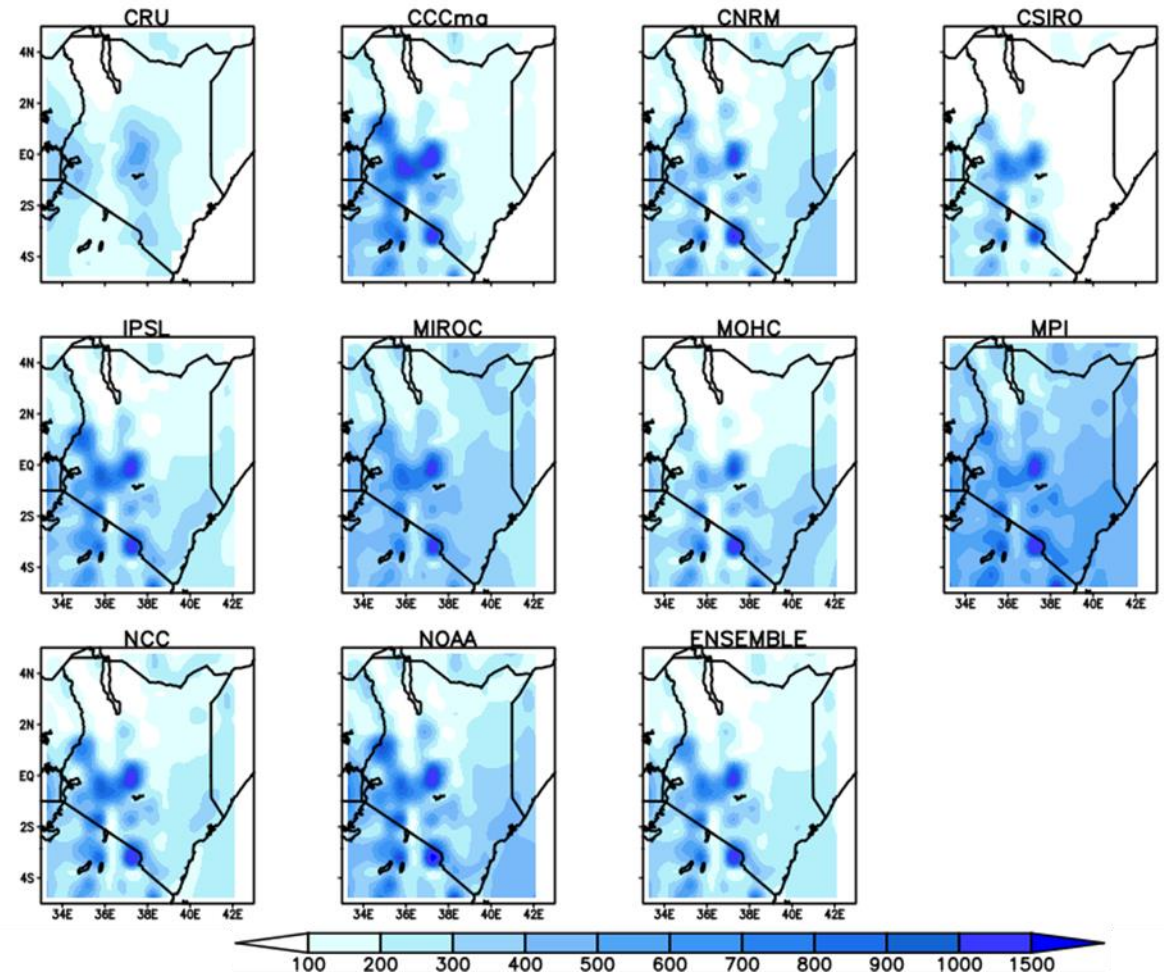

Figure 4-6: Performance of CORDEX RCA4 models in simulating the observed OND rainfall total (in mm) over Kenya for 1971-2000. Rainfall amount increases from the white shaded areas through to the blue shaded areas.

4.2.2.2 Rainfall Bias in the Simulated Dataset

The spatial distribution of the average bias of the simulated rainfall dataset against the observed rainfall datasets for the period 1971-2000 is presented in this section. Figures 4-7 and 4-8 present the average bias in rainfall during the MAM and OND seasons, respectively.

Most of the CORDEX models overestimate the rainfall over most parts of Kenya during the MAM season, except for the MOHC, NCC and NOAA models which tend to underestimate the observed rainfall amounts. Overestimation of rainfall is noted in the western and central parts of Kenya, particularly around Mt. Kenya region, especially by CSIRO, IPSL, MIROC and MPI models as shown in Figure 4-7.

Higher positive values of bias were observed during the OND season in contrast to the MAM season. The models simulate higher rainfall over the regions near the mountains and lakes

especially around Mt. Kenya and Mt. Kilimanjaro region, and the Lake Victoria region as indicated in Figure 4-8. The models do not properly simulate the mesoscale systems which are driven by the orographic drag, and the land-water contrasts.

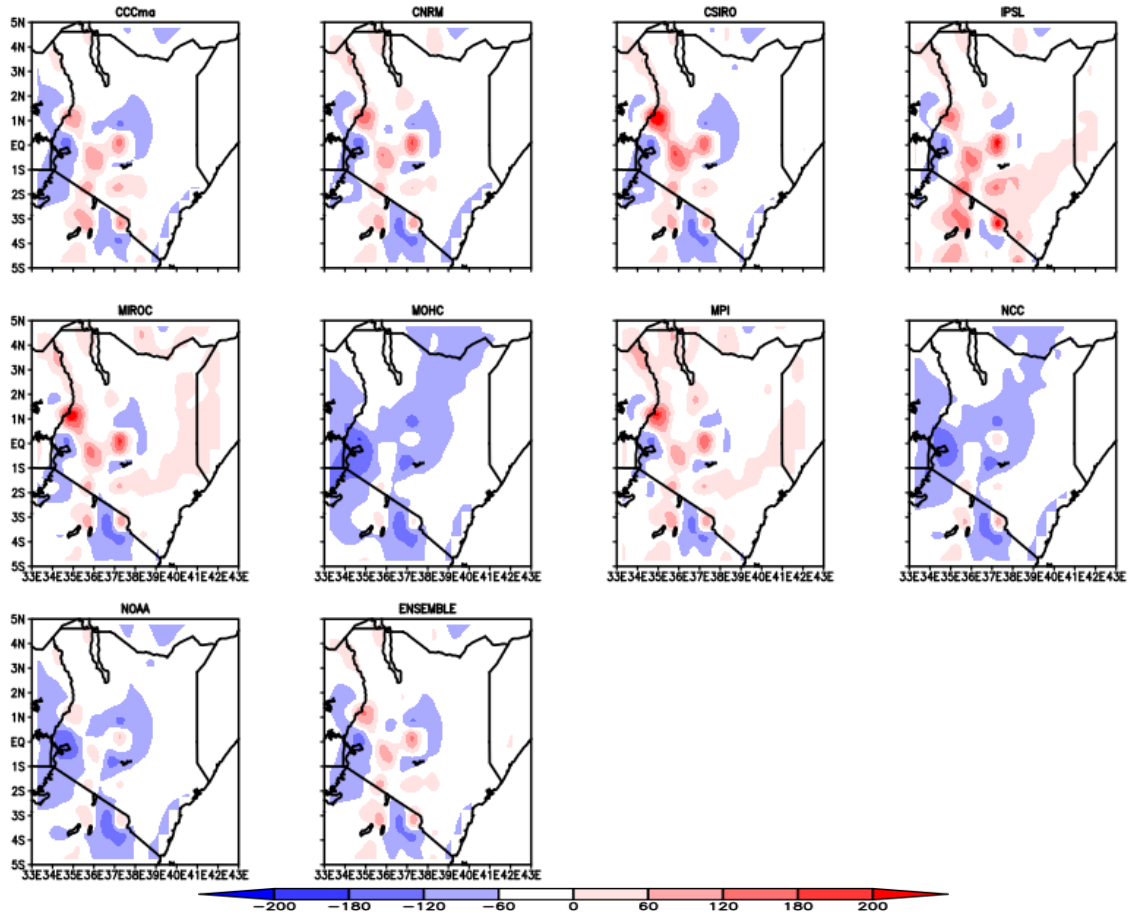

Figure 4-7: Bias of the average CORDEX simulated rainfall against the observed rainfall for the period 1971-2000 rainfall (in mm) during the MAM season over Kenya. Shades of red indicate overestimation while shades of blue indicate underestimation

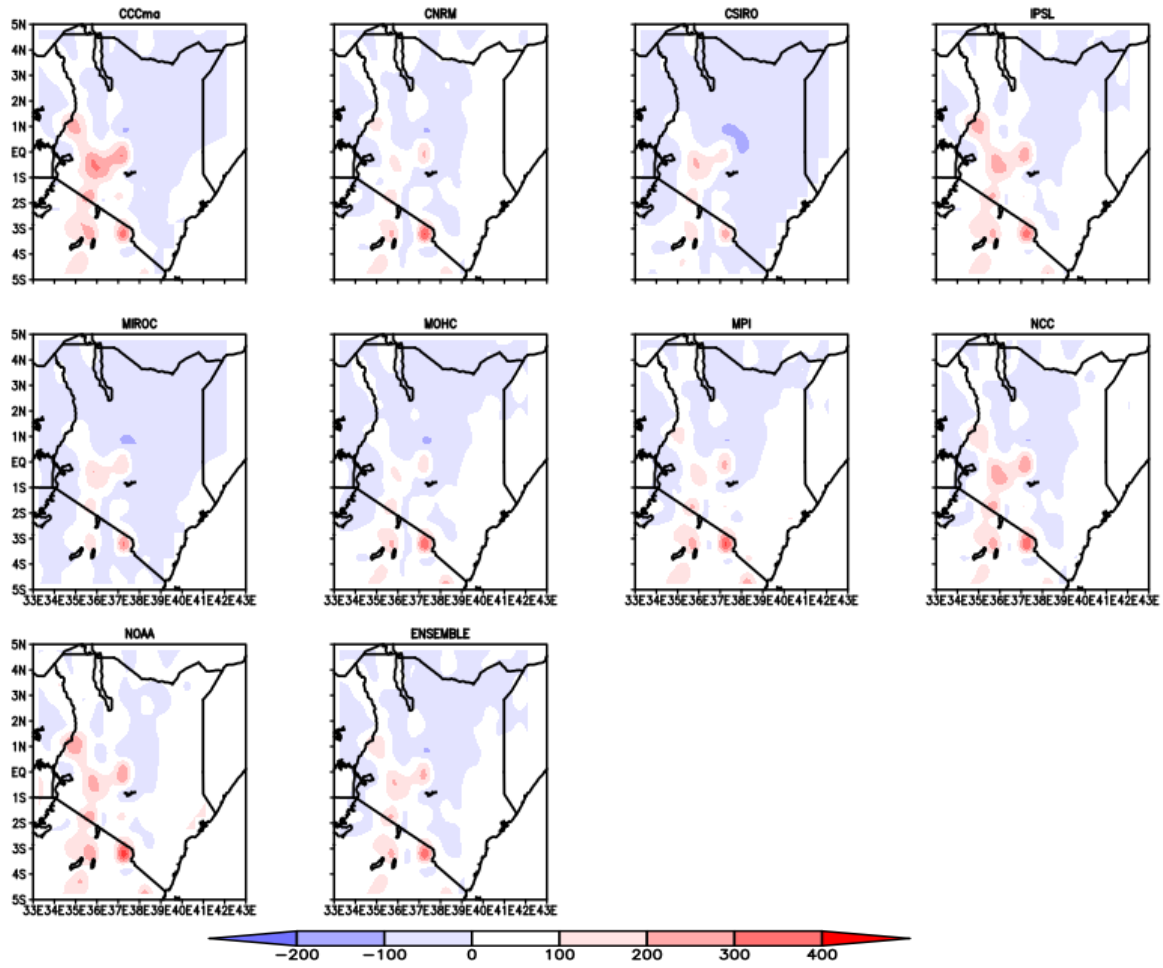

Figure 4-8: Bias of the average CORDEX simulated rainfall against the observed rainfall for the period 1971-2000 rainfall (in mm) during the OND season over Kenya. Shades of red indicate overestimation while shades of blue indicate underestimation

4.2.2.3 Normalised Root Mean Square Error in the Simulated Rainfall Datasets

The spatial distribution of the average NRMSE in the simulated rainfall dataset against the observed rainfall datasets for the period 1971-2000 are presented in this section. Figure 4-9 and 4-10 present average NRMSE during the MAM and OND seasons, respectively, which was generally high. The NRMSE measures the absolute error of the RCM in simulating the observed climate parameters of interest. The smaller the value of the NRMSE the better the RCM simulates the observed climatology, and vice versa.

During the MAM season lower values of NRMSE are observed over most parts in Kenya especially with the MOHC, NCC, NOAA, and the ensemble showing good simulation of observed data by the models. High values of NRMSE are noted around Mt. Kilimanjaro region, the western and central (around Mt. Kenya) parts of Kenya as shown in Figure 4-9.

High NRMSE show poor simulation of observed data by the models especially the mesoscale systems around the western and central parts of Kenya.

During the OND season, higher values of NRMSE are observed compared to the MAM season. High values of NRMSE are noted around Mt. Kilimanjaro, the western and central (around Mt. Kenya) parts of Kenya, especially with the CCCma, IPSL, NCC and NOAA models as shown in Figure 4-10.

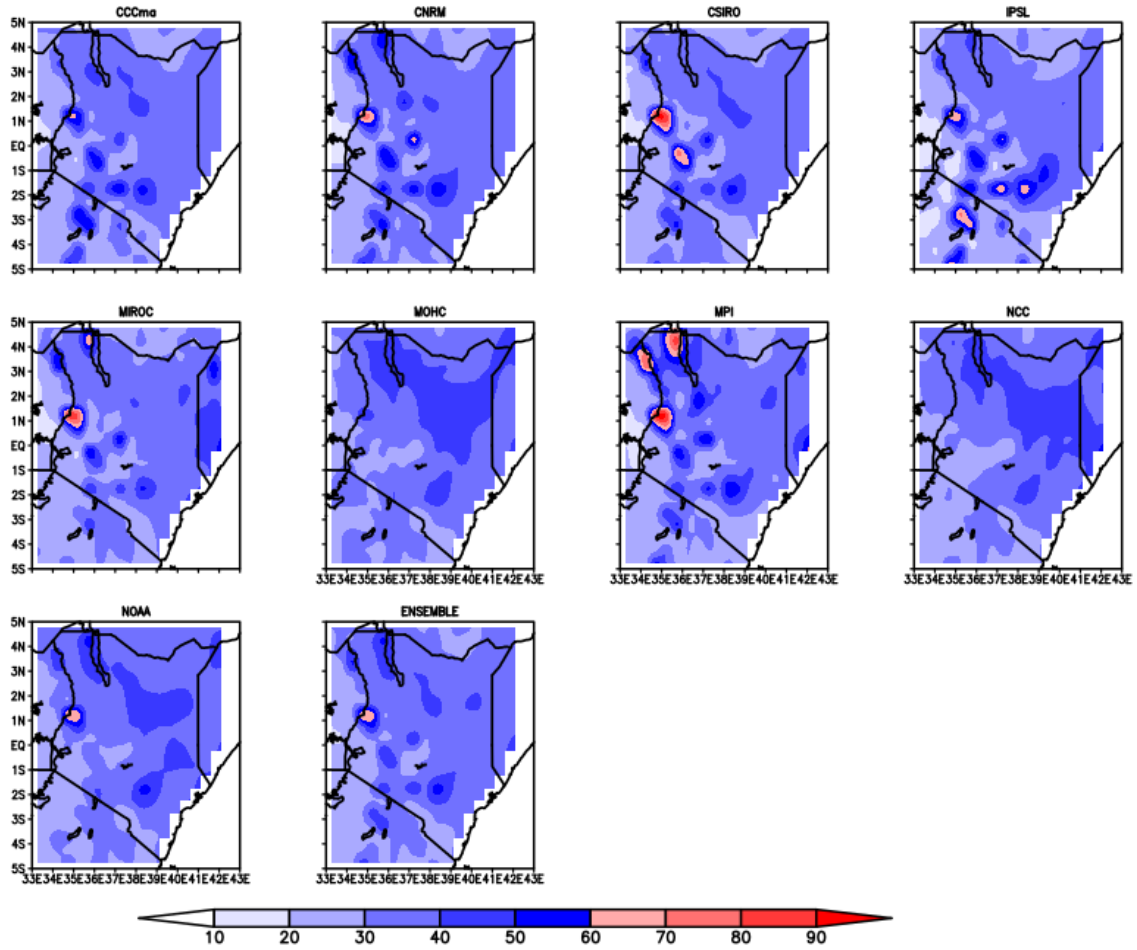

Figure 4-9: NMRSE of the average CORDEX simulated rainfall against the observed rainfall for the period 1971-2000 rainfall (in %) during the MAM season over Kenya. Shades of red indicate large error while shades of blue indicate small error.

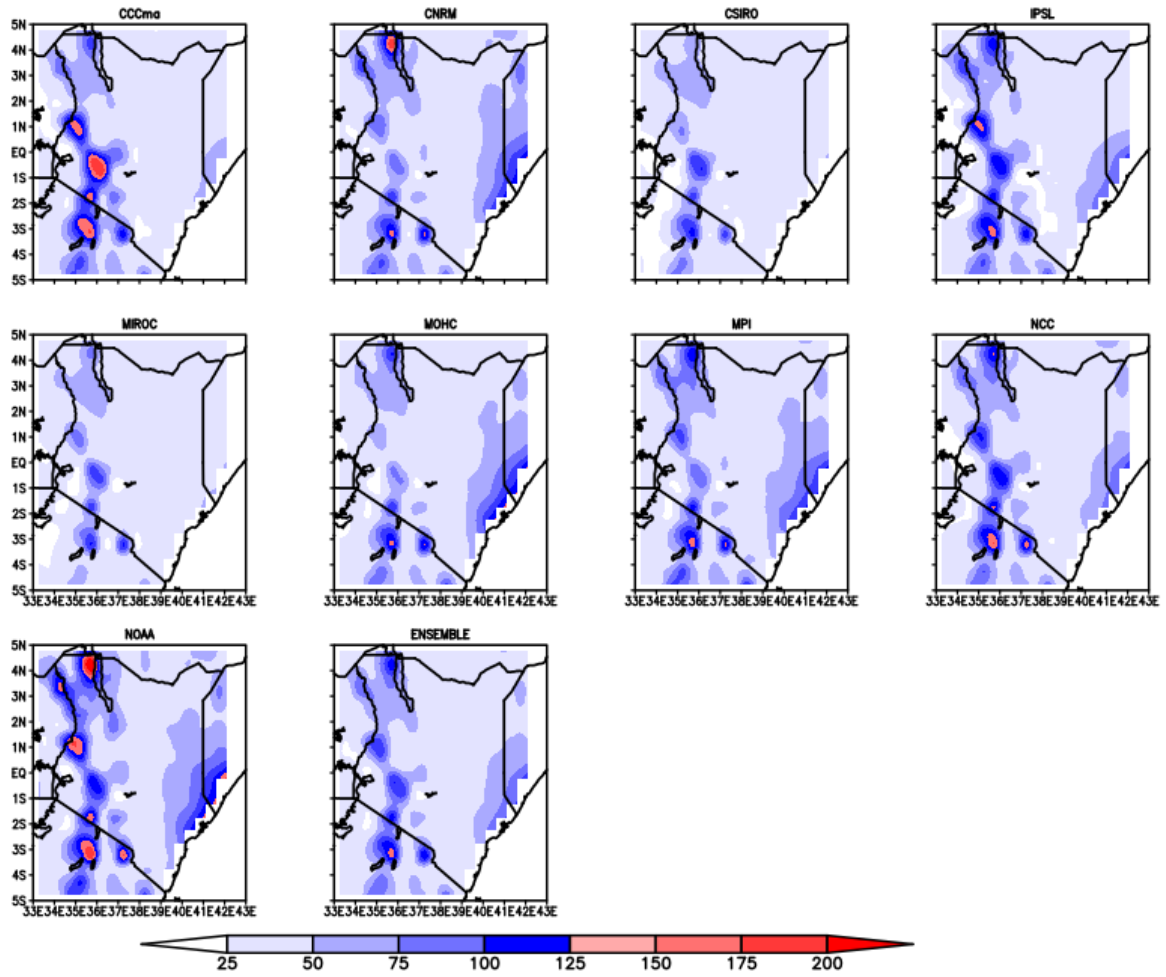

Figure 4-10: NMRSE of the average CORDEX simulated rainfall against the observed rainfall for the period 1971-2000 rainfall (in %) during the OND season over Kenya. Shades of red indicate large error while shades of blue indicate small error.

4.2.2.4 Bias-corrected Rainfall Climatology in Kenya

This section presents results on reduction of bias between the observed rainfall dataset and the ensemble of the CORDEX models. The rainfall ensemble, despite performing better than the individual CORDEX models, still showed notable biases. This necessitated bias correction to better simulate the observed rainfall before studying the temporal and spatial variability of rainfall and green gram crop modelling under present and future climate conditions. Figure 4-11 illustrates the average bias in rainfall after reducing bias using the scaling method for the MAM and OND seasons. Figure 4-12 presents the average NRMSE in rainfall after reducing bias during the MAM and OND seasons. The error in the rainfall ensemble is reduced as shown by lower values of bias (Figure 4-11) and NRMSE (Figure 4-12).

The bias corrected ensemble during the MAM (Figure 4-13) and OND (Figure 4-14) season shows improvement after being adjusted using the scaling method. Bias correction is able to reduce the disagreement between the observed dataset and the ensemble of the CORDEX models' dataset. Other studies have shown the importance of performing bias correction before using the data for climate impact studies (Ezéchiel *et al.*, 2016; Akhter *et al.*, 2017; Mutayoba and Kashaigili, 2017; Ayugi *et al.*, 2020).

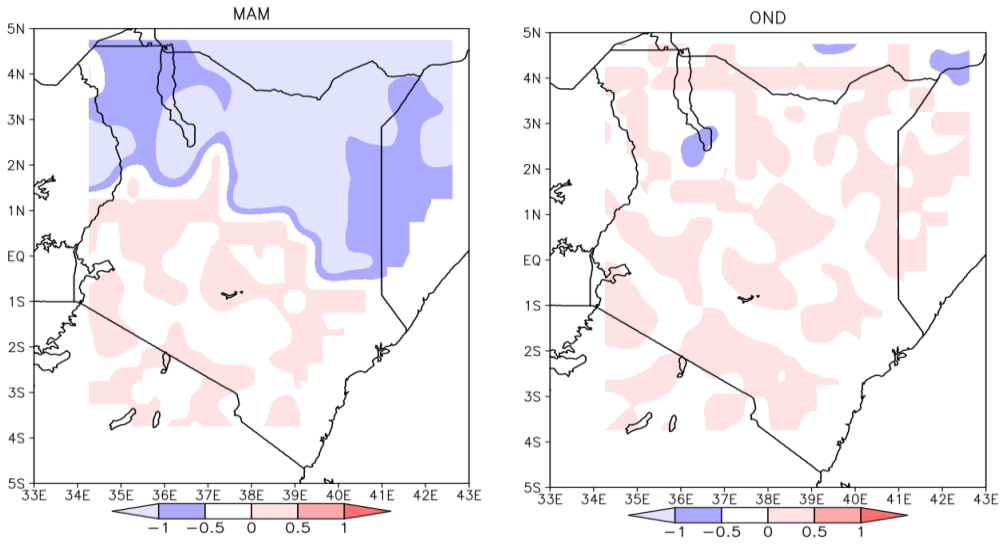

Figure 4-11: Deviation of the average bias corrected ensemble of simulated rainfall (mm) against the observed rainfall for the period 1971-2000 during the MAM and OND seasons over Kenya. Shades of red indicate overestimation while shades of blue indicate underestimation

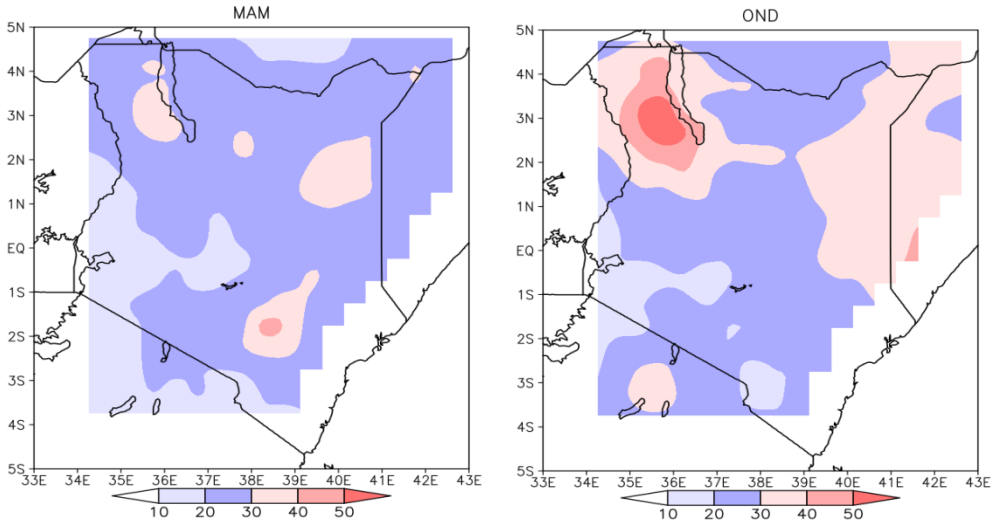

Figure 4-12: NMRSE of the average CORDEX simulated rainfall against the observed rainfall (mm) for the period 1971-2000 rainfall during the MAM and OND seasons over Kenya. Shades of red indicate large error while shades of blue indicate small error.

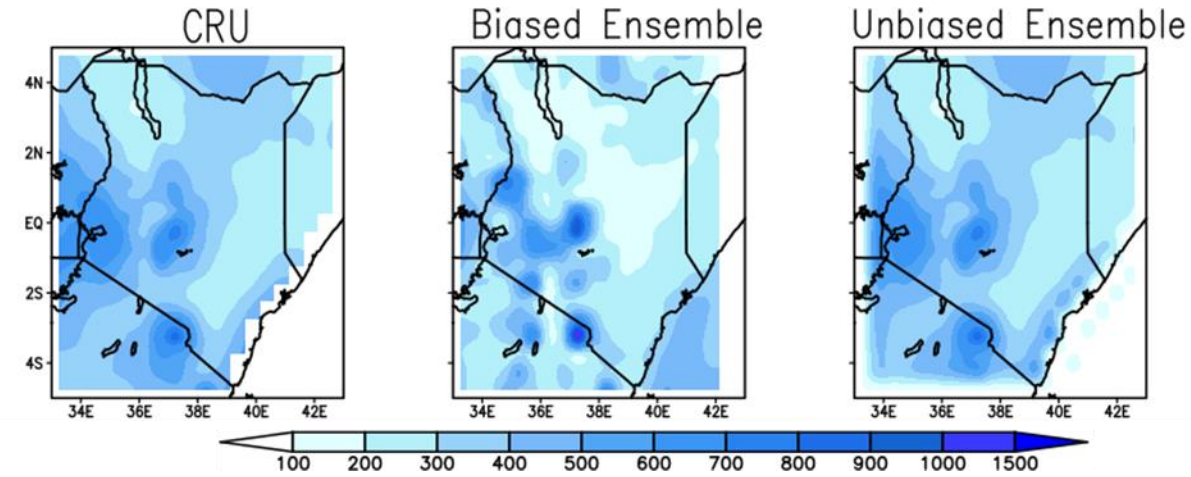

Figure 4-13: Performance of the CORDEX bias corrected ensemble in simulating the observed MAM rainfall total (in mm) over Kenya for 1971-2000. Rainfall amount increases from the white shaded areas through to the blue shaded areas

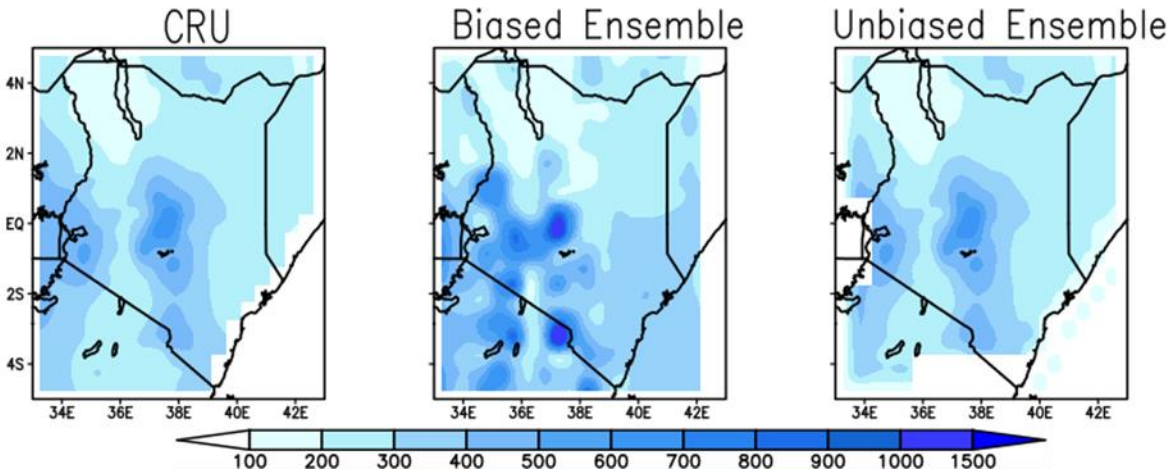

Figure 4-14: Performance of the CORDEX bias corrected ensemble in simulating the observed OND rainfall total (in mm) over Kenya for 1971-2000. Rainfall amount increases from the white shaded areas through to the blue shaded areas

4.2.3 Performance of the CORDEX RCA4 Models in Simulating the Spatial Climatology of Minimum Temperature in Kenya

This subsection presents results on observed and simulated climatology of minimum temperature during the MAM and OND seasons.

4.2.3.1 Climatology of Observed and Simulated Minimum Temperature over Kenya

The spatial distributions of the climatology of the observed minimum temperature for the MAM and OND seasons are represented in Figures 4-15 and 4-16, respectively.

The lowest temperature of the day is recorded early in the morning just before sunrise. The cooling of the atmosphere is cumulative and during the day the sun warms the earth's surface. Once the sun sets, the earth begins to cool off by radiating infra-red radiation into space. The air near the earth's surface becomes progressively cooler during the night until the early morning hours around sunrise when the sun begins to warm the earth once more.

During the MAM and OND seasons, all the models and their ensembles capture the observed pattern of the spatial distribution of temperature as illustrated in Figure 4-15 and Figure 4-16, respectively. Other studies have also shown that models are able to simulate temperature fairly well (Opijah *et al.*, 2017; Mukhala *et al.*, 2017; Warnatzsch and Reay, 2019).

Low values of minimum temperature are observed in central and western parts of Kenya which are the highland zones. High values of minimum temperature values are observed in the eastern and northern parts of Kenya which are the low lying areas. Temperature decreases

with altitude such that low altitude areas (eastern and northern Kenya) experience higher temperature than in the higher altitudes (western and central Kenya) which experience lower temperature. At higher altitude, the density of air is lower. Therefore, there are less greenhouse gases in the air. The high altitude areas, thus, lose more heat during the night when the earth cools off by radiating infra-red radiation into space leading to lower minimum temperatures being recorded. At lower altitudes the denser atmosphere absorbs the outgoing long wave radiation and re-directs it back leading to higher values of minimum temperature being recorded.

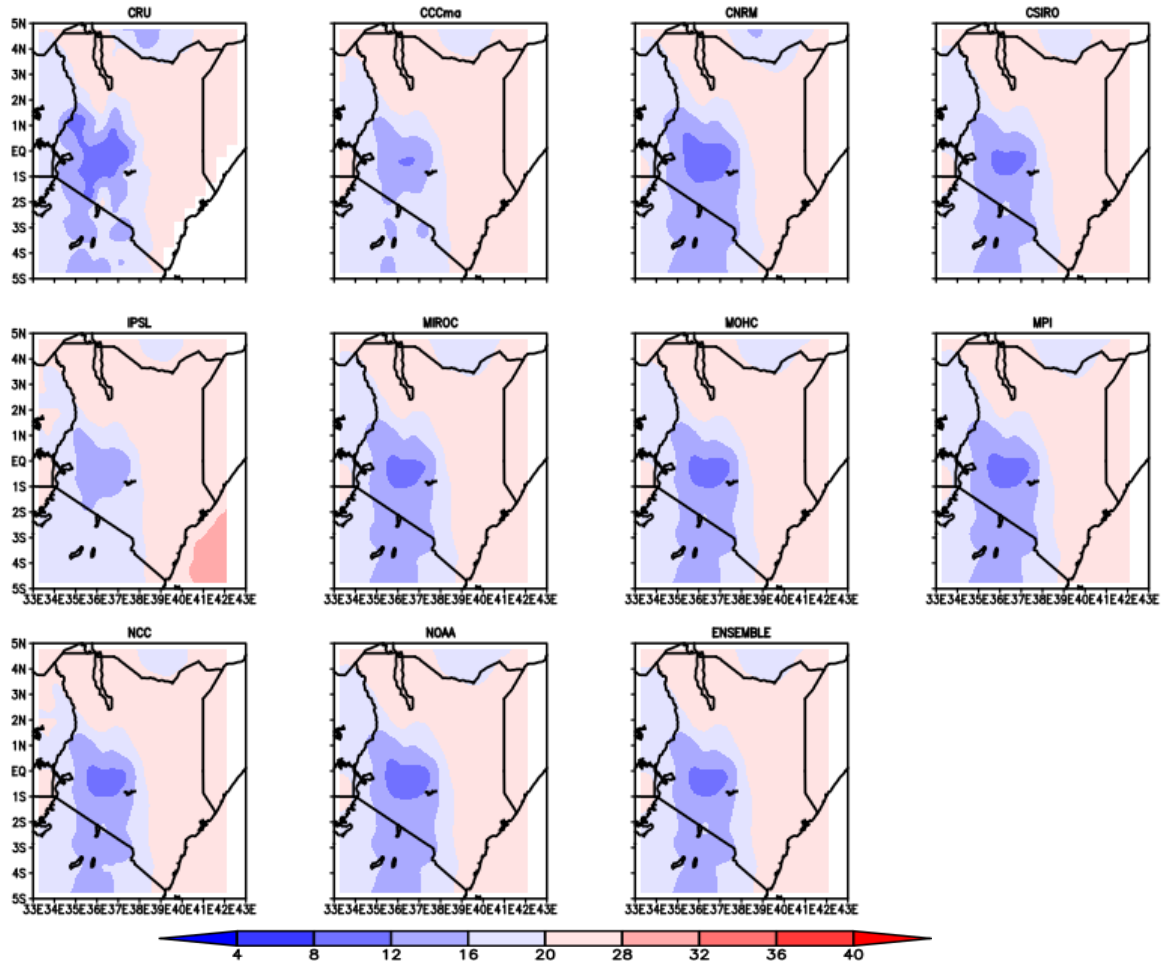

Figure 4-15: Performance of CORDEX models in simulating the observed mean minimum temperature in the MAM season (°C) during 1971-2000 over Kenya. The temperature increases from the blue shades through to the red shades

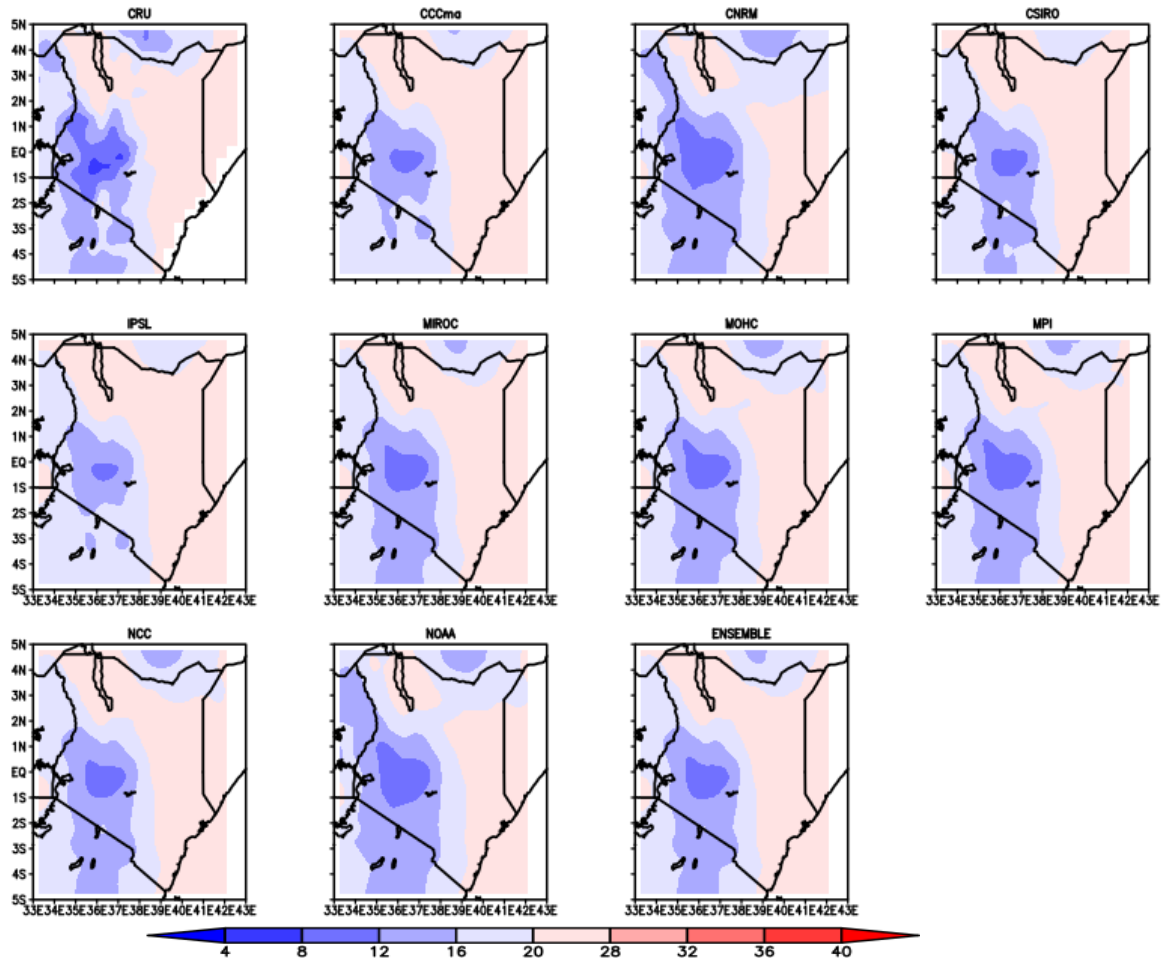

Figure 4-16: Performance of CORDEX models in simulating the observed mean minimum temperature in the OND season (in °C) during 1971-2000 over Kenya. The temperature increases from the blue shades through to the red shades

4.2.3.2 Bias of Minimum Temperature in the Simulated Dataset

This section presents the spatial distribution of the mean bias between the simulated minimum temperature data against the observed data for the period between 1971 and 2000. Figure 4-17 and 4-18 present the average bias during the MAM and OND seasons, respectively. Generally the CORDEX models and their ensemble are a good representation of the observed minimum temperature since they show low levels of bias during the MAM and OND seasons.

During the MAM season, some models, especially the CCCma, CSIRO, IPSL and NCC models, overestimate the minimum temperature in the western, north western, northern and central parts of the country. Negative values of bias are observed around Mount Kenya and Mount Kilimajaro region especially by the CNRM, MIROC, MPI, and NOAA models as

shown in Figure 4-17. The models, thus, do not properly capture the effect of altitude, radiation loss and atmosphere density on minimum temperature.

During the OND rainfall season, some models, especially the CCCma, CSIRO and IPSL, overestimate the minimum temperature in the western, north western, northern and central parts of the country. The underestimation of minimum temperature is most notable in the CNRM and NOAA models where the underestimation is in most parts of Kenya as shown in Figure 4-18. The model ensemble generally shows lower values of bias compared to the rest due its ability to smooth over the individual biases of each model. Minimum temperature is dependent on altitude which affects cloud cover and radiation loss from the earth during the night.

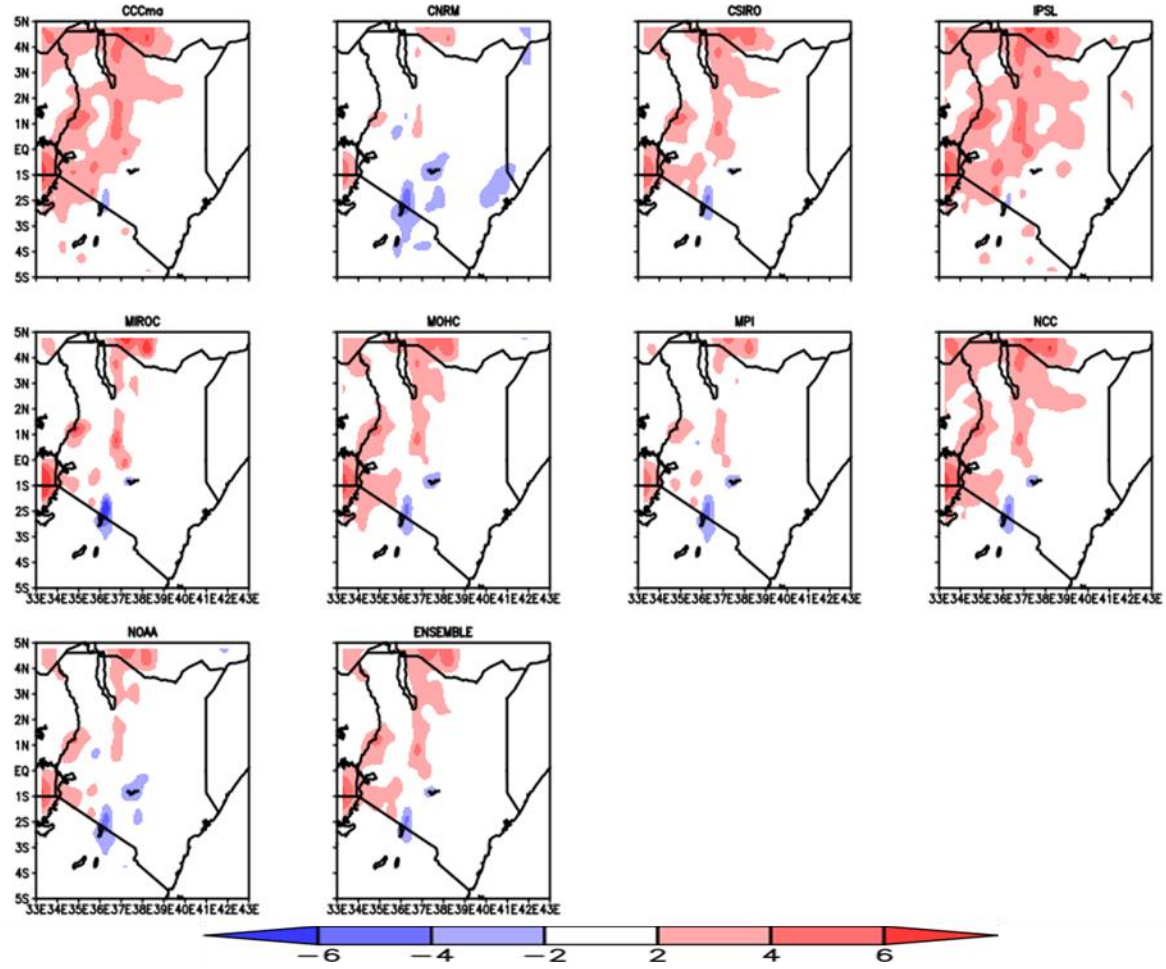

Figure 4-17: Bias of the average CORDEX simulated minimum temperature (in°C) against the observed minimum temperature from 1971 to 2000 during the MAM season over Kenya. Shades of red indicate overestimation while shades of blue indicate underestimation

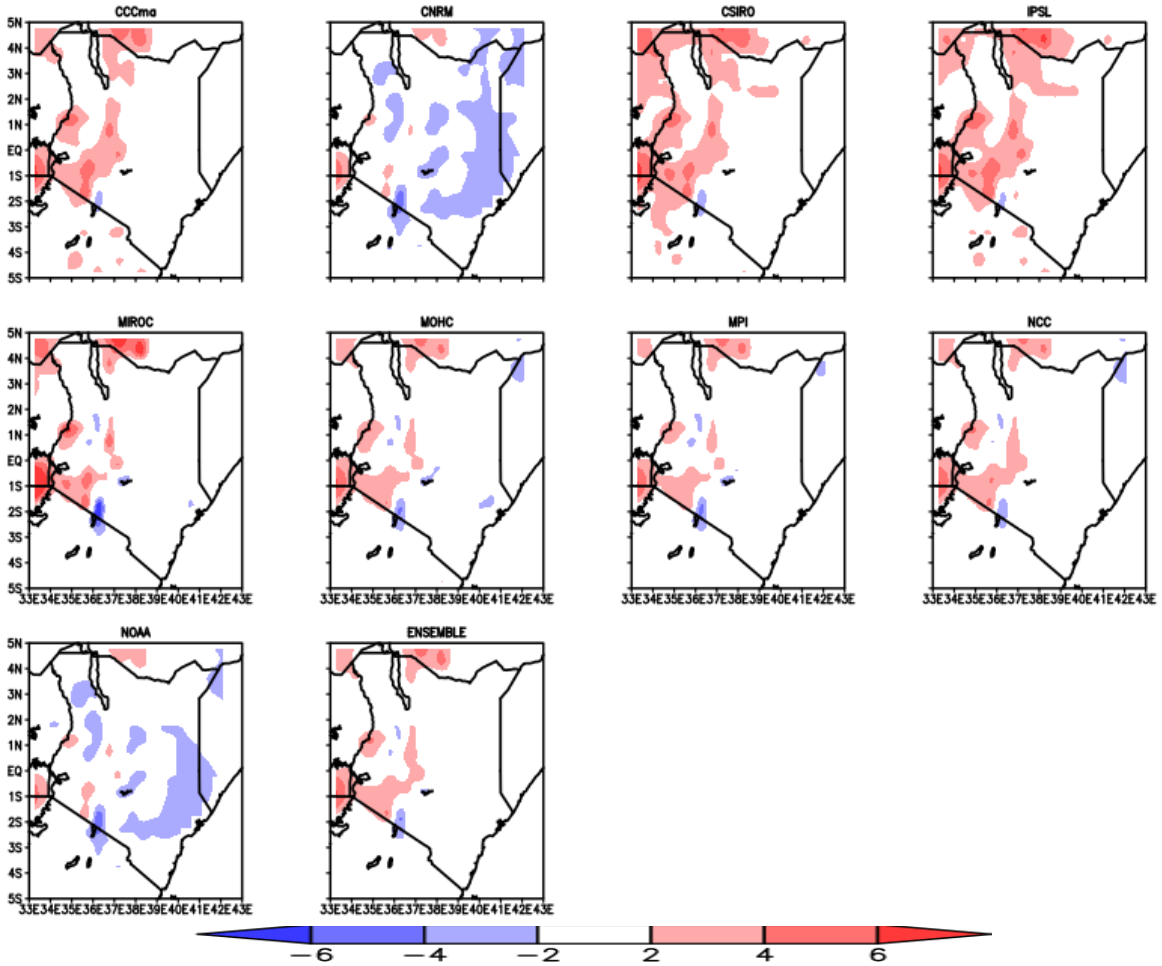

Figure 4-18: Bias of the average CORDEX simulated minimum temperature (in°C) against the observed minimum temperature from 1971 to 2000 during the OND season over Kenya. Shades of red indicate overestimation while shades of blue indicate underestimation

4.2.3.3 Normalised Root Mean Square Error in the Simulated Minimum Temperature Datasets

The spatial distribution of the average NRMSE in the simulated minimum temperature values against the observed minimum temperature values for the period 1971-2000 are presented in this section. Figure 4-19 and 4-20 depict the average NRMSE during the MAM and OND seasons respectively. The NRMSE measures the absolute error of the RCM in simulating the observed climate parameters of interest. The smaller the value of the NRMSE the better the RCM simulates the observed climatology, and vice versa.

During the MAM season higher values of NRMSE are observed in the central and western regions of the country. Lower values of NRMSE are observed in the southern and eastern

region of the Country indicating that the models and their ensemble are able to simulate the minimum temperature patterns in the low lying areas with more accuracy as shown in Figure 4-19.

During the OND season higher values of NRMSE are observed in the northern and western region of the country. Lower values of the NRMSE are observed in the southern and eastern region of the Country indicating that the models and their ensemble are able to simulate the minimum temperature patterns with more accuracy as shown in Figure 4-20.

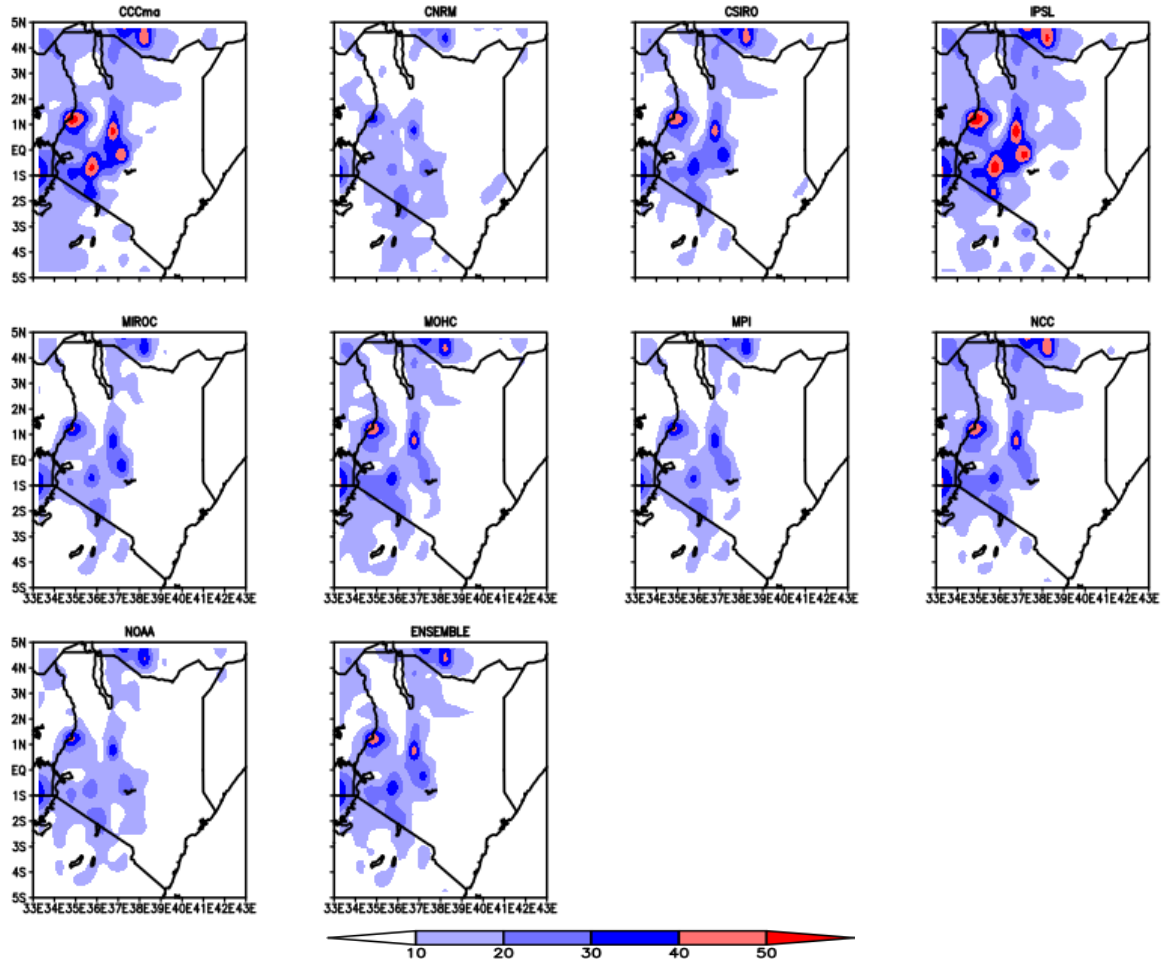

Figure 4-19: NRMSE of the average CORDEX simulated minimum temperature against the observed minimum temperature for the period 1971-2000 minimum temperature (in %) during the MAM season over Kenya. Shades of red indicate large error while shades of blue indicate small error.

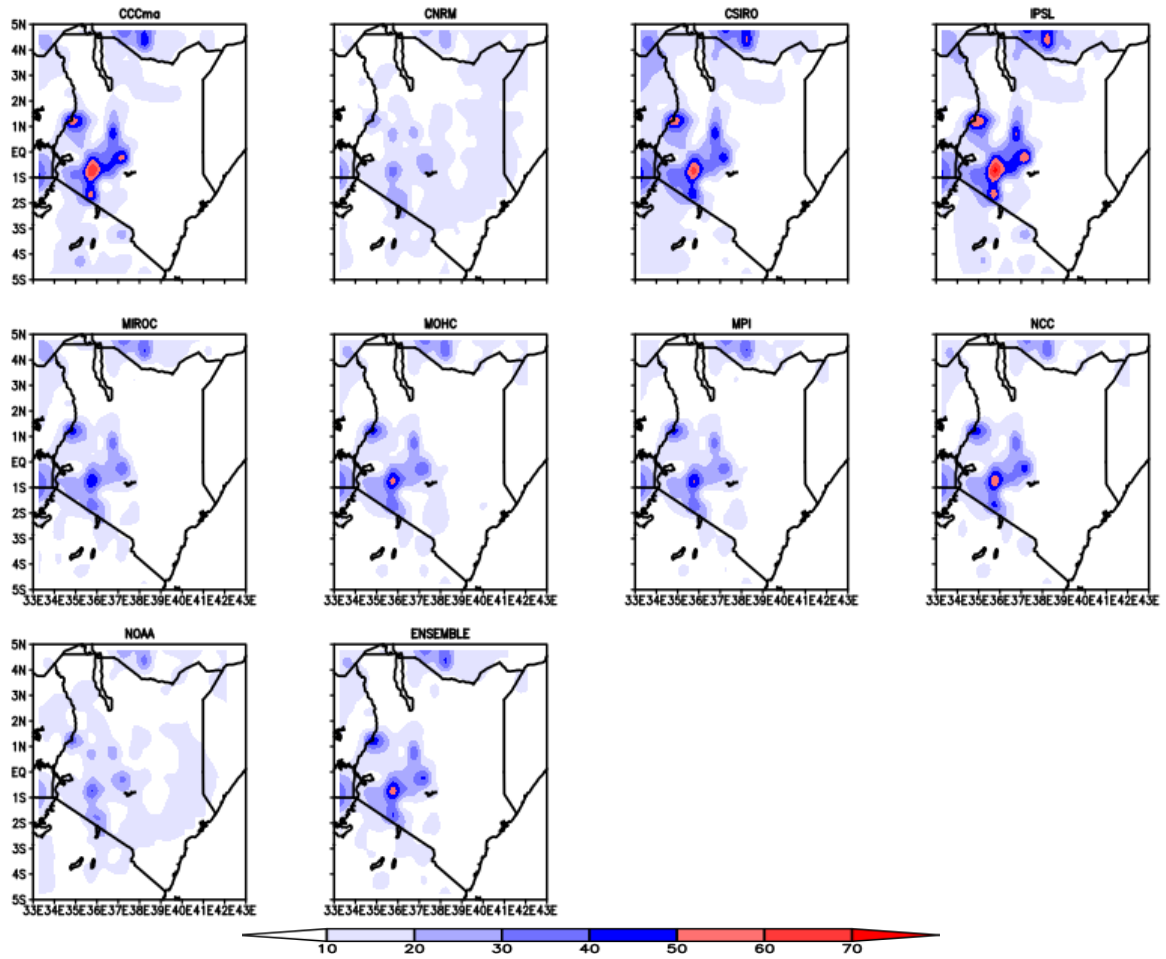

Figure 4-20: NRMSE of the average CORDEX simulated minimum temperature against the observed minimum temperature for the period 1971-2000 minimum temperature (in %) during the OND season over Kenya. Shades of red indicate large error while shades of blue indicate small error.

4.2.4 Performance of the CORDEX RCA4 Models in Simulating the Spatial Climatology of Maximum Temperature in Kenya

This subsection presents results on observed and simulated climatology of maximum temperature during the MAM and OND seasons.

4.2.4.1 Climatology of Observed and Simulated Maximum Temperature over Kenya

The spatial distribution of the climatology of the observed maximum temperature for the MAM and OND seasons are displayed in Figures 4-21 and 4-22 respectively.

The maximum temperature of the day is recorded in the afternoon three to four hours before sunset. The earth's surface becomes progressively warmer as the sun heats the earth reaching its maximum temperature a few hours before sunset. The maximum temperature of the day is

determined by the amount of reflected heat, in the form of long-wave radiation, trapped in the atmosphere.

In Figure 4-21, all the models and their ensemble can simulate the observed spatial distribution of maximum temperature during the MAM season reasonably well. Low maximum temperatures are observed in the high ground areas including the central parts of Kenya, and the highlands west of the Rift Valley. High values of maximum temperature are mainly concentrated in the north-eastern and north-western regions of Kenya which are the low-lying areas. Temperature decreases with altitude such that low altitude areas (north-western, north-eastern, eastern and coastal Kenya) experience higher temperature than the higher altitude areas (western and central Kenya) which experience lower temperature. Maximum temperature is affected by altitude due to air density and the balance between incoming solar radiation and outgoing terrestrial radiation. Low altitude areas have a higher concentration of air leading to more absorption of heat and in turn higher records of maximum temperature. The spatial distribution of maximum mean temperature during OND generally follows that of the MAM season as shown in Figure 4-22.

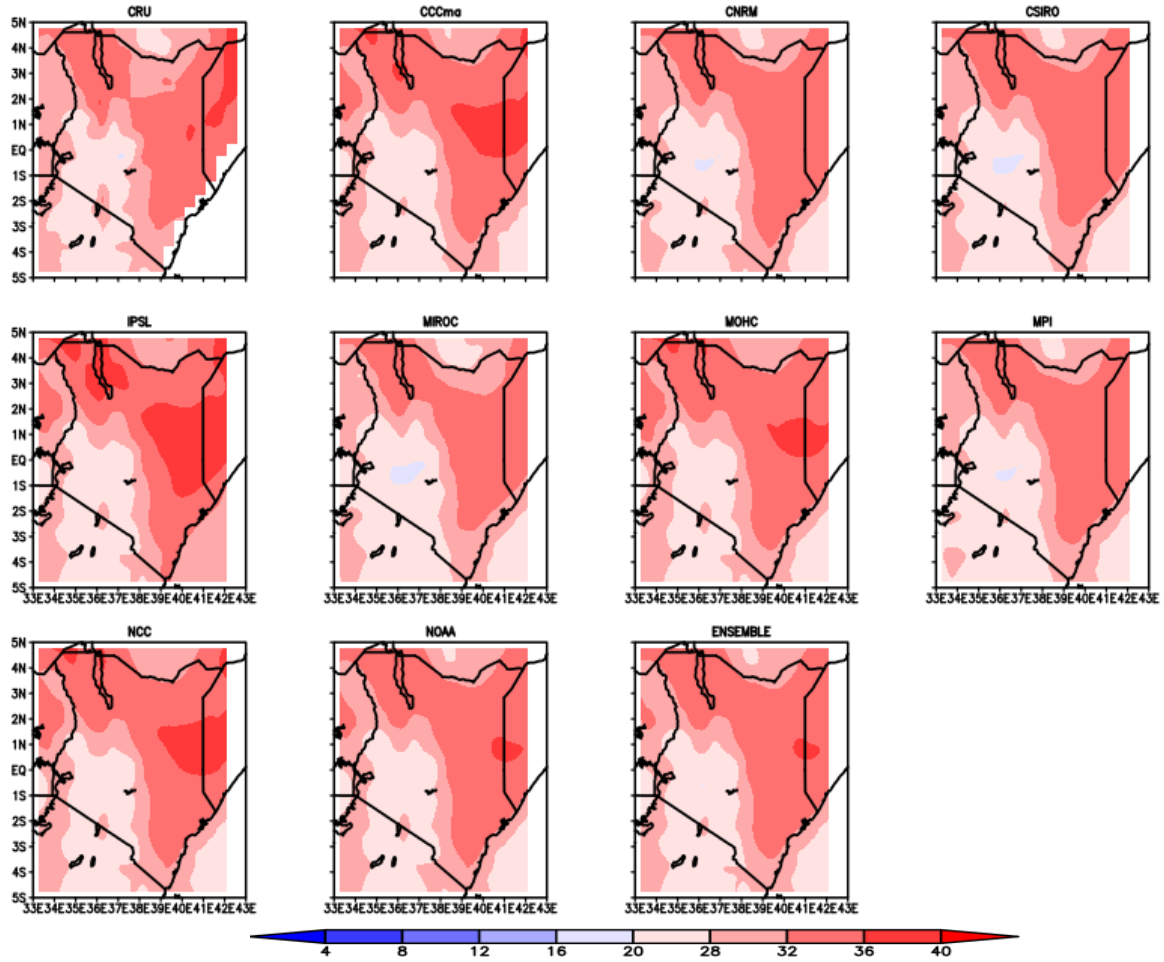

Figure 4-21: Performance of CORDEX RCA4 models in replicating the observed maximum mean temperature in the MAM season (in °C) during 1971-2000 over Kenya. The temperature increases from the blue shades through to the red shades

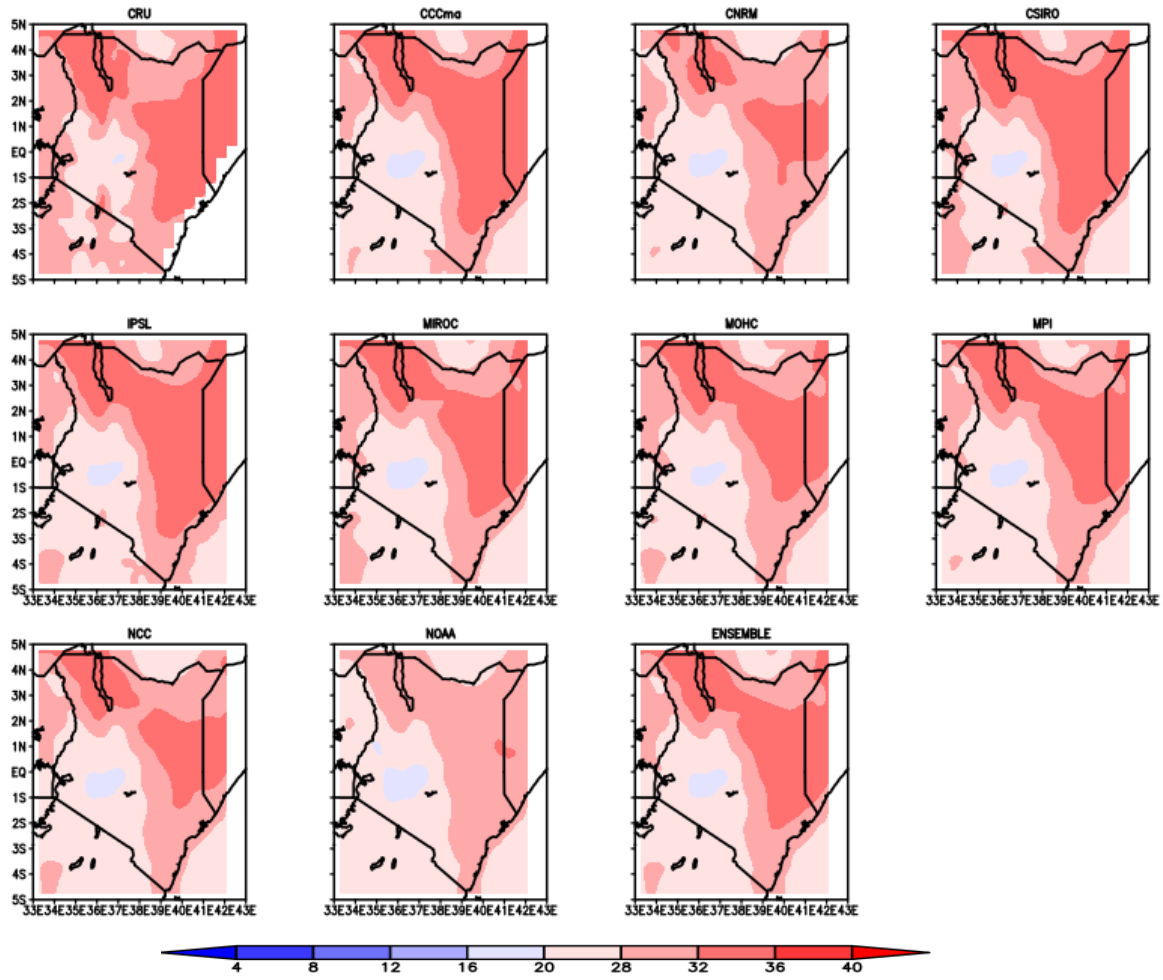

Figure 4-22: Performance of CORDEX RCA4 models in replicating the observed maximum mean temperature in the OND season (°C) during 1971-2000 over Kenya. The temperature increases from the blue shades through to the red shades

4.2.4.2 Maximum Temperature Bias in the Simulated Datasets

This section presents the spatial distribution of the mean bias between the simulated maximum temperature data against the observed data from 1971 to 2000. Figure 4-23 and 4-24 display the average bias during the MAM and OND seasons, respectively. Generally the CORDEX models and their ensemble show low levels of bias during the MAM and OND seasons, thus the models are a good representation of the observed maximum temperature.

In Figure 4-23, during the MAM season, underestimation of maximum temperature is noted in the western and south western regions of the country especially with the CNRM, CSIRO, MIROC and MPI models. Positive values of bias are noted in the northern region of the Country. Positive values of bias mean that the models overestimate maximum temperature in the northern parts of Kenya. Maximum temperature is affected by altitude due to air density

and the balance between incoming solar radiation and outgoing terrestrial radiation. Low altitude areas have a higher concentration of air leading to more absorption of heat and in turn higher records of maximum temperature.

In Figure 4-24, during the OND season underestimation of maximum temperature is observed in most parts of the Country by all the models, but especially in the western and south western regions. Overestimation of maximum temperature is observed over the northern part of the country by the CCCma, CSIRO and IPSL models as presented in Figure 4-24.

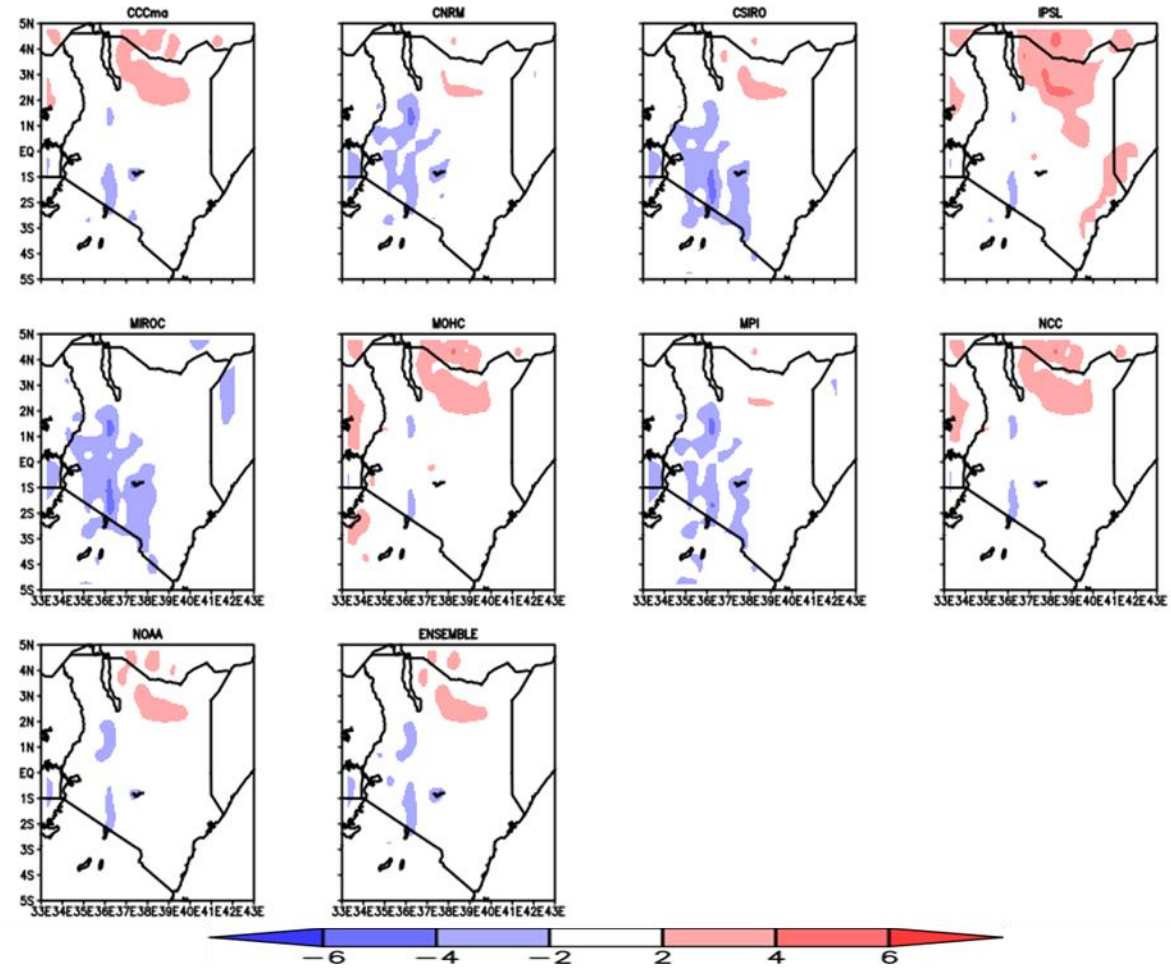

Figure 4-23: Bias of the average CORDEX simulated maximum temperature (in°C) against the observed maximum temperature from 1971 to 2000 during the MAM season over Kenya. Shades of red indicate overestimation while shades of blue indicate underestimation

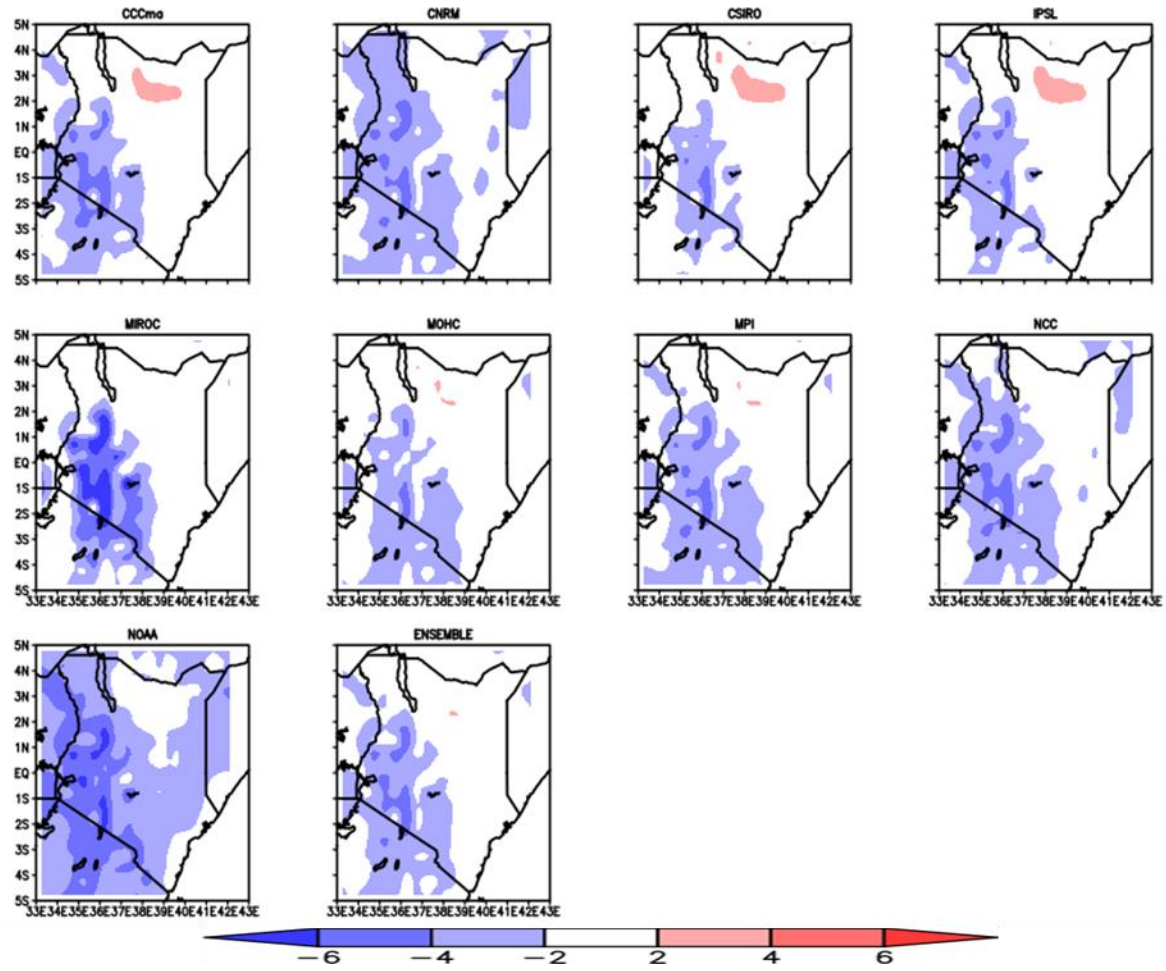

Figure 4-24: Bias of the average CORDEX simulated maximum temperature (in°C) against the observed maximum temperature from 1971 to 2000 during the OND season over Kenya. Shades of red indicate overestimation while shades of blue indicate underestimation

4.2.4.3 Normalised Root Mean Square Error in the Simulated Maximum Temperature Datasets against the Observed Maximum Temperature

The spatial distribution of the average NRMSE in the simulated maximum temperature dataset against the observed maximum temperature datasets from 1971 to 2000 are presented in this section. Figures 4-25 and 4-26 display the average NRMSE during the MAM and OND seasons, respectively. The NRMSE measures the absolute error of the RCM in simulating the observed climate parameters of interest. The smaller the value of the NRMSE the better the RCM simulates the observed climatology and vice versa.

During the MAM and OND seasons, low values of NRMSE are observed in most parts of the country. The models and their ensemble are able to simulate the observed climatology with

higher accuracy. Higher values are noted in the western and northern regions of the Country as shown in Figure 4-25 and Figure 4-26.

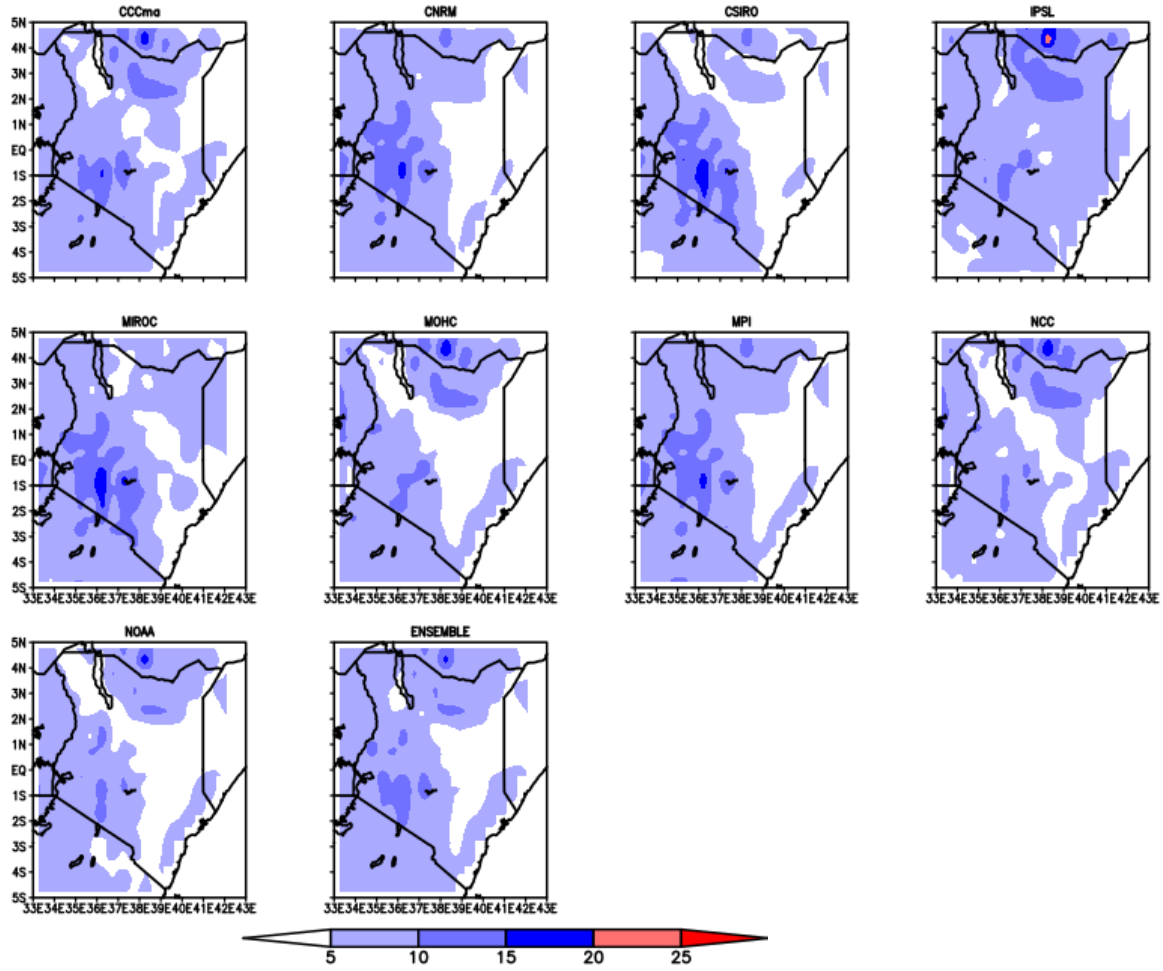

Figure 4-25: NRMSE of average (1971-2000) CORDEX simulated maximum temperature against the observed maximum temperature (%) from 1971 to 2000 during the MAM season over Kenya. Shades of red in the IPSL model indicate large error while shades of blue indicate small error.

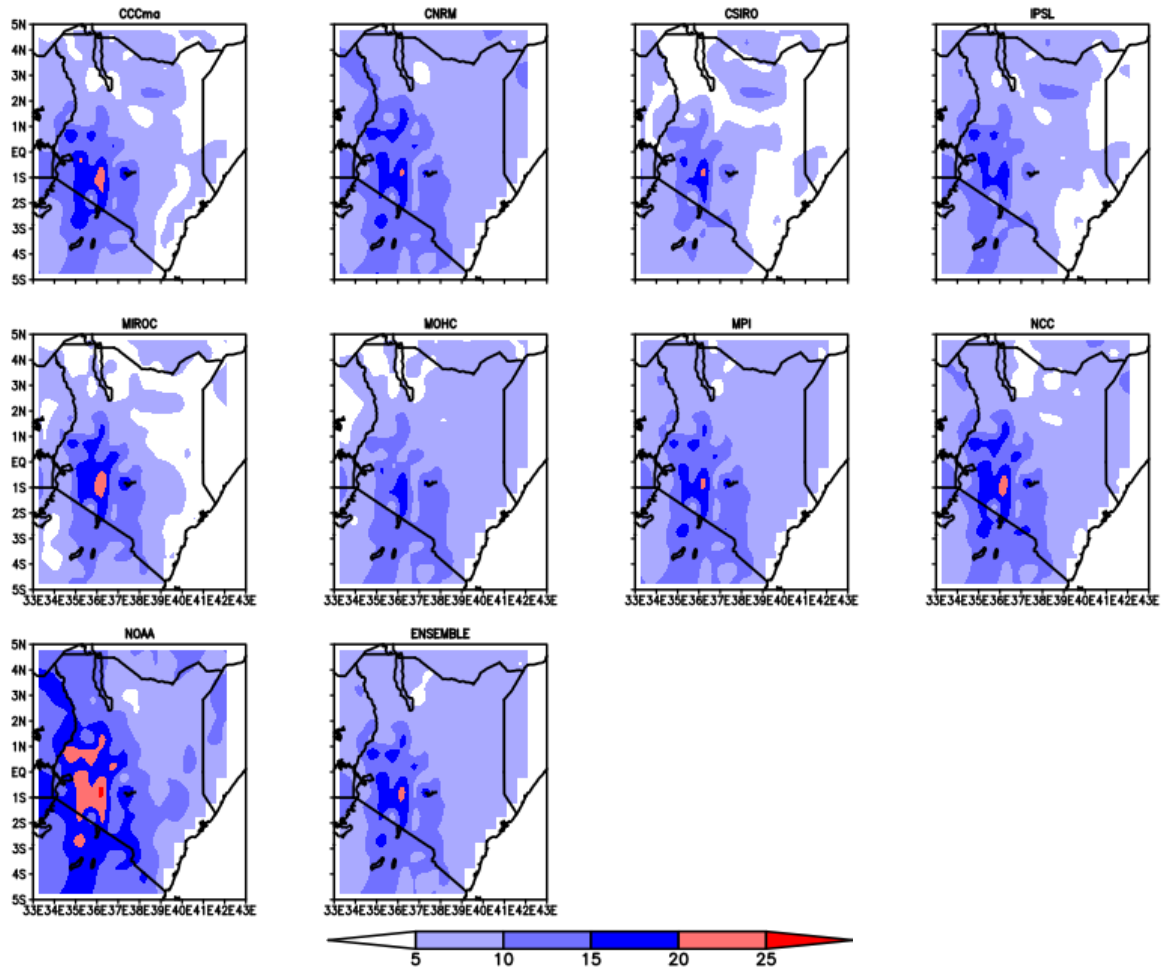

Figure 4-26: NRMSE of average (1971-2000) CORDEX simulated maximum temperature against the observed maximum temperature (%) from 1971 to 2000 during the OND season over Kenya. Shades of red indicate large error while shades of blue indicate small error.

4.2.5 Temporal Variability of Seasonal Climate in Kenya

This section presents the results of the significance of the Mann Kendall test and Sen's estimate at a significance level equalling 0.001, 0.01, 0.05, 0.1. The Sen Slope was also expressed as a percentage of the average parameter per unit time (% Δ).

4.2.5.1 Temporal Variation of Seasonal Rainfall in Kenya

This subsection presents results on the temporal variation of rainfall in Kenya during the MAM and OND season. Table 4-2 and Table 4-3 show the results of the time series of total rainfall for the baseline, RCP 4.5 and RCP 8.5 scenarios, during the MAM and OND seasons, respectively.

Under the baseline condition, the rainfall during the MAM season shows a generally increasing trend except for Voi, but statistical significance was not recorded for any of the stations; the magnitude of trend ranged between -4.4% and 26.0% (Table 4-2). The OND season showed an increasing trend in all stations, but statistical significance was not recorded in any of the stations; the magnitude of trend ranged between 4.0% and 40.4% (Table 4-3). The insignificance in trend for both seasons means we cannot decisively state that rainfall is decreasing or increasing in these regions and this could be attributed to the variable nature of the rainfall.

Under the RCP 4.5 condition, the rainfall during MAM season showed an increasing trend for most stations except Kakamega, Kisumu, Nakuru and Narok Table (4-2). Statistical positive significance was recorded for Mandera, Marsabit, Moyale, Voi, Wajir and Kitui; the magnitude of trend ranged between -8.5% and 85.1%. The OND season showed an increasing trend for all stations, for which statistical positive significance was recorded for the Kakamega and Lodwar stations; the magnitude of trend ranged between 6.4% and 51.6% (Table 4-3). This increase in rainfall can be attributed to global warming due to the projected increase in greenhouse gases, which could lead to higher temperatures and, therefore, enhanced convection near the surrounding Lakes and Indian Ocean, if conditions are favourable in terms of an unstable atmosphere, availability of condensation nuclei and a lifting mechanism rainfall could be enhanced.

Under the RCP 8.5 condition the rainfall during MAM season showed an increasing trend for most stations except Dagoretti, Nakuru, Nanyuki, Narok and Kitui. Statistical positive significance was recorded for Mandera, Marsabit, Moyale, Wajir and Lodwar; the magnitude of trend ranged between -6.4% and 52.6% (Table 4-2). The OND season showed an increasing trend all stations except Kisumu and Nakuru. Statistical positive significance was recorded for the Marsabit and Moyale stations; the magnitude of trend ranged between -5.7% and 27.5% (Table 4-3). This increase in rainfall can be attributed to global warming due to the projected increase in greenhouse gases which could lead to higher temperatures and therefore enhanced convection near the surrounding Lakes and Indian Ocean, if conditions are favourable in terms of an unstable atmosphere, availability of condensation nuclei and a lifting mechanism rainfall could be enhanced.

Other studies have found rainfall to be highly variable with the OND season exhibiting greater consistency compared to the MAM season (Liebmann *et al.*, 2014; Yang *et al.*, 2014).

Rainfall over the region is regulated by large scale systems like the ENSO circulation, which has a significant influence on rainfall during the OND season (Endris *et al*., 2013) and which is linked with wet conditions (El Niño) and dry conditions (La Niña). Moreover, the Indian Ocean Dipole (IOD) significantly influences rainfall during the OND season than the MAM seasonal (Behera et al., 2005).

Table 4-2: Time Series Analysis of Total MAM Rainfall (mm) for the Baseline, RCP 4.5 and RCP 8.5 Scenarios (Z Denotes the Mann Kendall Statistic, Sig Denotes the Level of Significance Denotes the Sen's Slope, % Δ the Percentage of the Sen's Slope over Mean Quantity per Unit Time, and NA Denotes Data that was not Available)

	Baseline				RCP 4.5				RCP 8.5			
Station	**Z**	**Sig**	**Q**	**% Δ**	**Z**	**Sig**	**Q**	**% Δ**	**Z**	**Sig**	**Q**	**% Δ**
Dagoretti	1.4		1.9	12.5	1.4		2.9	18.5	-0.8		-1.0	-6.3
Garissa	1.2		0.6	12.6	1.9	+	3.8	61.7	0.6		0.7	10.6
Kakamega	1.2		2.6	12.3	-0.1		-0.6	-2.7	0.2		0.9	3.7
Kisumu	1.0		1.7	9.4	-1.0		-4.0	-21.2	0.5		0.7	3.7
Lamu	NA	NA	NA	NA	NA	NA	NA	NA	NA	NA	NA	NA
Mandera	0.6		0.3	5.9	2.7	**	3.6	56.8	2.5	*	3.1	42.8
Marsabit	0.6		0.6	7.6	2.8	**	6.9	73.0	2.9	**	3.8	37.9
Mombasa	NA	NA	NA	NA	NA	NA	NA	NA	NA	NA	NA	NA
Moyale	0.0		0.0	0.3	2.8	**	3.8	37.2	2.9	**	3.8	35.3
Nakuru	0.2		0.3	2.7	-0.6		-1.0	-10.3	0.0		0.0	-0.3
Nanyuki	0.4		0.5	3.9	1.9	+	2.8	21.8	-1.0		-0.8	-6.0
Narok	1.0		1.7	14.7	-0.4		-1.0	-8.5	-0.7		-0.8	-6.4
Voi	-0.6		-0.3	-4.4	2.1	*	3.2	38.4	-0.2		-0.2	-2.5
Wajir	1.8	+	1.5	26.0	3.9	***	5.9	85.1	2.0	*	1.7	23.4
Lodwar	0.9		0.5	16.0	1.7	+	2.4	55.2	2.1	*	2.4	52.6
Kitui	1.4		1.6	14.2	2.5	*	5.7	46.4	-0.7		-0.8	-5.9

Key: *** represents significance in trend at $\alpha = 0.001$, ** represent significance in trend at $\alpha = 0.01$, * represents significance in trend at $\alpha = 0.05$, + represents significance in trend at $\alpha = 0.1$, a blank cell means the significance level greater than 10%

Table 4-3: Time Series Analysis of Total OND Rainfall (mm) for the Baseline, RCP 4.5 and RCP 8.5 Scenarios (Z Denotes the Mann Kendall Statistic, Sig Denotes the Level of Significance Denotes the Sen's Slope, % Δ the Percentage of the Sen's Slope over Mean Quantity per Unit Time, and NA Denotes Data that was not Available)

	Baseline				RCP 4.5				RCP 8.5			
Station	**Z**	**Sig**	**Q**	**% Δ**	**Z**	**Sig**	**Q**	**% Δ**	**Z**	**Sig**	**Q**	**% Δ**
Dagoretti	0.4		0.4	4.0	1.9	+	1.7	16.9	1.0		0.8	8.3
Garissa	1.4		0.5	9.3	1.7	+	1.9	26.4	0.9		1.0	13.8
Kakamega	1.0		2.0	16.5	2.1	*	3.5	24.9	0.5		0.9	6.3
Kisumu	1.1		1.6	15.5	1.3		2.0	17.6	-0.3		-0.6	-5.7
Lamu	NA	NA	NA	NA	NA	NA	NA	NA	NA	NA	NA	NA

	Baseline				RCP 4.5				RCP 8.5			
Station	**Z**	**Sig**	**Q**	**% Δ**	**Z**	**Sig**	**Q**	**% Δ**	**Z**	**Sig**	**Q**	**% Δ**
Mandera	1.2		0.5	11.6	1.4		1.3	27.3	1.8	+	1.4	25.8
Marsabit	0.5		0.5	8.5	1.8	+	2.0	26.8	2.3	*	2.2	27.5
Mombasa	NA	NA	NA	NA	NA	NA	NA	NA	NA	NA	NA	NA
Moyale	0.8		0.5	8.6	0.9		1.3	17.2	2.2	*	2.1	27.5
Nakuru	0.9		0.4	6.1	1.0		0.4	6.4	-0.4		-0.1	-1.2
Nanyuki	1.2		1.0	6.6	1.3		1.5	9.8	0.9		0.6	3.7
Narok	0.4		0.2	4.1	1.3		0.8	13.2	0.0		0.0	0.5
Voi	0.5		0.2	2.6	1.6		1.7	17.6	1.1		1.1	10.8
Wajir	1.6		0.8	18.5	1.8	+	1.7	30.5	1.8	+	1.4	24.3
Lodwar	1.4		0.6	40.4	2.2	*	0.9	51.6	1.0		0.5	24.5
Kitui	1.0		0.8	6.0	1.6		2.2	13.7	1.1		1.7	10.0

Key: *** represents significance in trend at α = 0.001, ** represent significance in trend at α = 0.01, * represents significance in trend at α = 0.05, + represents significance in trend at α = 0.1, a blank cell means the significance level greater than 10%

4.2.5.2 Temporal Variation of Seasonal Maximum Temperature

This subsection presents results on the temporal variation of maximum temperature in Kenya during the MAM and OND seasons. Table 4-4 and Table 4-5 show the results of the time series of maximum temperature for the baseline, RCP 4.5 and RCP 8.5 scenarios, during the MAM and OND seasons, respectively.

Under the baseline condition the maximum temperature during MAM season shows an increasing trend for all stations (Table 4-4). Statistical significance was recorded for most of the stations except for Kakamega and Kisumu; the magnitude of trend ranged between 1.1% and 2.9%. The increase in maximum temperature during the MAM season was attributed to global warming owing to increased anthropogenic greenhouse gas emissions. The OND season showed a decreasing trend for all stations, statistical negative significance was recorded for the Garissa, Lamu, Mandera, Marsabit, Mombasa, Moyale, Voi, Wajir and Lodwar stations; the magnitude of trend ranged between -2.8% and -0.9% (Table 4-5).

Under the RCP 4.5 condition, the maximum temperature during MAM season showed an increasing trend in all stations, statistical positive significance was recorded for all stations; the magnitude of trend ranged between 1.3% and 3.8% (Table 4-4). The increase in maximum temperature during the MAM season was attributed to global warming owing to increased anthropogenic greenhouse gas emissions. The OND season showed a decreasing trend for most stations except Kakamega, Kisumu, Mandera, Nakuru, Nanyuki and Lodwar

stations, statistical significance was recorded for the Mandera and Voi stations; the magnitude of trend ranged between -2.2% and 2.4% (Table 4-5).

Under the RCP 8.5 condition the maximum temperature during the MAM season showed an increasing trend in all stations, statistical positive significance was recorded in all stations; the magnitude of trend ranged between 3.2% and 5.3% (Table 4-4). The OND season showed a positive trend in most stations except the Garissa, Lamu, Moyale, Voi and Wajir stations; statistical significance was recorded in the Lamu, Mombasa, Nakuru, Nanyuki and Narok stations; the magnitude of trend ranged between -1.0% and 2.6% (Table 4-5). The increase in maximum temperature during the MAM season was attributed to global warming owing to increased anthropogenic greenhouse gas emissions.

Table 4-4: Time Series Analysis of Mean MAM Maximum Temperature (in °C) of the Baseline, RCP 4.5 and RCP 8.5 Scenarios (Z Denotes the Mann Kendall Statistic, Sig Denotes the Level of Significance; Q Denotes the Sen's Slope and % Δ Percentage of the Sen's Slope over Mean Quantity per Unit Time)

	Baseline				RCP 4.5				RCP 8.5			
Station	**Z**	**Sig**	**Q**	**% Δ**	**Z**	**Sig**	**Q**	**% Δ**	**Z**	**Sig**	**Q**	**% Δ**
Dagoretti	3.2	**	0.0	2.3	4.9	***	0.0	2.8	5.3	***	0.0	5.3
Garissa	3.1	**	0.0	1.9	3.5	***	0.0	1.3	5.2	***	0.0	3.6
Kakamega	1.5		0.0	1.3	5.3	***	0.0	2.8	5.1	***	0.0	3.4
Kisumu	1.2		0.0	1.1	5.5	***	0.0	2.9	5.0	***	0.0	3.4
Lamu	4.6	***	0.0	2.8	4.3	***	0.0	1.6	5.5	***	0.1	4.6
Mandera	4.1	***	0.0	1.9	5.1	***	0.0	1.8	5.7	***	0.0	3.6
Marsabit	3.1	**	0.0	2.1	4.8	***	0.0	1.6	5.1	***	0.0	3.2
Mombasa	4.5	***	0.0	2.7	4.9	***	0.0	1.8	5.7	***	0.0	4.2
Moyale	4.5	***	0.0	2.9	4.9	***	0.0	1.8	5.1	***	0.0	3.8
Nakuru	2.8	**	0.0	2.7	5.4	***	0.0	3.8	5.4	***	0.0	5.1
Nanyuki	2.8	**	0.0	2.2	5.3	***	0.0	3.1	5.6	***	0.0	4.2
Narok	2.4	*	0.0	2.1	5.2	***	0.0	3.2	5.1	***	0.0	5.3
Voi	3.4	***	0.0	2.6	3.1	**	0.0	1.4	5.0	***	0.1	4.2
Wajir	3.8	***	0.0	2.1	4.4	***	0.0	1.5	5.4	***	0.0	3.6
Lodwar	3.8	***	0.0	1.9	5.3	***	0.0	1.9	5.6	***	0.0	3.6
Kitui	2.0	*	0.0	1.8	4.4	***	0.0	2.1	4.6	***	0.0	4.1

Key: *** represents significance in trend at $\alpha = 0.001$, ** represents significance in trend at $\alpha = 0.01$, * represents significance in trend at $\alpha = 0.05$, + represents significance in trend at $\alpha = 0.1$, a blank cell means the significance level greater than 10%

Table 4-5: Time Series Analysis of Mean OND Maximum Temperature (in °C) of the Baseline, RCP 4.5 and RCP 8.5 Scenarios (Z Denotes the Mann Kendall Statistic, Sig Denotes the Level of Significance; Q Denotes the Sen's Slope and % Δ Percentage of the Sen's Slope over Mean Quantity per Unit Time)

	Baseline				RCP 4.5				RCP 8.5			
Station	**Z**	**Sig**	**Q**	**% Δ**	**Z**	**Sig**	**Q**	**% Δ**	**Z**	**Sig**	**Q**	**% Δ**
Dagoretti	-1.8	+	0.0	-1.9	-1.3		0.0	-1.2	0.8		0.0	0.6
Garissa	-3.5	***	0.0	-2.0	-1.5		0.0	-1.4	-0.8		0.0	-0.4
Kakamega	-1.1		0.0	-1.3	0.4		0.0	0.4	1.4		0.0	1.1
Kisumu	-1.0		0.0	-1.0	0.8		0.0	0.7	1.8	+	0.0	1.4
Lamu	-4.2	***	0.0	-2.8	-1.9	+	0.0	-1.3	-2.1	*	0.0	-1.0
Mandera	-2.5	*	0.0	-1.1	2.4	*	0.0	1.3	1.1		0.0	0.9
Marsabit	-2.6	**	0.0	-1.3	-0.5		0.0	-0.3	0.1		0.0	0.1
Mombasa	-3.9	***	0.0	-1.4	-0.7		0.0	-0.3	2.0	*	0.0	0.6
Moyale	-3.1	**	0.0	-2.1	-0.6		0.0	-0.7	-0.8		0.0	-0.8
Nakuru	-1.0		0.0	-1.1	1.0		0.0	0.9	3.7	***	0.0	2.6
Nanyuki	-1.3		0.0	-1.1	0.9		0.0	0.8	3.5	***	0.0	2.2
Narok	-1.0		0.0	-1.1	-0.5		0.0	-0.4	2.0	*	0.0	1.4
Voi	-3.8	***	0.0	-2.1	-2.2	*	0.0	-1.8	-0.5		0.0	-0.3
Wajir	-3.2	**	0.0	-2.0	-0.6		0.0	-0.6	-0.8		0.0	-0.5
Lodwar	-2.1	*	0.0	-0.9	1.0		0.0	0.6	1.7	+	0.0	0.8
Kitui	-1.6		0.0	-1.3	-1.6		0.0	-1.0	1.2		0.0	0.6

Key: *** represents significance in trend at α = 0.001, ** represents significance in trend at α = 0.01, * represents significance in trend at α = 0.05, + represents significance in trend at α = 0.1, a blank cell means the significance level greater than 10%

4.2.5.3 Temporal Variation of Seasonal Minimum Temperature

This subsection presents results on the temporal variation of minimum temperature in Kenya during the MAM and OND seasons. Table 4-6 and Table 4-7 show the results of the time series of maximum temperature for the baseline, RCP 4.5 and RCP 8.5 scenarios, during the MAM and OND seasons, respectively.

Under the baseline condition the minimum temperature during MAM season shows an increasing trend for all stations (Table 4-6). Statistical significance was recorded for most of the stations except Mandera, Marsabit and Lodwar. The magnitude of trend ranged between 0.1% and 5.7%. The OND season showed an increasing trend in minimum temperature for all stations, statistical significance was recorded for the Dagoretti, Kakamega, Kisumu, Moyale, Narok and Wajir stations; the magnitude of trend ranged between -2.2% and 2.4% (Table 4-7). The increase in minimum temperature could be attributed to global warming as a result of

increased anthropogenic greenhouse gas emissions which prevent the loss of terrestrial radiation by absorbing it and storing it in the surface boundary layer.

Under the RCP 4.5 condition the minimum temperature during MAM season showed an increasing trend in all stations, statistical positive significance was recorded all stations; the magnitude of trend ranged between 2.3% and 7.7% (Table 4-6). The OND season showed an increasing trend in minimum temperature for all stations, statistical significance was recorded for all stations; the magnitude of trend ranged between 2.6% and 9.4% (Table 4-7). The increase in minimum temperature could be attributed to global warming as a result of the increased anthropogenic greenhouse gas emissions which prevent the loss of terrestrial radiation by absorbing it and storing it in the surface boundary layer.

Under the RCP 8.5 condition the minimum temperature during MAM season showed an increasing trend in minimum temperature in all stations, statistical positive significance was recorded for all stations; the magnitude of trend ranged between 4.7% and 10.6% (Table 4-6). The OND season showed an increasing trend in minimum temperature in all stations, statistical significance was recorded in all stations; the magnitude of trend ranged between 3.9% and 11.3% (Table 4-7). The increase in minimum temperature could be attributed to global warming as a result of the increased anthropogenic greenhouse gas emissions which prevent the loss of terrestrial radiation by absorbing it and storing it in the surface boundary layer.

Table 4-6: Time Series Analysis of Mean MAM Minimum Temperature (in °C) of the Baseline, RCP 4.5 and RCP 8.5 Scenarios (Z Denotes the Mann Kendall Statistic, Sig Denotes the Level of Significance; Q Denotes the Sen's Slope and % Δ Percentage of the Sen's Slope over Mean Quantity per Unit Time)

	Baseline				**RCP 4.5**				**RCP 8.5**			
Station	**Z**	**Sig**	**Q**	**% Δ**	**Z**	**Sig**	**Q**	**% Δ**	**Z**	**Sig**	**Q**	**% Δ**
Dagoretti	4.5	***	0.0	5.7	5.4	***	0.0	7.7	6.0	***	0.1	10.3
Garissa	3.0	**	0.0	2.0	5.1	***	0.0	3.7	5.9	***	0.1	5.5
Kakamega	3.3	***	0.0	3.6	5.0	***	0.0	6.2	5.9	***	0.0	7.0
Kisumu	3.6	***	0.0	3.6	5.1	***	0.0	6.2	6.0	***	0.1	7.6
Lamu	3.0	**	0.0	1.9	4.8	***	0.0	2.9	5.7	***	0.0	4.7
Mandera	0.1		0.0	0.1	3.8	***	0.0	2.3	5.5	***	0.0	4.9
Marsabit	0.5		0.0	0.5	4.0	***	0.0	2.9	5.5	***	0.0	4.8
Mombasa	4.0	***	0.0	2.5	5.0	***	0.0	3.2	5.7	***	0.0	4.8
Moyale	2.9	**	0.0	2.1	4.6	***	0.0	3.4	5.7	***	0.0	5.5

	Baseline				RCP 4.5				RCP 8.5			
Station	**Z**	**Sig**	**Q**	**Station**	**Z**	**Sig**	**Q**	**Station**	**Z**	**Sig**	**Q**	**Station**
Nakuru	3.3	**	0.0	4.0	5.1	***	0.0	8.0	5.8	***	0.0	10.6
Nanyuki	2.4	*	0.0	2.6	5.3	***	0.0	5.5	6.0	***	0.0	7.9
Narok	4.3	***	0.0	5.4	5.3	***	0.0	7.6	5.7	***	0.1	10.4
Voi	4.4	***	0.0	3.5	5.4	***	0.0	4.6	5.8	***	0.1	6.3
Wajir	2.3	*	0.0	1.5	4.8	***	0.0	3.3	5.7	***	0.1	5.4
Lodwar	1.1		0.0	1.1	4.6	***	0.0	3.8	5.7	***	0.0	4.8
Kitui	3.5	***	0.0	3.4	5.4	***	0.0	5.3	5.7	***	0.0	7.3

Key: *** represents significance in trend at α = 0.001, ** represents significance in trend at α = 0.01, * represents significance in trend at α = 0.05, + represents significance in trend at α = 0.1, a blank cell means the significance level greater than 10%

Table 4-7: Time Series Analysis of Mean OND Minimum Temperature (in °C) of the Baseline, RCP 4.5 and RCP 8.5 Scenarios (Z Denotes the Mann Kendall Statistic, Sig Denotes the Level of Significance; Q Denotes the Sen's Slope and % Δ Percentage of the Sen's Slope over Mean Quantity per Unit Time)

	Baseline				RCP 4.5				RCP 8.5			
Station	**Z**	**Sig**	**Q**	**% Δ**	**Z**	**Sig**	**Q**	**% Δ**	**Z**	**Sig**	**Q**	**% Δ**
Dagoretti	1.7	+	0.0	1.7	4.1	***	0.0	3.8	5.4	***	0.0	5.7
Garissa	2.6	*	0.0	1.8	5.1	***	0.0	3.9	6.4	***	0.0	5.5
Kakamega	1.1		0.0	0.9	3.8	***	0.0	3.6	5.0	***	0.0	5.5
Kisumu	1.4		0.0	1.1	3.7	***	0.0	3.6	5.3	***	0.0	5.8
Lamu	3.0	**	0.0	1.8	5.0	***	0.0	3.3	6.0	***	0.0	4.3
Mandera	4.4	***	0.0	4.6	5.2	***	0.1	6.5	5.6	***	0.1	7.8
Marsabit	3.4	***	0.0	3.3	4.6	***	0.0	4.9	5.8	***	0.1	6.3
Mombasa	2.0	*	0.0	1.0	4.5	***	0.0	2.6	5.7	***	0.0	3.9
Moyale	1.6		0.0	1.4	4.3	***	0.0	3.3	4.8	***	0.0	4.6
Nakuru	4.7	***	0.0	6.9	5.6	***	0.0	9.3	6.3	***	0.1	11.3
Nanyuki	4.4	***	0.0	6.1	5.2	***	0.0	8.5	6.6	***	0.1	10.5
Narok	1.8	+	0.0	1.3	4.3	***	0.0	3.5	5.1	***	0.0	5.2
Voi	2.4	*	0.0	1.3	4.9	***	0.0	3.1	6.2	***	0.0	5.0
Wajir	1.4		0.0	0.9	4.6	***	0.0	3.3	5.3	***	0.0	4.4
Lodwar	3.5	***	0.0	3.0	5.1	***	0.0	4.8	5.6	***	0.1	6.5
Kitui	3.5	***	0.0	4.3	4.5	***	0.0	5.9	6.2	***	0.1	7.8

Key: *** represents significance in trend at α = 0.001, ** represents significance in trend at α = 0.01, * represents significance in trend at α = 0.05, + represents significance in trend at α = 0.1, a blank cell means the significance level greater than 10%

4.2.6 Spatial Variation of Seasonal Climate in Kenya

This subsection presents the results of the spatial variability of rainfall and temperature under baseline period from 1971 to 2000, and the future climate scenarios (RCP 4.5 and 8.5 scenarios from 2021 to 2050). The spatial plots of the future rainfall, maximum and minimum temperature climatology of the MAM and OND seasons are shown in Figure 4-27 to Figure 4-32.

4.2.6.1 Spatial Variation of Seasonal Rainfall in Kenya

Figure 4-27 and Figure 4-28 present the spatial variation of rainfall during the MAM and OND seasons, respectively. The rainfall amount under both the RCP 4.5 and 8.5 scenarios is expected to increase spatially; the increase is higher under the RCP 8.5 when compared to the RCP 4.5 scenario. Other studies using the CMIP3/5 found that rainfall will increase in the future over East Africa due to global warming because of increased anthropogenic greenhouse emissions (Otieno and Anyah, 2013; Peterson *et al*., 2013; Tierney *et al*., 2015). The increased level of greenhouse emissions will favour higher temperatures which could enhance convection and if the conditions are favourable yield higher amounts of rainfall. However, other studies using observed station data have found that rainfall will reduce in East Africa during the MAM season and increase in the OND season (Ongoma and Chen, 2017; Ongoma *et al*., 2018; Mumo *et al*., 2019). The increase in rainfall during the OND season over East Africa has been attributed to the warming of the western Indian Ocean (Liebmann *et al.*, 2014). The reduction in MAM rainfall over East Africa has been associated with changes in sea surface temperatures over the Pacific Ocean instead of anthropogenic effect (Yang *et al.*, 2014).

The discrepancy between the GCM projections and observed climate in East Africa is called the ‘East Africa climate paradox’ (Rowell *et al.*, 2015). Brands *et al*., (2013), has associated this discrepancy to the insufficiency of observed data required for model parameterization over the region. Additionally, rainfall biases in CMIP3/5 have been attributed to several factors like a double ITCZ, an extreme equatorial Pacific cold tongue, and a weak Atlantic meridional overturning flow (Lee and Wang, 2014).

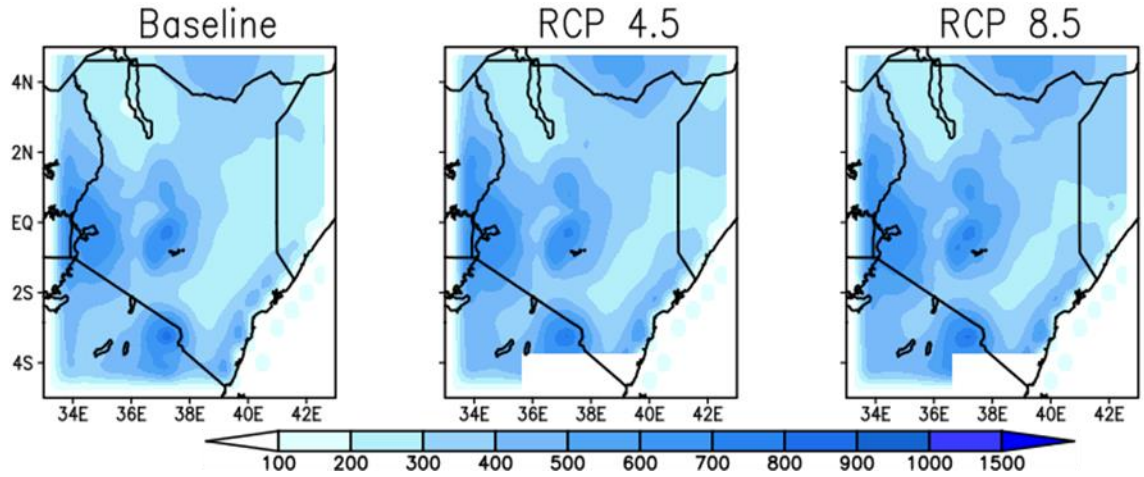

Figure 4-27: Spatial comparison of the total mean MAM rainfall under the baseline (1971-2000), RCP 4.5 and RCP 8.5 scenarios (2021 -2050) in Kenya. Rainfall amount increases from the white shaded areas through to the red shaded areas

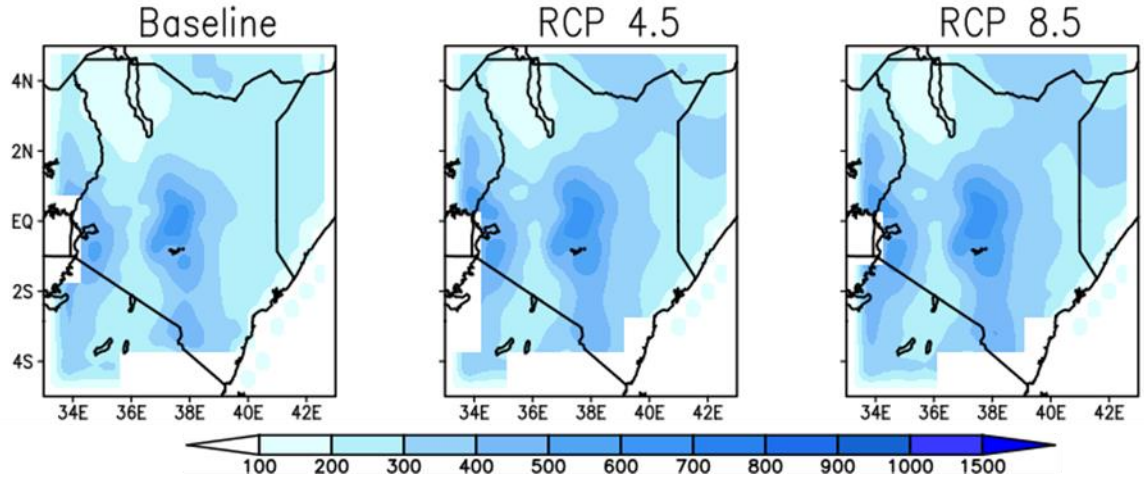

Figure 4-28: Spatial comparison of the total mean OND rainfall under the baseline (1971-2000), RCP 4.5 and RCP 8.5 scenarios (2021 -2050) in Kenya. Rainfall amount increases from the white shaded areas through to the red shaded areas

4.2.6.2 Spatial Variation of Seasonal Maximum Temperature in Kenya

Figure 4-29 and Figure 4-30 present the spatial variation of maximum temperature during the MAM and OND seasons respectively. Maximum temperature increases from west to east during both MAM (Figure 4-29) and OND (Figure 4-30) seasons. The MAM season shows increased temperatures in the north western and eastern region of the country during both the RCP 4.5 and RCP 8.5 scenarios.

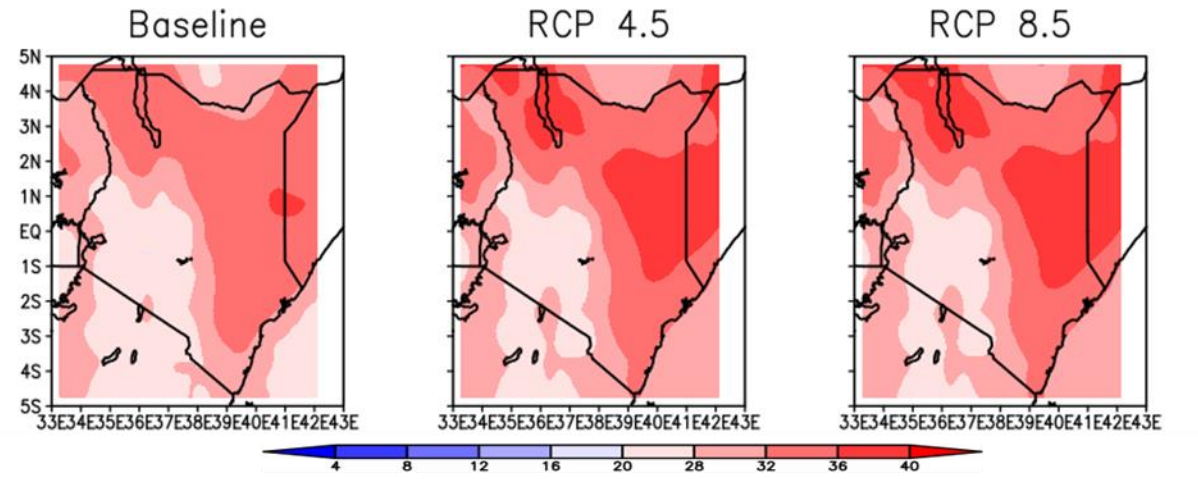

Figure 4-29: Spatial comparison of the Mean MAM maximum temperature under the Baseline (1971-2000), RCP 4.5 and RCP 8.5 scenarios (2021-2050) in Kenya. Maximum temperature increases from the white shaded areas through to the red shaded areas

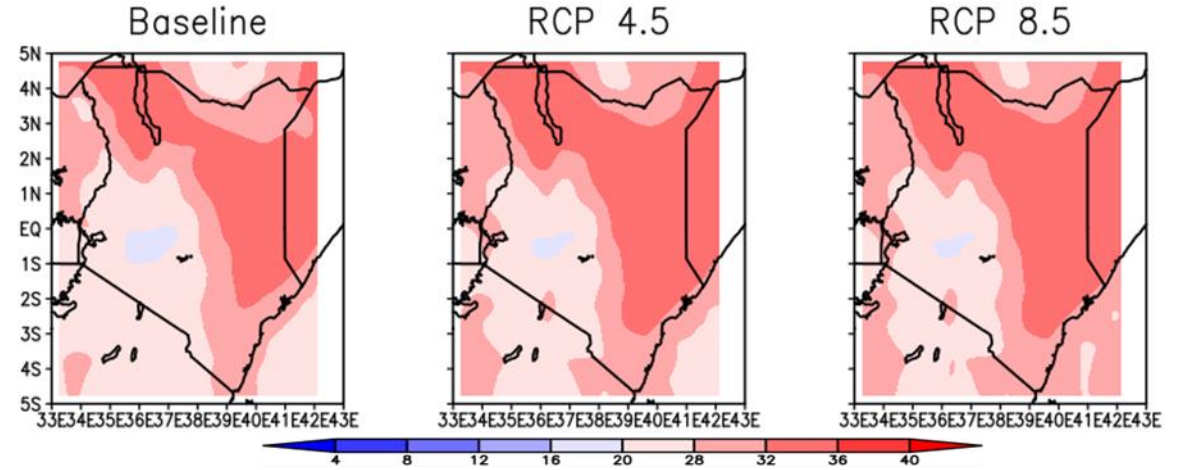

Figure 4-30: Spatial comparison of the Mean OND maximum temperature under the Baseline (1971-2000), RCP 4.5 and RCP 8.5 scenarios (2021-2050) in Kenya. Maximum temperature increases from the white shaded areas through to the red shaded areas

4.2.6.3 Spatial Variation of Seasonal Minimum Temperature in Kenya

Figure 4-31 and Figure 4-32 present the spatial variation of maximum during the MAM and OND seasons respectively. Minimum temperature increases from west to east during both MAM (Figure 4-31) and OND (Figure 4-32) seasons. The pattern of minimum temperature varies only slightly under both RCP 4.5 and RCP 8.5 scenarios in the MAM and OND seasons.

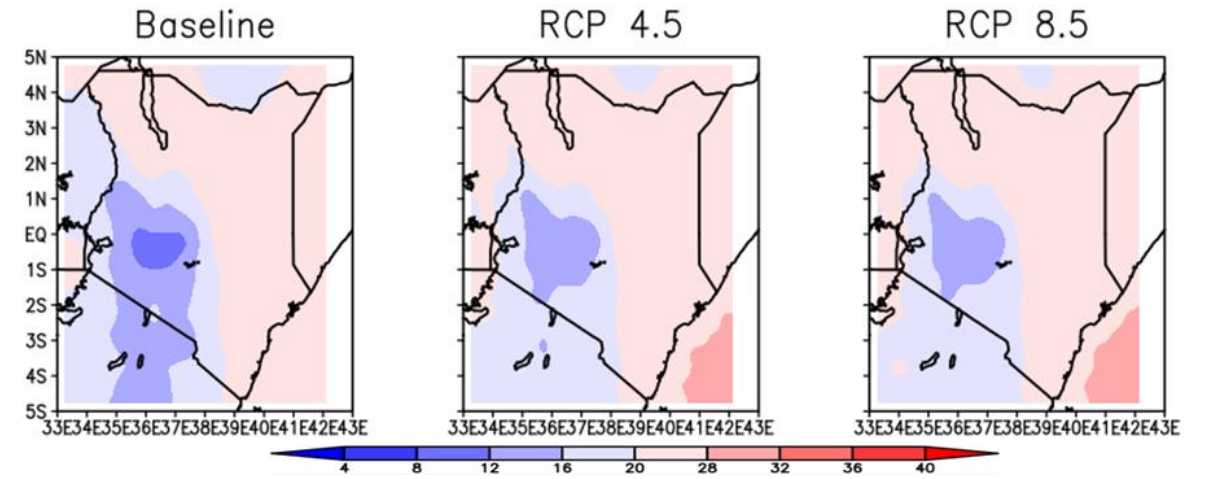

Figure 4-31: Spatial comparison of the mean MAM minimum temperature under the Baseline (1971-2000), RCP 4.5 and RCP 8.5 scenario (2021-2050) in Kenya. minimum temperature increases from the white shaded areas through to the red shaded areas

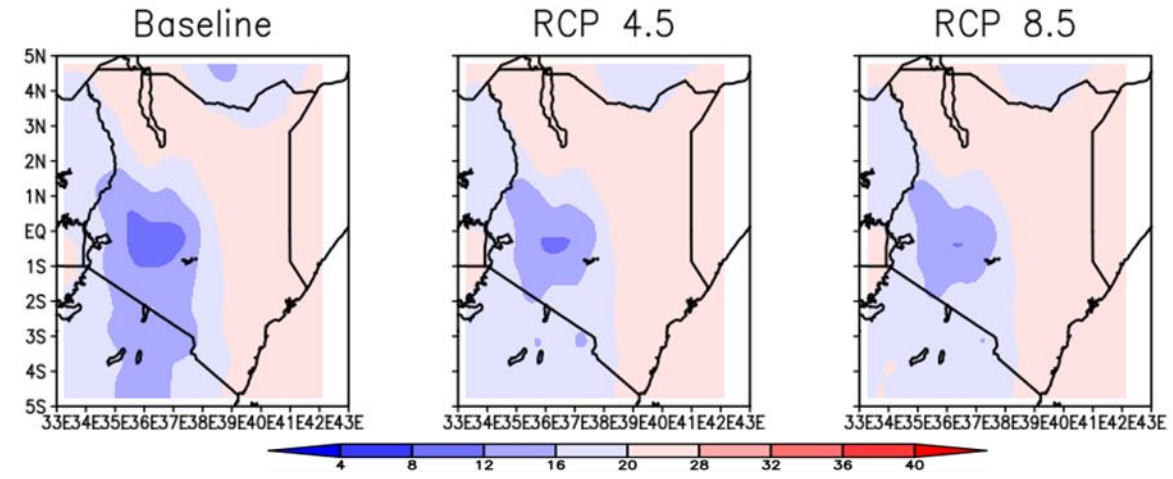

Figure 4-32: Spatial comparison of the mean OND minimum Temperature under the Baseline (1971-2000), RCP 4.5 and RCP 8.5 scenario (2021-2050) in Kenya. Minimum temperature increases from the white shaded areas through to the red shaded areas

4.3 Analysis of the Suitability of Land over the Study Area for Green Gram Production under Past and Future Climate Scenarios

This section presents results from the weighted overlay of climate (past and future rainfall and temperature), soil (pH, depth, texture, drainage, and CEC) and altitude. The first step in analysing the suitability of green gram production involved reclassification of soil, climate and altitude parameters based on Table 3-4 which shows the conditions under which green gram performs best. The bias corrected ensemble of rainfall and the ensemble of temperature from the CORDEX RCA4 models have been used in the analysis. When making a suitability

map for green gram production, the variation in suitability is only accredited to climate parameters under past and future scenarios.

4.3.1 Reclassification of Soil and Altitude Parameters in Terms of their Suitability for Green Gram Production

This subsection presents the results on the reclassification of soil and altitude depending on their suitability levels as in Table 3-4. Figure 4-33 presents the results for the reclassification of soil and altitude parameters into four classes (S1, S2, S3 and N). The factors highly limiting the suitability of green gram were depth, pH, drainage and altitude.

The soil Cation Exchange Capacity (CEC) in the study area falls into three classes of suitability in terms of green gram production with most of the area being suitable (Figure 4-33). The soil CEC has an impact on the acidity and availability of nutrients in the soil. Generally, soils with a high CEC do not require much liming as compared to those soils with low CEC (Moore and Blackwell, 1998). Soils with CEC greater than 10meq/100g in general experience little cation leaching making application of N and K fertilizer more realistic during the rainy season. Soils with a low CEC less that 5meq/100g are prone to deficits of magnesium, potassium, and other cations (CUCE, 2007).

The soil texture in the study area falls into three classes of suitability in terms of green gram production with most of the area being suitable (Figure 4-33). Green gram is suitable for most soil textures but prefers fertile, deep, well-drained loams or sandy loams (Oplinger *et al*., 1990; Morton *et al*., 1982; SASOL, 2015; Infonet, 2018, Meena, 2013). The legumes are most suitable to clayey soils (SASOL, 2015) but do not preform well on heavy clay soils with poor drainage and are somewhat tolerant of saline soils (Grealish *et al*., 2008, Oplinger *et al*., 1990). Sandy soils require good fertilizer and water supply and organic soils need drainage and raised beds since their water tables occur at or near the soil surface (Grealish *et al*., 2008).

The soil pH in the study area falls into four classes of suitability in terms of green gram production with most of the area being not suitable (Figure 4-33). Green gram is well adjusted to a pH range of 5 to 8 (Grealish *et al*., 2008; SASOL, 2015; Infonet, 2018, Meena, 2013; Hanumantharao *et al*., 2016). The performance of green gram is best when the soil has a pH between 6.2 and 7.2. Otherwise, the plants depict signs of serious iron chlorosis and micronutrient deficits on alkaline soils (Morton *et al*., 1982; Oplinger *et al*., 1990). They require slightly acidic soils for the best growth (Morton *et al*., 1982).

The soil depth of the study area falls into four classes of suitability in terms of green gram production (Figure 4-33). Soil depth is the approximate space in centimetres where root development is unhindered by any chemical or physical barrier. This may be in the form of an impassable or contaminated layer.

The altitude of the study area falls into four classes of suitability in terms of green gram production with the not suitable class being located in the central and western part of the country (Figure 4-33). Green gram performs best at a height of 0-1600m above sea level (SASOL, 2015) but not exceeding 2,000 m altitude (SASOL, 2015).

The drainage of the soil falls into four classes of suitability in terms of green gram production (Figure 4-33). Green gram performs best in well drained soils. Regions with poor drainage can be amended by constructing fallows to boost drainage during the rainy season which can further improve green gram suitability.

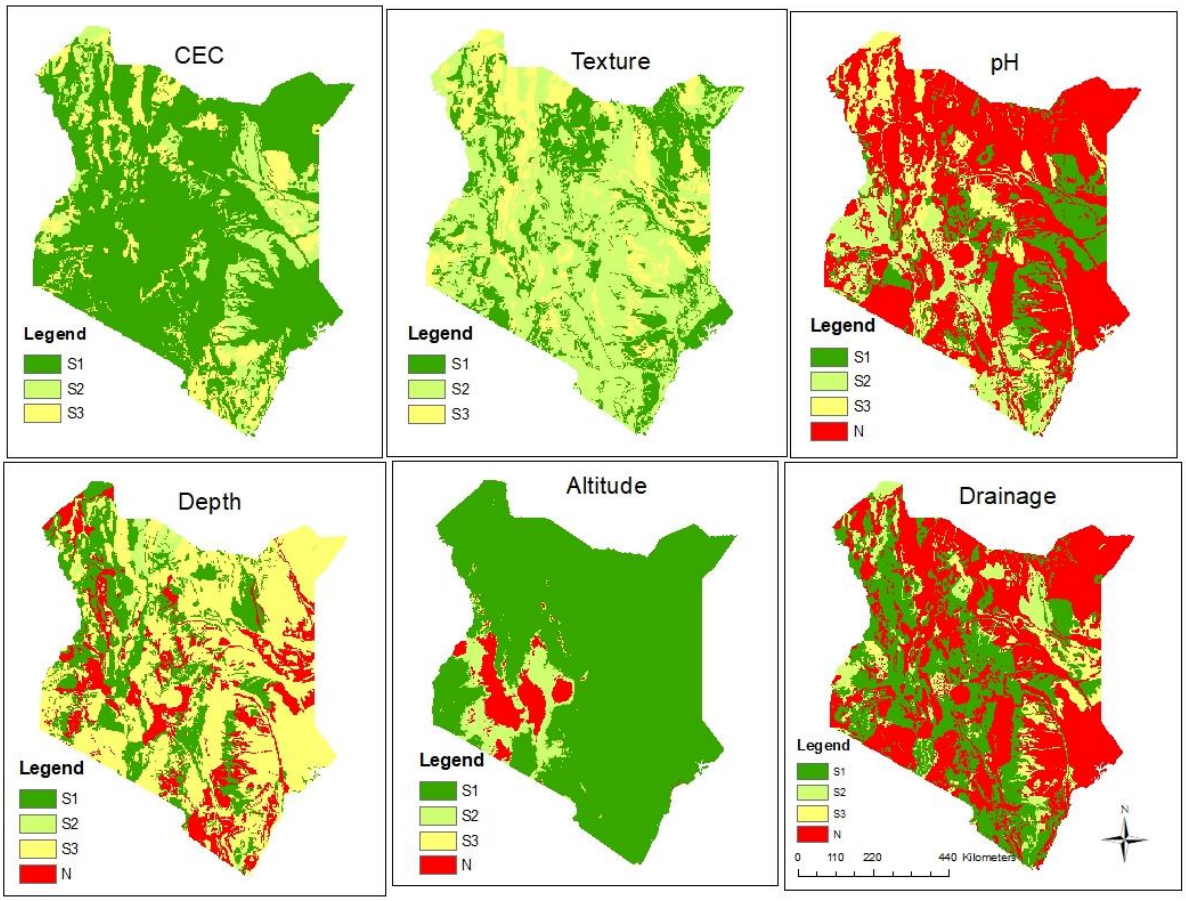

Figure 4-33: Reclassified maps of soil Cation Exchange Capacity (CEC), texture, pH, depth, altitude and drainage. The dark green colour shading (S1) represents the most suitable areas, light green shading (S2) represents the moderately suitable areas, yellow shading (S3) represents the marginally suitable areas, and red shading (N) represents areas that are not suitable for green gram production in Kenya based on these classifications.

4.3.2 Reclassification of Temperature and Rainfall under Present (1971-2000) and Future (2021-2050) RCP 4.5 and RCP 8.5 scenarios in Relation to their Suitability for Green Gram Production

This subsection presents the results of the reclassification of temperature and rainfall depending on their suitability levels for green gram production (Table 3-4) under present (1971-2000) and future (2021-2050) RCP 4.5 and RCP 8.5 scenarios. Figure 4-34 shows the areas in Kenya that are either suitable or not suitable for green gram production in terms of mean temperature using the ensemble of the CORDEX RCA4 models. Figure 4-35 shows the areas in Kenya that are either suitable or not suitable for green gram production in terms of rainfall using the bias corrected ensemble of the CORDEX RCA4 models.

In Figure 4-3, during the MAM season under present conditions, most of the country is highly suitable for green gram production in terms of mean temperature. In the future under the RCP 4.5 scenario areas in the north western and eastern part of the country will not be suitable for green gram production. Under the RCP 8.5 scenario the areas in the north western and eastern parts of the country will also not be suitable for green gram production. Under the RCP 4.5 and RCP 8.5 conditions during the MAM season, regions around the north-western and eastern parts of the country will not be suitable for green gram production since these areas experience a mean temperature greater than 30 °C. A temperature range of 28 to 30 °C is recognized as the best for green gram growth (Mogosti, 2006; Morton *et al*., 1982).

During the OND season under the present conditions, most of Kenya is highly suitable for the production of green gram in terms of mean temperature as shown in Figure 4-34. Under the present conditions areas that are not suitable are noted around Nyandarua and Nyeri Counties since these regions experience mean temperatures lower than 15 °C which, according to Mogosti (2006), are not suitable for green gram production. In the future, under the RCP 4.5 scenario most of the country will be highly suitable for green gram production. Under the RCP 8.5 scenario most of the country will also be highly suitable for green gram production.

In Figure 4-35 during the MAM season under present condition most of the country is suitable for green gram production in terms of total rainfall. In the future under the RCP 4.5 most of the country will be suitable for green gram production. Under the RCP 8.5 scenario most of the country will also be suitable for green gram production. The area highly suitable for green gram production in terms of rainfall under present conditions increases under the RCP 4.5 and RCP 8.5 scenarios to include the north eastern part of the country due to increase in rainfall.

During the OND season areas that are not suitable for green gram production under the present conditions are located in the north western parts of the country in terms of rainfall as shown in Figure 4-35. Under the RCP 4.5 scenario the north western part of the country is not suitable for green gram production. Under the RCP 8.5 scenario the north western part of the country is also not suitable for green gram production. Areas that are not suitable for production are located around the north-west part of Kenya during the OND season for all scenarios since the total rainfall amounts are lower than 75 mm per season. Water stress reduces the rate of nutrients uptake, budding, flowering, leaf area development and

photosynthesis instigating a reduction in yield (Malik, 2006). A rainfall amount of between 250 and 350 mm per season is considered best for sustained growth (Gaiser *et al.*, 2001).

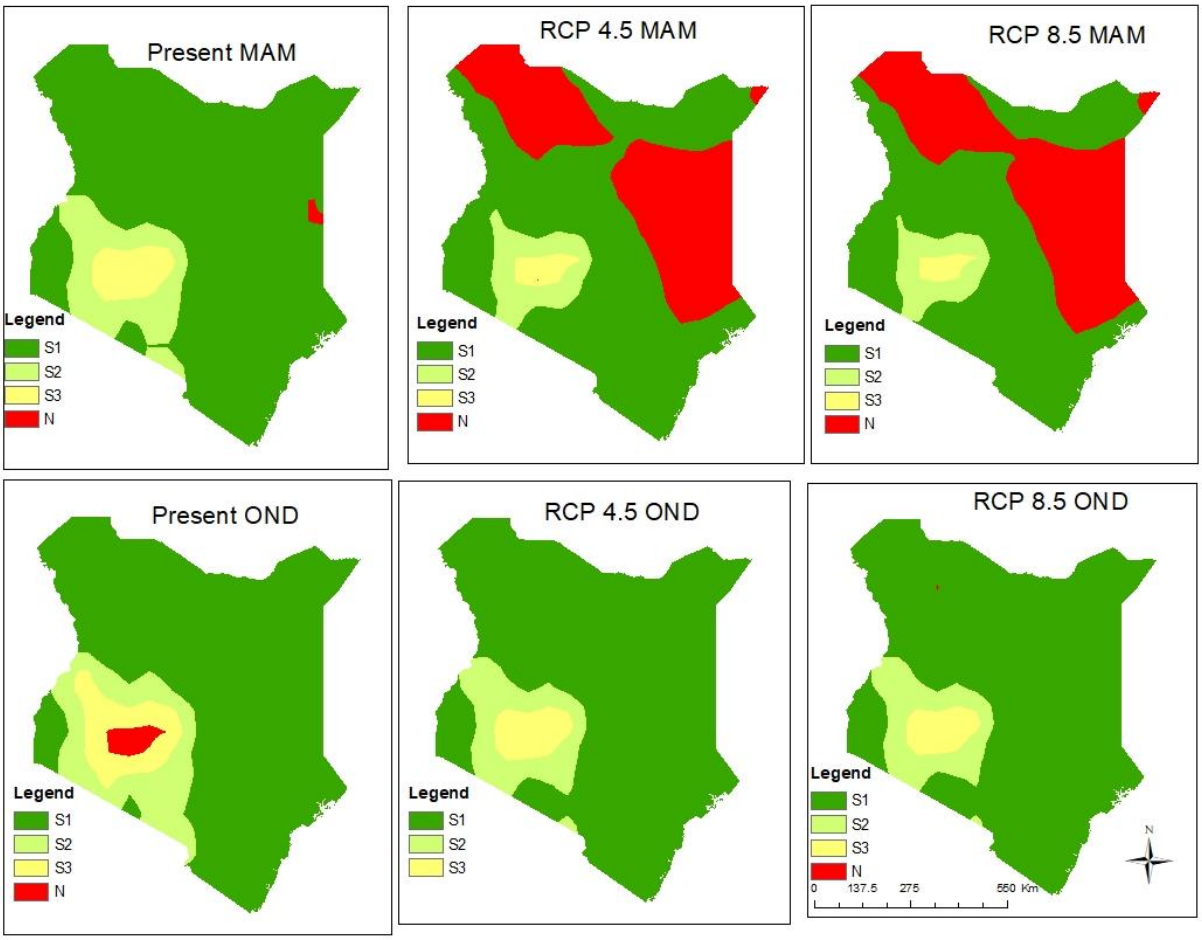

Figure 4-34: Reclassified maps of present and future mean temperature (in °C) layers during the MAM (top row) and OND (bottom row) seasons. The dark green colour shading (S1) represents the most suitable areas, light green shading (S2) represents the moderately suitable areas, yellow shading (S3) represents the marginally suitable areas, and red shading (N) represents areas that are not suitable for green gram production in Kenya based on these classifications.

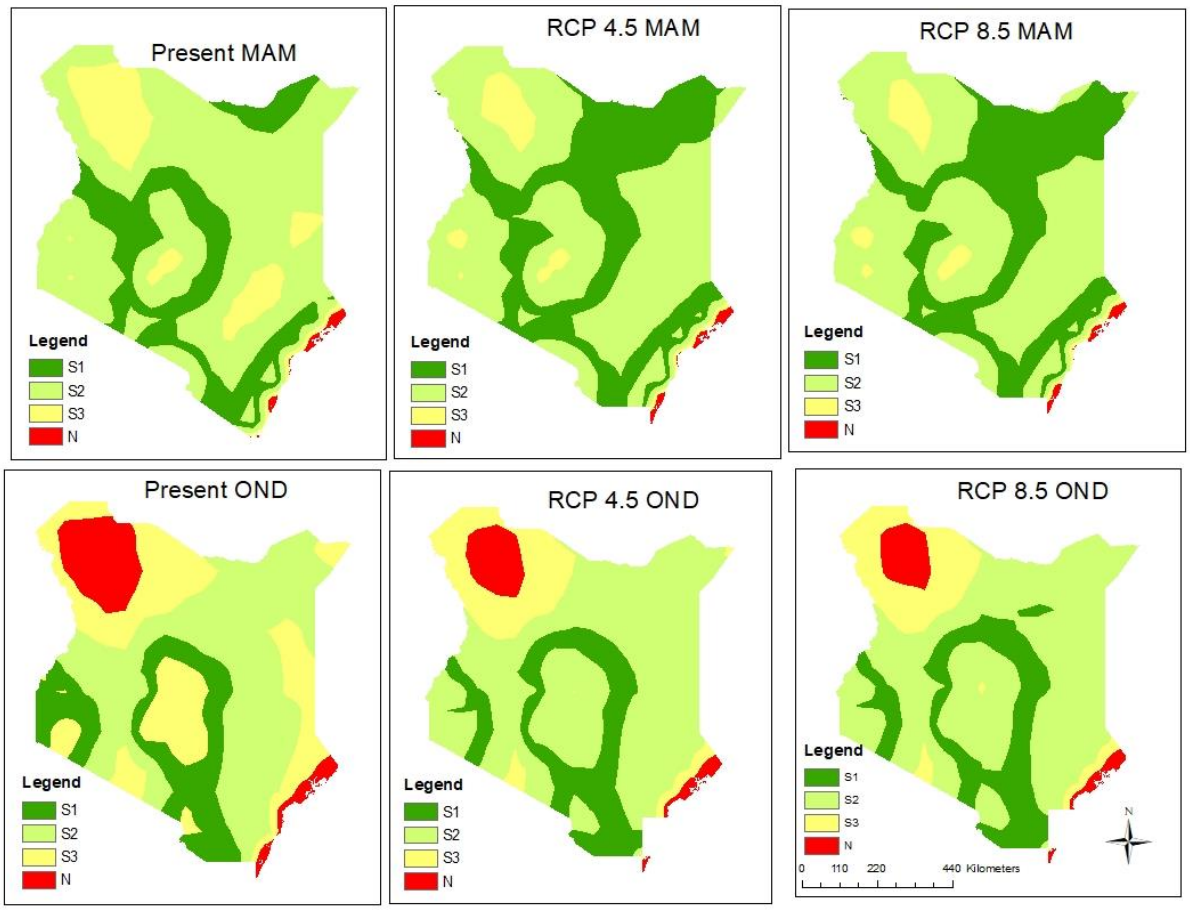

Figure 4-35: Reclassified maps of present and future total rainfall (in mm) during the MAM (top row) and OND (bottom row) seasons. The green colour shading (S1) represents the most suitable areas, light green shading (S2) represents the moderately suitable areas, yellow shading (S3) represents the marginally suitable areas, and red shading (N) represents areas that are not suitable for green gram production in Kenya based on these classifications.

4.3.3 Overall Suitability of Green Gram Production in Kenya Obtained from a Weighted Overlay of Prevailing and Projected Climate, Soil and Altitude Parameters

This subsection presents the results of the green gram suitability maps. The suitability maps were obtained through the weighted overlay of climate under the prevailing and projected RCP 4.5 and RCP 8.5 scenarios, soil and altitude parameters whose weights were obtained as shown in Table 4-8. Figure 4-36 presents areas suitable for green gram production under historical climate data (1971-2000). Figure 4-37 presents areas suitable for green gram production in the future under RCP 4.5 scenario for the years 2021 to 2050. Figure 4-38

presents areas suitable for green gram production under future RCP 8.5 scenario for the years 2021 to 2050.

Table 4-8 shows that rainfall is the most important factor to the growth of green grams by 33% followed by temperature by 20%. Soil parameters in terms of the depth, texture, CEC, pH and drainage account for 6.5%, 5.0%, 9.0%, 9.5% and 12.4% of the weighted overlay for green gram production, respectively. Altitude accounted for the 8% of the weighted overlay for green gram production.

Figure 4-36 shows areas suitable for green gram production during the MAM and OND seasons under historical conditions. During the MAM season areas highly suitable for green gram production are found in the lower eastern, coastal, central and lower Rift Valley regions. During the OND season, areas highly suitable for green gram production are found in the western, lower eastern and coastal regions.

Figure 4-37 shows areas suitable for green gram production during the MAM and OND seasons under the RCP 4.5 scenario. During the MAM season, areas highly suitable for green gram production are found in the lower eastern, coastal, central and lower Rift Valley regions. During the OND season areas highly suitable for green gram production are found in the lower eastern, lower Rift Valley and coastal regions.

Figure 4-38 shows areas suitable for green gram production during the MAM and OND seasons under the RCP 8.5 scenario. During the MAM season areas highly suitable for green gram production are found in the lower eastern, coastal, and central and lower rift valley regions. During the OND season areas highly suitable for green gram production are found in the lower eastern, lower rift valley and coastal regions.

Figure 4-36 (historical), Figure 4-37 (RCP 4.5), and Figure 4-38 (RCP 8.5) show that most of the country is currently moderately suitable for the production of green gram during the MAM and OND season, with highly suitable classes being found in Counties like Kitui, Makueni, Machakos, Isiolo, Samburu, Narok and West Pokot.

Table 4-8: Weights obtained through the Analytical Hierarchy Process Showing the Contribution of each Parameter in the Weighted Overlay of Green gram Production

	Rainfall	Temperature	Depth	Texture	CEC	pH	Drainage	Slope	Weights	Rank
Rainfall	1	3.00	4.00	4.00	4.00	4.00	4.00	4.00	33.0%	1
Temperature	0.33	1	3.00	3.00	3.00	3.00	3.00	3.00	20.2%	2
Depth	0.25	0.33	1	2.00	0.50	0.50	0.50	2.00	6.5%	6
Texture	0.25	0.33	0.50	1	0.33	0.33	0.33	2.00	5.0%	7
CEC	0.25	0.33	2.00	3.00	1	1.00	0.50	2.00	9.0%	5
pH	0.25	0.33	2.00	3.00	1.00	1	0.50	3.00	9.5%	4
Drainage	0.25	0.33	2.00	3.00	2.00	2.00	1	3.00	12.4%	3
Altitude	0.25	0.33	0.50	0.50	0.5	0.33	0.33	1	4.3%	8

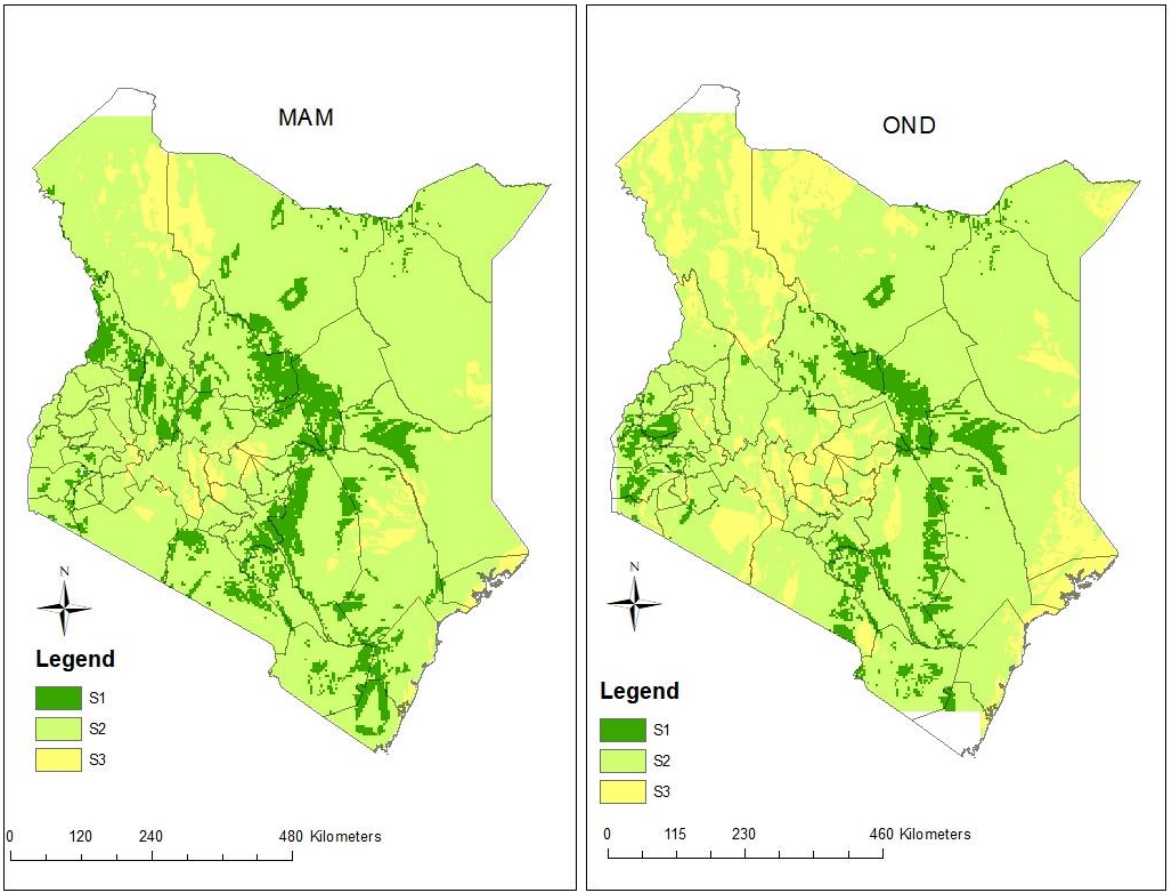

Figure 4-36: Present lands suitable for green gram production during the MAM (left) and OND (right) season. The dark green colour shading (S1) represents the most suitable areas, light green shading (S2) represents the moderately suitable areas, and yellow shading (S3) represents the marginally suitable areas, for green gram production in Kenya based on these classifications.

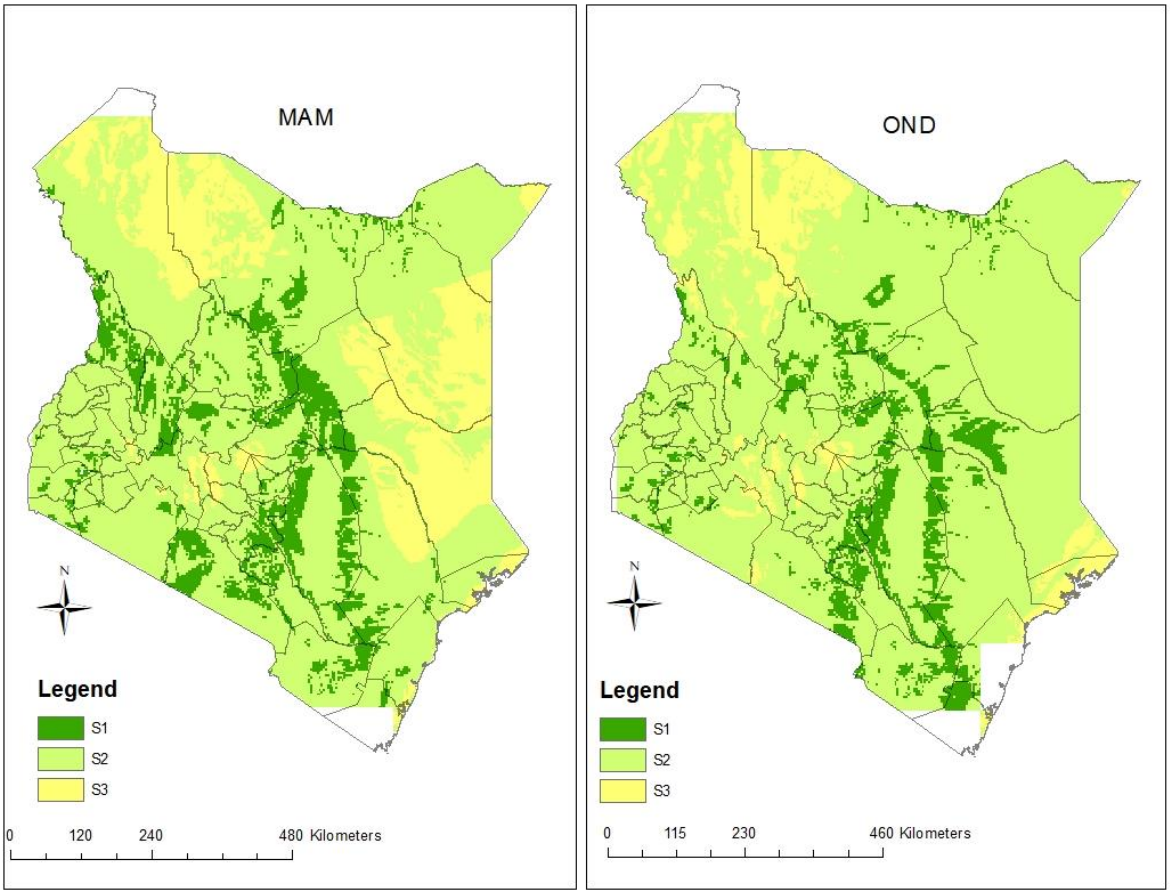

Figure 4-37: Future land suitable for green gram production during the MAM (left) and OND (right) season under the RCP 4.5 scenario for the years 2021 to 2050. The dark green colour shading (S1) represents the most suitable areas, light green shading (S2) represents the moderately suitable areas, and yellow shading (S3) represents the marginally suitable areas, for green gram production in Kenya based on these classifications.

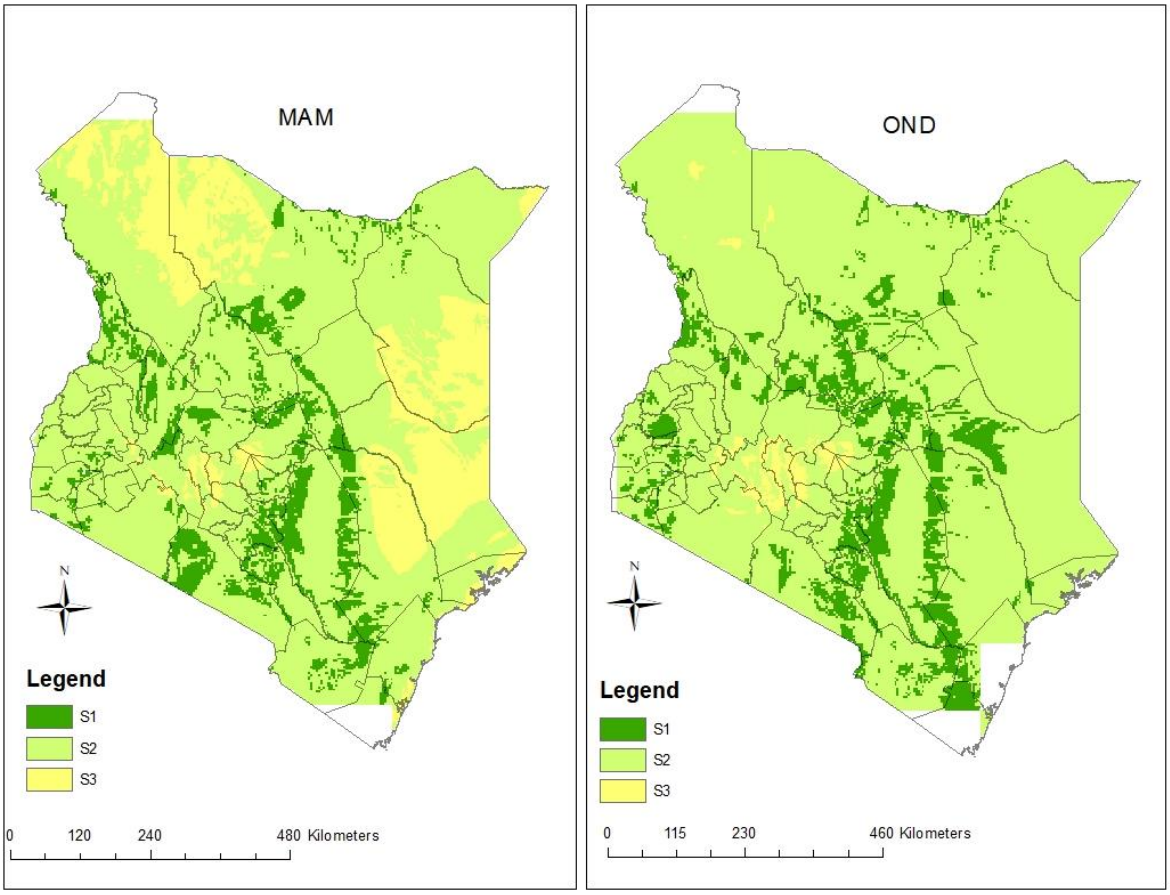

Figure 4-38: Future land suitable for green gram production during the MAM (left) and OND (right) season under the RCP 8.5 scenario for the years 2021 to 2050. The dark green colour shading (S1) represents the most suitable areas, light green shading (S2) represents the moderately suitable areas, and yellow shading (S3) represents the marginally suitable areas, for green gram production in Kenya based on these classifications.

Table 4-9 shows the area in km^2 suitable for green gram production during the MAM and OND seasons under baseline and future climate scenarios. Table 4-10 shows the percentage change in area between the present and the future climate scenarios. The change in the suitable area is only based on climatic parameters and not on the conditions of soil and altitude.

During the MAM season, the area presently highly suitable for green gram production (67842.62 km^2) is expected to increase slightly by 1.1% to 68600.4 km^2 under the RCP 4.5 scenario. The area is projected to reduce by -9.6% to 61307.8 km^2 under the RCP 8.5 scenario. During the OND season the area currently highly suitable for green gram production (49633.4 km^2) is projected to increase under the RCP 4.5 scenario by 22.2%. The

area is projected to increase by 58.5% under the RCP 8.5 scenario, due to favourable rainfall and temperature conditions in the future.

During the MAM season the area presently moderately suitable for green gram production (470972 km^2) is estimated to reduce by 16.8% to 391768.9 km^2 under the RCP 4.5 scenario. The area is projected to decrease by 14.1% to 404721.1 km^2 under the RCP 8.5 forcing. During the OND season the area currently moderately suitable for green gram production (423463.3 km^2) is projected to increase by 7.9% to 457128.1 km^2 under the RCP 4.5 scenario. The area is projected to increase by 15.3% to 488043.8 km^2 (15.3%) under the RCP 8.5 condition.

During the MAM season the area currently marginally suitable for green gram production (41552.37 km^2) is projected to increase by 188.8% to 119997.7 km^2 under the RCP 4.5 scenario. The area is projected to increase by 175% to 114275.8 km^2 under the RCP 8.5 condition. During the OND season the area currently marginally suitable (111174.4 km^2) is projected to reduce by 45.9% to 60173.4 km^2. The area is projected to reduce by 88.5% to 12777.6 km^2 under the RCP 8.5 scenario.

Table 4-9: Changes in Land Suitable for Green gram Production (in km^2) under the Baseline and Future RCP 4.5 and 8.5 Climate Scenarios during the MAM and OND Seasons

	HISTORICAL		**RCP 4.5**		**RCP 8.5**	
	MAM (km^2)	**OND (km^2)**	**MAM (km^2)**	**OND (km^2)**	**MAM (km^2)**	**OND (km^2)**
S1	67842.6	45729.4	68600.4	55885.1	61307.8	72464.8
S2	470972	423463.3	391768.9	457128.1	404721.1	488043.8
S3	41552.4	111174.4	119997.7	60173.4	114275.8	12777.6

Table 4-10: Percentage Changes in Land Suitable for Green gram Production between Baseline and Future RCP 4.5 and RCP 8.5 Climate Scenarios during the MAM and OND Seasons

	RCP 4.5		**RCP 8.5**	
	MAM	**OND**	**MAM**	**OND**
S1	1.1%	22.2%	-9.6%	58.5%
S2	-16.8%	7.9%	-14.1%	15.3%
S3	188.8%	-45.9%	175.0%	-88.5%

4.4 Simulation of the Impact of Changing Climate on Green Gram Production

This section presents the results of the effect of changing climate on the yield of four green gram varieties planted at the SEKU farm. The APSIM module is able to simulate nine cultivars of the green gram crop. The varieties calibrated in APSIM include: Satin, a dull green seed resembling KS20; Celera, a small seeded, shiny green seed with hard seed levels resembling N26, and Berken and Emerald, medium-large and shiny green seeds resembling Tosha and Biashara varieties respectively (Gentry and Gordon, 2010). The calibrated Biashara, Tosha, KS20 and N26 were used to simulate the effect of changing climate on the yield, biomass and days to physiological maturity of green gram.

4.4.1 Weather Conditions during the Growing Period

Land was prepared at the beginning of the season and sowing done when at least 30 mm of rainfall had been received to enable sufficient moisture in the soil for sustained germination of the green gram varieties. This threshold in some cases occurred in the middle of the season. Table 4-11 shows the pattern of rainfall, solar radiation, and minimum and maximum temperature during the growing season when the experiments were conducted.

Rainfall of 250 to 350 mm per season is considered as optimal for green gram production (Gaiser *et al*. 2001; SASOL, 2015; Infonet, 2018). The OND season of 2018 received rainfall amount of 302.5 mm, which favoured good yield during the season. The MAM season of 2019 received rainfall amount of 132.9 mm which resulted in reduced yields. The OND season of 2019 received higher than the optimal amount required of 464.7 mm which resulted in increased biomass and less yield compared to the 2018 OND season.

The temperature during all the growing seasons remained optimal as shown in Table 4-11. A temperature of 21 to 30 °C is considered ideal for seed germination and plant growth (Mogosti, 2006; Morton *et al*., 1982). The temperature should always be above 15 °C during crop growth (Mogosti, 2006).

Table 4-11: Distribution of Monthly Total Rainfall (mm), Mean Maximum and Minimum Temperature, and Mean Solar Radiation during the Growing Season when the Green gram Experiments were Conducted at the SEKU Farm. NRD Denotes the Number of Rainy Days with at Least 0.85 mm of Rainfall

Experiment 1 OND 2018					
Months	**Total rainfall (mm)**	**NRD**	**Maximum temperature (°C)**	**Minimum temperature (°C)**	**Radiation MJ m^{-2} day^{-1}**
Nov	127.2	11	28.7	18.3	18.2
Dec	171.6	14	27.2	17.7	17.6
Jan	3.5	1	29.0	16.5	19.2
Total/Mean	302.5	26	28.3	17.5	18.3
Experiment 2 MAM 2019					
Months	**Total rainfall (mm)**	**NRD**	**Maximum temperature (°C)**	**Minimum temperature (°C)**	**Radiation MJ m^{-2} day^{-1}**
Apr	98.8	10	31.5	20.1	17.5
May	33.8	5	27.5	18.3	15.6
Jun	0.1	0	26.5	17.1	12.1
Jul	0.2	0	27.1	15.7	13.6
Total /Mean	132.9	15	28.2	17.8	14.7
Experiment 3 OND 2019					
Months	**Total rainfall (mm)**	**NRD**	**Maximum temperature (°C)**	**Minimum temperature (°C)**	**Radiation MJ m^{-2} day^{-1}**
Oct	381.2	20	27.1	18.2	17.1
Nov	4.4	1	26.6	18.1	17.0
Dec	79.1	8	26.6	18.4	14.6
Total/Mean	464.7	29	26.8	18.2	16.2

4.4.2 The Performance of APSIM Green Gram Module in Simulating the Observed Yield, Biomass and Days to Maturity

This section presents results on the performance of the APSIM green gram model in simulating the observed yield, biomass and days to maturity. The green gram model was calibrated for four varieties of the legume which are Biashara, Tosha, N26 and KS20 varieties. Table 4-12 shows the genetic coefficients used to model the green gram varieties. Table 4-13 shows the observed and simulated yield, biomass and days to maturity for the green gram varieties when experiments were conducted. Table 4-14 shows the results of the strength of the relationship between the observed and simulated green gram varieties.

Table 4-12 shows the calculated number of growing degree days it takes for each green gram variety to develop through seven phenological phases. The APSIM green gram model uses 7.5 °C base temperature, 30 °C optimal temperature and 40 °C extreme temperature as the key values in the calculation of degree days (Carberry, 2007; Chauhan *et al.,* 2010).

Table 4-13 shows the observed versus and simulated yield, biomass and days to maturity for each green gram variety. The APSIM model generally underestimates the observed yield, biomass and days to maturity. The yield during the OND season of 2018 was better compared to the MAM 2019 and OND 2019 season. The differences in yield, biomass and days to maturity were attributed to changes in rainfall (Table 4-11) since temperature remained optimal for production as discussed in the preceding section. Table 4-14 represent the strength of the relationship between the observed and modelled varieties which was good and the model was approved for future climate studies.

Table 4-12: The Genetic Coefficients used to Model the Four Varieties of Green gram Biashara, Tosha, KS20 and N26

			Green gram Variety			
PHENOLOGY	**Source**	**Units**	**Biashara**	**Tosha**	**KS20**	**N26**
Emergence	C	°C days	95.2	95.2	95.2	95.2
Emergence To End Of Juvenile Phase	C	°C days	430	430	400	508
Juvenile To Floral Initiation	D	Hours	5	5	5	5
Floral Initiation To Flowering	D	Hours	25	25	25	25
Flowering To Start Of Grain Filling	C	°C days	206	206	178	205
Start of Grain Filling to Maturity	C	°C days	313	320	313	304
Start of Grain Filling To End Of Grain Filling	D	°C days	30	27.5	25	25.5

C: Calibrated; D: Default

Table 4-13: Observed and Simulated Yield, Biomass and Days to Maturity for each Green gram Variety for the Growing Season when the Green gram Experiments were Conducted. Obs and Sim denote the Observed and Simulated Parameters, Respectively

OND 2018									
Variety	**Yield (kg/ha)**			**Biomass (kg/ha)**			**Days to maturity**		
	Obs	**Sim**	**% error**	**Obs**	**Sim**	**% error**	**Obs**	**Sim**	**% error**
Biashara	1071.2	654	-38.9	1954.3	1738	-11.1	71	65	-8.5
N26	995.8	771.2	-22.6	2773.6	2416.3	-12.9	75	69	-8.0
KS20	798.1	403.6	-49.4	1859.3	1334.7	-28.2	62	60	-3.2
Tosha	854.2	601.6	-29.6	2631.9	1887.7	-28.3	69	65	-5.8
MAM 2019									
Variety	**Yield (kg/ha)**			**Biomass (kg/ha)**			**Days to maturity**		
	Obs	**Sim**	**% error**	**Obs**	**Sim**	**% error**	**Obs**	**Sim**	**% error**
Biashara	510.5	380.6	-25.4	1405.9	1169.1	-16.8	66	60	-9.1
N26	570.2	409.9	-28.1	1748.6	1491.3	-14.7	70	64	-8.6
KS20	405.4	288.2	-28.9	1615.1	1005.9	-37.7	60	57	-5.0
Tosha	614.6	379.3	-38.3	1558.1	1252.8	-19.6	59	61	+3.4
OND 2019									
Variety	**Yield (kg/ha)**			**Biomass (kg/ha)**			**Days to maturity**		
	Obs	**Sim**	**% error**	**Obs**	**Sim**	**% error**	**Obs**	**Sim**	**% error**
Biashara	850.4	616.9	-27.5	2080.6	1614.7	-22.4	73	68	-6.8
N26	894.3	611.3	-31.6	2463.5	1911.4	-22.4	77	72	-6.5
KS20	760.2	449.7	-40.8	1994.2	1357.6	-31.9	64	64	0
Tosha	721.8	549.1	-23.9	2503.2	1632.4	-34.8	71	68	-4.2

Table 4-14: Results of the Strength of the Relationship between the Observed and Modelled Green gram Varieties using the Coefficient of Determination (R^2) NRMSE, and Bias Tests of Skill

Variety	**R^2**			**NRMSE (%)**			**BIAS**		
	Yield (kg/ha)	**Biomass (kg/ha)**	**Days to maturity**	**Yield (kg/ha)**	**Biomass (kg/ha)**	**Days to maturity**	**Yield (kg/ha)**	**Biomass (kg/ha)**	**Days to maturity**
Biashara	92.6	85.9	99.0	35.3	18.0	8.1	16.1	17.5	2.4
N26	94.9	92.5	99.0	27.8	17.5	7.7	14.9	19.7	2.4
KS20	87.0	91.2	99.3	45.5	32.5	3.4	16.6	24.3	1.3
Tosha	87.8	91.2	92.1	30.5	30.7	4.7	14.8	25.3	1.3

4.5.6 Climate Characteristics between the Baseline and Future Climate Scenarios in Kitui County, Kenya

This section presents the results of the simulated yield, biomass and days to maturity of green gram under the baseline (1971-2000) and the future climate (2021-2050) using the RCP 4.5 and RCP 8.5 scenario for a highly suitable region in Kitui County in Kenya. Table 4-15 presents the results on the distribution of total annual and seasonal rainfall, mean annual and seasonal maximum and minimum temperature and mean annual and seasonal solar radiation under the baseline and future RCP 4.5 and 8.5 scenarios.

Table 4-15 shows an increase in total rainfall, minimum and maximum temperature during both future RCP 4.5 and RCP 8.5 scenarios. The projected increase in the rainfall and temperature is more during the RCP 8.5 scenario in comparison to the RCP 4.5 scenario. This is because the RCP 8.5 scenario represents higher concentration of greenhouse gases compared to the RCP 4.5 scenario. The increased level of greenhouse emissions will favour higher temperatures which could enhance moisture evaporation and if conditions are favourable yield higher amounts of rainfall.

Table 4-15: Distribution of Mean Total Annual and Seasonal Rainfall, Mean Annual and Seasonal Maximum and Minimum Temperature, and Mean Annual and Seasonal Solar Radiation under Baseline (1971-2000), RCP 4.5 (2021-2050) and RCP 8.5 (2021-2050) Scenarios in Kitui County, Kenya

	Scenario	Total rainfall (mm)	Maximum temperature (°C)	Minimum temperature (°C)	Radiation MJ m^{-2} day^{-1}
Annual	**Baseline**	765.8	26.7	15.4	18.1
	RCP 4.5	850.0	27.9	16.9	18.1
	RCP 8.5	870.0	28.1	17.1	18.1
MAM	**Baseline**	298.9	27.1	16.2	18.2
	RCP 4.5	318.9	28.2	17.6	18.2
	RCP 8.5	328.5	28.4	17.9	18.2
OND	**Baseline**	345.3	25.6	15.9	18.4
	RCP 4.5	394.2	26.8	17.4	18.4
	RCP 8.5	400.1	27.0	17.6	18.4

4.5.7 The Effect of Climate Change on Green Gram Yield, Biomass and Days to Maturity in Kitui County Kenya

This subsection presents the results of the effect of climate change on four green gram varieties modelled using the APSIM Model in Kitui County, Kenya. Figure 4-39 presents the

effects of climate change on green gram yield during the MAM season. Figure 4-40 presents the effects of climate change on green gram yield during the OND season. Figure 4-41 presents the effects of climate change on green gram biomass during the MAM season. Figure 4-42 presents the effects of climate change on green gram biomass during the OND season. Figure 4-43 presents the effects of climate change on green gram days to maturity during the MAM season. Figure 4-44 presents the effects of climate change on green gram days to maturity during the OND season. Table 4-16 shows the actual values of the mean of the yield, biomass and days to maturity during the MAM season for the historical, RCP 4.5 and RCP 8.5 scenarios. Table 4-17 show the actual values of the mean of the yield, biomass and days to maturity during the OND season for the historical, RCP 4.5 and RCP 8.5 scenarios.

During the MAM and OND seasons under the RCP 4.5 and RCP 8.5 scenarios, there is a decline in yield, biomass, and days to maturity as displayed in Figure 4-39, Figure 4-40, Figure 4-41, Figure 4-42, Figure 4-43, and Figure 4-44. The decline in yield, biomass and days to maturity is slightly larger during the RCP 8.5 scenario in comparison to the RCP 4.5 scenario in both MAM and OND seasons. This is because the RCP 8.5 scenario represents higher concentrations of greenhouse gas emissions leading to more rainfall when compared to the RCP 4.5 scenario. The projected increase in rainfall amount under both the RCP 4.5 and RCP 8.5 scenarios will translate to a decreased yield due to reduced pod setting (Mogosti, 2006; Oplinger *et al*., 1990). The increase in temperature will result in reduction of the days to maturity for green gram.

Table 4-16 and Table 4-17 reinforce the result during the MAM and OND season under both RCP 4.5 and RCP 8.5 scenarios there is a decline in yield, biomass and days to maturity. The decline in yield, biomass and days to maturity is slightly larger under the RCP 8.5 scenario than the RCP 4.5 scenario in both seasons. Overall the yield is greater during the OND season compared to the MAM season due to more favourable weather conditions.

Kenya, currently, only produces 460kg/ha of green grams (Kilimo Trust, 2017). The study found that despite the decrease in yield, potential production under the future climate scenarios was still above 460kg/ha. There is, thus, potential to expand on the current production of green grams. Therefore, despite the decrease in the future green gram is still a lucrative crop since farmers still stand to increase their current production.

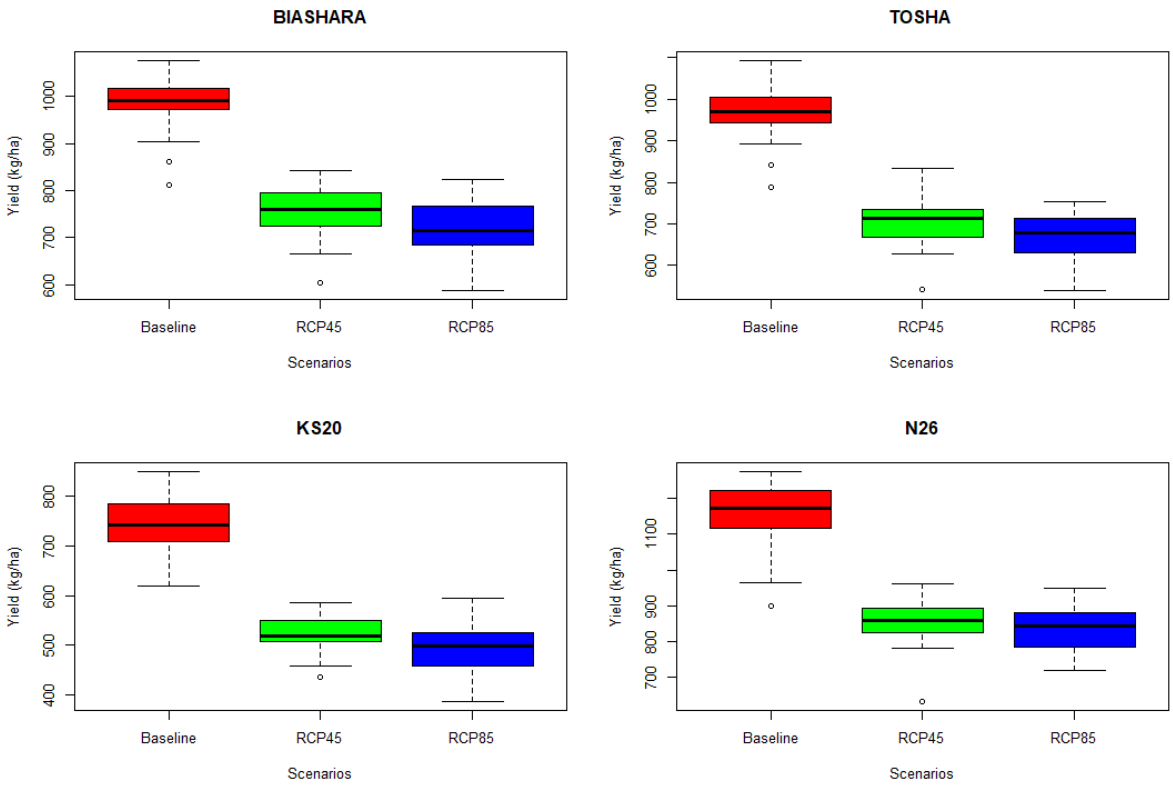

Figure 4-39: The effect of changing climate on green gram yield (kg/ha) over the study area for four varieties during the MAM season. The varieties are Biashara, Tosha, KS20 and N26. The red colour represents yield during the baseline period (1971-2000), the green colour represents yield under the RCP 4.5 scenario (2021-2050) and the blue colour represents the yield during the RCP 8.5 scenario (2021-2050)

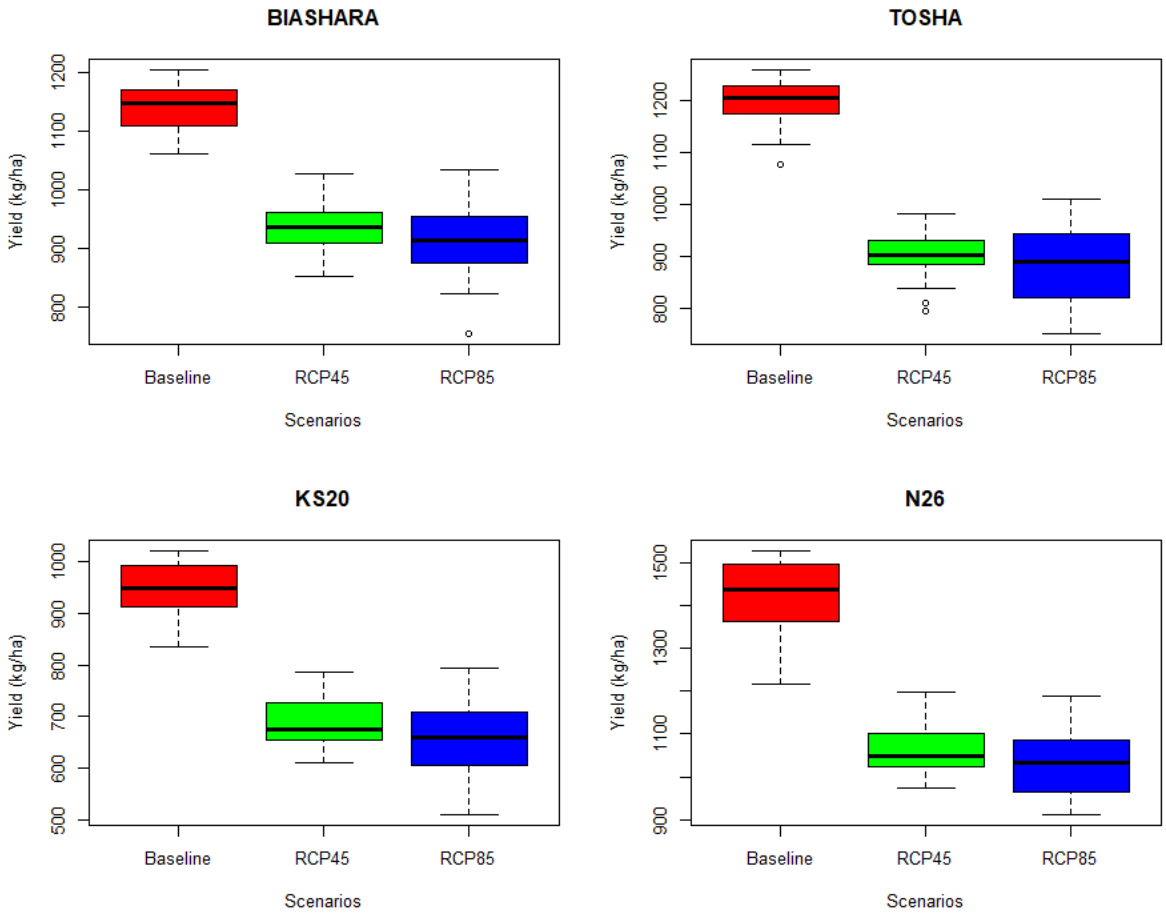

Figure 4-40: The effect of changing climate on green gram yield (kg/ha) over the study area for four varieties during the OND season. The varieties are Biashara, Tosha, KS20 and N26. The red colour represents yield during the baseline period (1971-2000), the green colour represents yield under the RCP 4.5 scenario (2021-2050) and the blue colour represents the yield during the RCP 8.5 scenario (2021-2050)

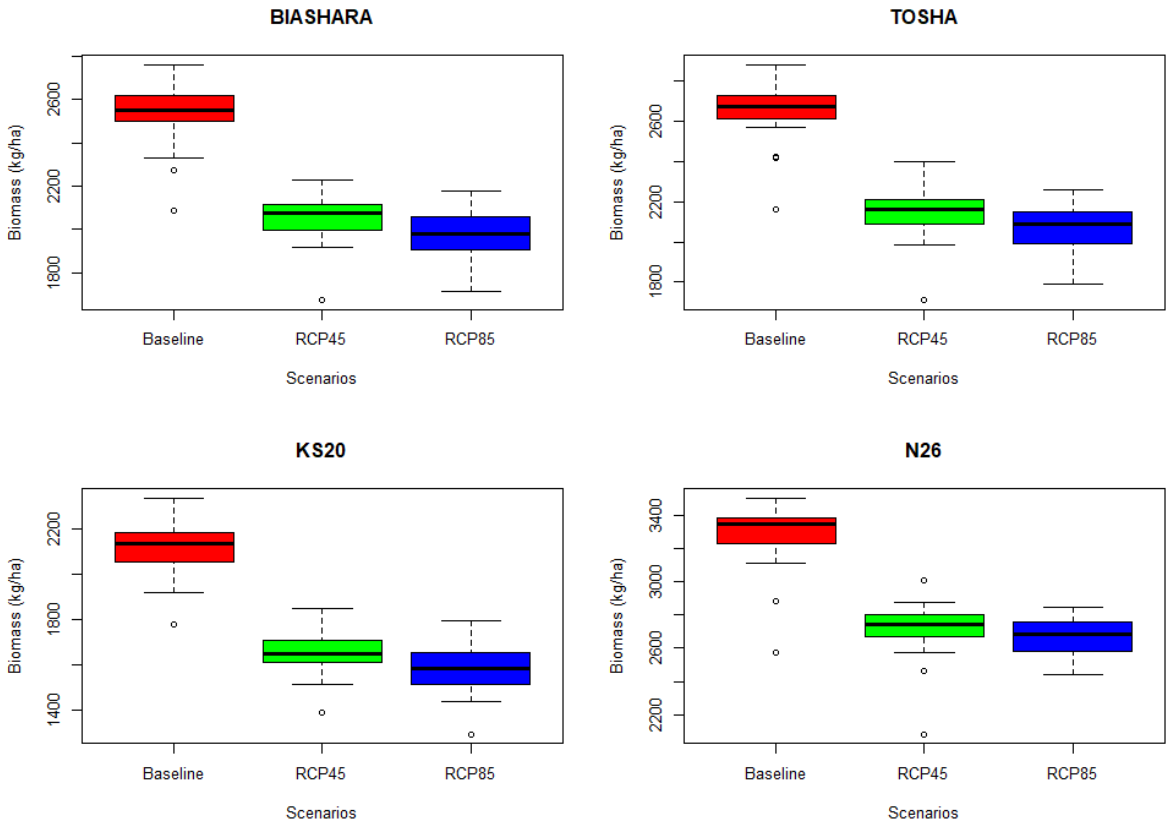

Figure 4-41: The effect of changing climate on green gram biomass (kg/ha) over the study area for four varieties during the MAM season. The varieties are Biashara, Tosha, KS20 and N26. The red colour represents biomass during the baseline period (1971-2000), the green colour represents biomass under the RCP 4.5 scenario (2021-2050) and the blue colour represents the biomass during the RCP 8.5 scenario (2021-2050)

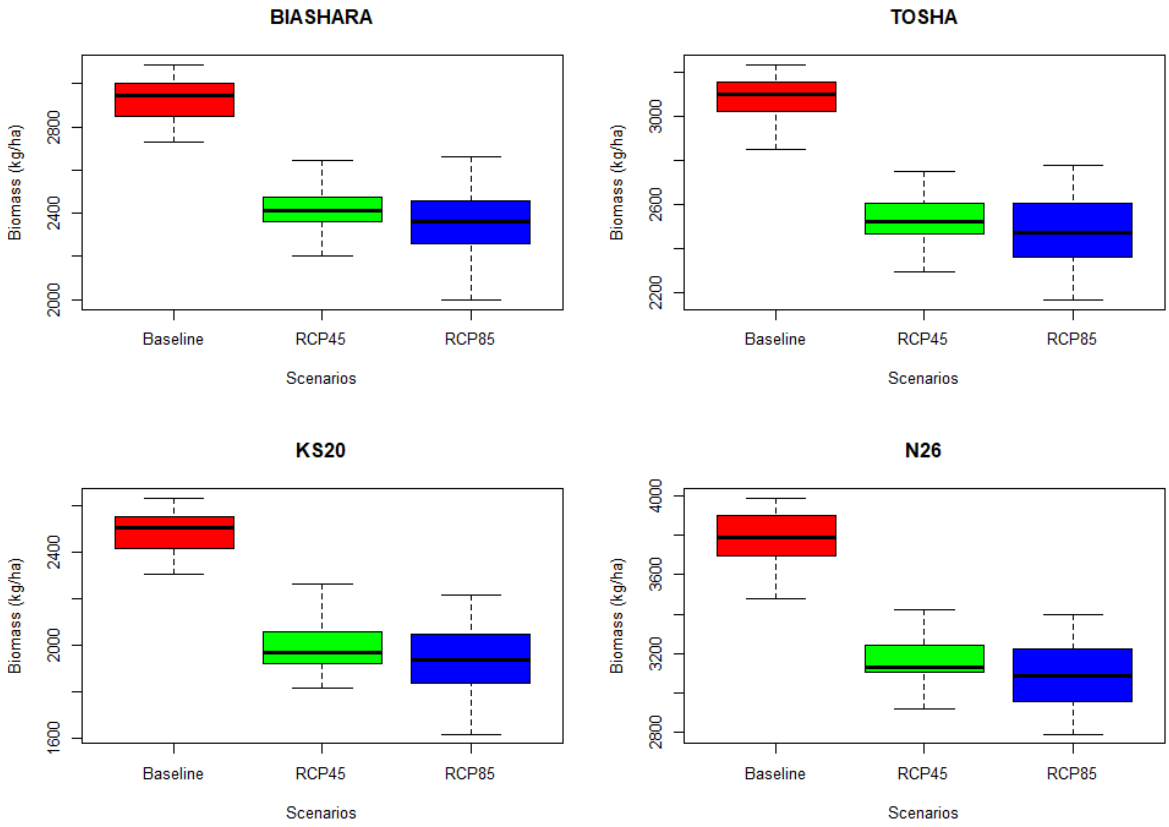

Figure 4-42: The effect of changing climate on green gram biomass (kg/ha) over the study area for four varieties during the OND season. The varieties are Biashara, Tosha, KS20 and N26. The red colour represents biomass during the baseline period (1971-2000), the green colour represents biomass under the RCP 4.5 scenario (2021-2050) and the blue colour represents the biomass during the RCP 8.5 scenario (2021-2050)

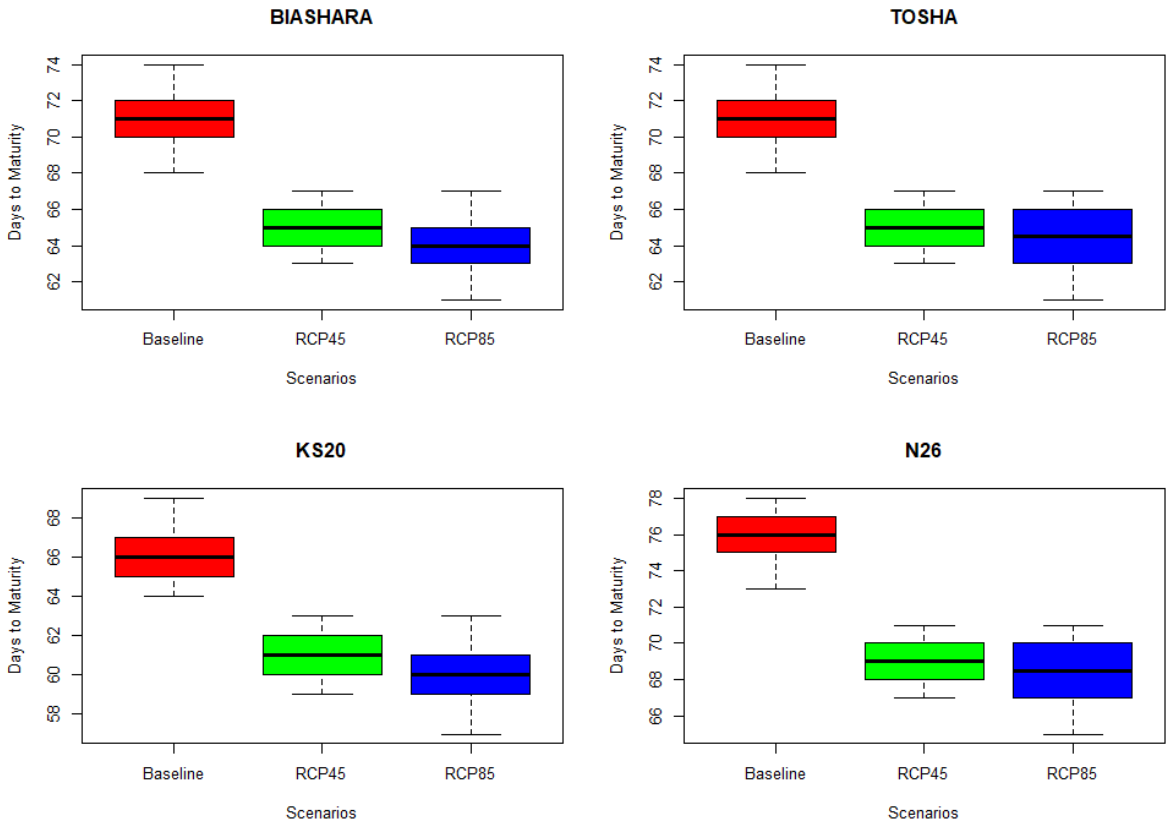

Figure 4-43: The effect of changing climate on green gram days to maturity over the study area for four varieties during the MAM season. The varieties are Biashara, Tosha, KS20 and N26. The red colour represents days to maturity during the baseline period (1971-2000), the green colour represents days to maturity under the RCP 4.5 scenario (2021-2050) and the blue colour represents the days to maturity during the RCP 8.5 scenario (2021-2050)

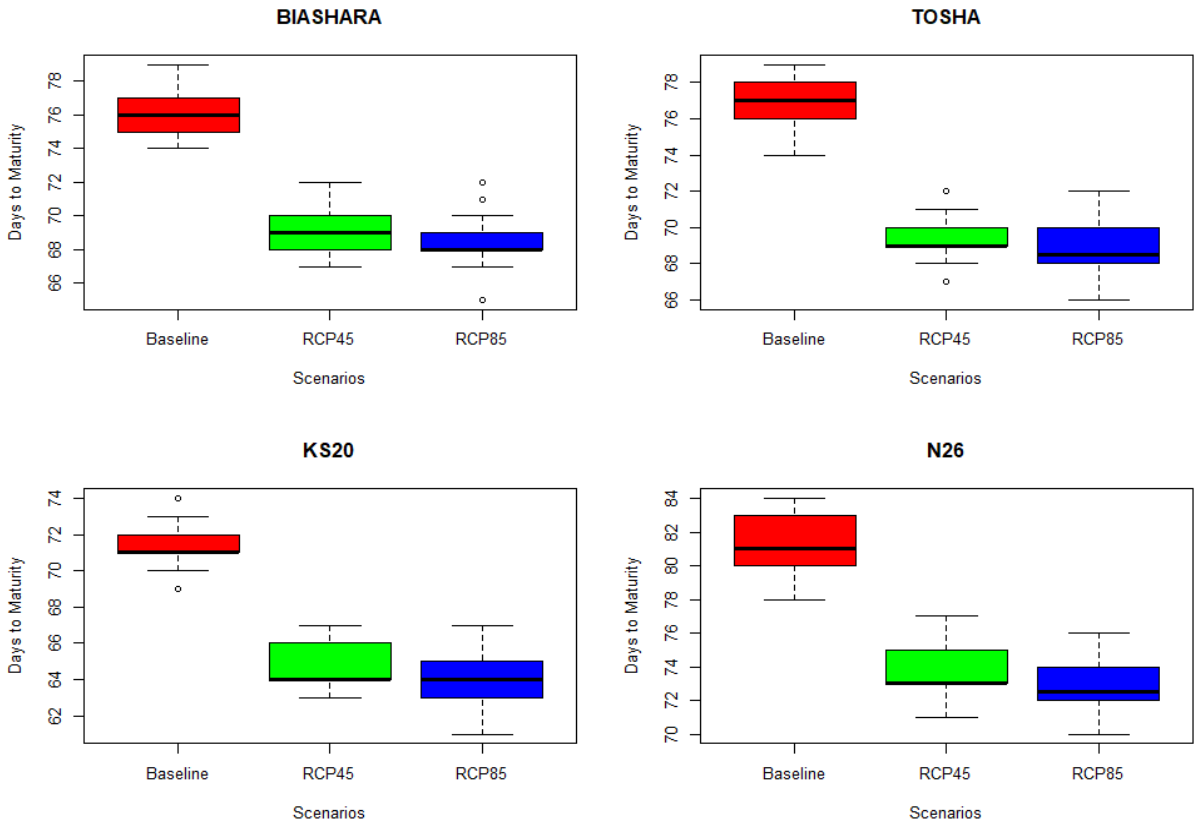

Figure 4-44: The effect of changing climate on green gram days to maturity over the study area for four varieties during the OND season. The varieties are Biashara, Tosha, KS20 and N26. The red colour represents days to maturity during the baseline period (1971-2000), the green colour represents days to maturity under the RCP 4.5 scenario (2021-2050) and the blue colour represents the days to maturity during the RCP 8.5 scenario (2021-2050)

Table 4-16: Comparison of Yield under the Baseline Period (1971-2000) and under the RCP 4.5 (2021-2050) and RCP 8.5 (2021-2050) Scenarios for Four Green gram Varieties during the MAM Growing Season

MAM	Variety	Past (1971-2000)	RCP4.5 (1921-2050)	RCP8.5 (1921-2050)
YIELD (kg/ha)	Biashara	984.5	858.1	835.6
	Tosha	967.0	785.4	759
	Ks20	743.5	683.2	668.2
	Nylon	1154.0	830.9	815.9
BIOMASS (kg/ha)	Biashara	2534.6	2293.4	2260.2
	Tosha	2658.0	2334.7	2303.2
	Ks20	2121.2	2108.3	2085.2
	Nylon	3285.5	2585.6	2576.5
MATURITY (days)	Biashara	70.9	65	64
	Tosha	71.2	65.2	64.3
	Ks20	66.2	60.8	59.9
	Nylon	75.7	69.3	68.3

Table 4-17: Comparison of Yield under the Baseline Period (1971-2000) and under the RCP 4.5 (2021-2050) and RCP 8.5 (2021-2050) Scenarios for Four Green gram Varieties during the OND Growing Season

OND	Variety	Past (1971-2000)	RCP4.5 (1921-2050)	RCP8.5 (1921-2050)
YIELD (kg/ha)	Biashara	1139.3	935.4	911.9
	Tosha	1196.9	903.7	874.2
	Ks20	944.9	684.9	657.5
	Nylon	1425	1066.3	1030.6
BIOMASS (kg/ha)	Biashara	2923.9	2416	2358.8
	Tosha	3085	2532.4	2476.9
	Ks20	2484.8	1991.5	1935.3
	Nylon	3788.5	3153.3	3092.9
MATURITY(days)	Biashara	76.4	69.2	68.4
	Tosha	76.8	69.4	68.7
	Ks20	71.5	64.7	64
	Nylon	81.4	73.6	72.8

CHAPTER 5: CONCLUSIONS AND RECOMMENDATIONS

This chapter presents the conclusions and recommendations of the study.

5.1 Conclusions

This study set out to model the suitability of green gram production in Kenya by determining the temporal and spatial variability of climate parameters in Kenya, identifying present and future suitability for green gram production in Kenya, and simulating the effects of climate change on green gram yield in Kenya.

5.1.1 Spatial and Temporal Variation of Rainfall and Maximum and Minimum Temperature in Kenya

5.1.1.1 Minimum Temperature Distribution

The lowest temperature of the day is recorded in the early morning just before sunrise. The cooling of an object is cumulative. During the day the sun warms the surface of the earth. Once the sun sets, the earth begins to cool off by radiating infra-red radiation into space. The earth's surface becomes progressively cooler during the night until the early morning hours around sunrise when the sun begins to warm the earth once more.

Low values of minimum temperature are observed in central and western regions of Kenya which are the highland zones. High values of minimum temperature values are observed in the eastern and northern regions of Kenya which are the low lying areas. Temperature decreases with altitude such that low altitude areas (eastern and northern Kenya) experience higher temperature than in the higher altitudes (western and central Kenya) which experience lower temperature. At higher altitude, the amount of atmosphere is lower, therefore, there is lower concentration of less greenhouse gases in the air. The high altitude areas thus lose more heat during the night when the earth cools off by radiating infra-red radiation into space leading to lower minimum temperatures being recorded. At lower altitudes the thicker atmosphere absorbs the outgoing terrestrial radiation and re-directs some of it back to earth leading to higher values of minimum temperature being recorded.

During the MAM season, some models especially, the CCCma, CSIRO, IPSL and NCC models, overestimate minimum temperature in the western, north western, northern and central regions of the country. Negative values of bias are observed around Mount Kenya and Mount Kilimanjaro region especially by the CNRM, MIROC, MPI, and NOAA models. The

models thus do not properly capture the effect of altitude, radiation loss and atmosphere content on minimum temperature.

During the OND rainfall season, some models especially with the CCCma, CSIRO and IPSL overestimate the minimum temperature in the western, north western, northern and central parts of the country. The underestimation of minimum temperature is most notable in the CNRM and NOAA models where the underestimation is in most parts of Kenya. The model ensemble generally shows lower values of bias compared to the rest due to its ability to smooth over the individual biases of each model. Minimum temperature is dependent on altitude which affects atmosphere content and radiation loss from the earth during the night.

Under the baseline condition, the minimum temperature during the MAM season shows an upward trend that is significant from a statistical point of view for most of the stations, except for Mandera, Marsabit and Lodwar. The OND season showed an upward statistically significant trend for the Dagoretti, Kakamega, Kisumu, Moyale, Narok and Wajir stations.

Under the RCP 4.5 condition, the minimum temperature during the MAM season showed an upward statistically significant trend for all stations at the 5% level. The OND season showed an upward statistically significant trend for all stations at the 5% level. The increase in minimum temperature could be attributed to global warming as a result of the increased anthropogenic greenhouse gas emissions which prevent the loss of terrestrial radiation by absorbing it and storing it in the surface boundary layer.

The minimum temperature during the MAM season under the RCP 8.5 condition exhibited an increasing trend that was statistically significant at all stations at the 5% level. The OND season showed an increasing trend that was statistically significant at all stations at the 5% level. The increase in minimum temperature could be attributed to global warming as a result of increased anthropogenic greenhouse gas emissions which prevent the loss of terrestrial radiation by absorbing it and storing it in the surface boundary layer.

5.1.1.2 Maximum Temperature Distribution

The maximum temperature of the day is recorded in the afternoon three to four hours before sunset. The earth's surface becomes progressively warmer as the sun heats the earth reaching its maximum temperature a few hours before sunset.

Low values of maximum temperature were recorded in the high altitude areas including the central parts of Kenya, and the highlands west of the Rift Valley. High values of maximum

temperature are mainly concentrated in the north western, northern, north eastern, eastern and south eastern parts of Kenya which are the low lying areas. The models simulate the effect of altitude on maximum temperature fairly well.

During the MAM season, underestimation of maximum temperature is noted in the western and south western regions of the country, especially with the CNRM, CSIRO, MIROC and MPI models. Positive values of bias are noted in the northern region of the Country. Positive values of bias mean the models overestimate maximum temperature in the northern parts of Kenya. Maximum temperature is affected by altitude due to air density, low altitude areas have a higher concentration of air leading to more absorption of heat and in turn higher records of maximum temperature.

During the OND season, underestimation of maximum temperature is observed in most parts of the Country by all the models, but especially in the western and south western regions. Overestimation of maximum temperature is observed over the northern part of the country by the CCCma, CSIRO and IPSL model.

The model ensemble showed lower values of bias when compared with the individual models. This was attributed to the ensemble's ability to smooth out the individual biases. The ensemble was used to assess the space and time variation of maximum temperature under the baseline, RCP 4.5 and RCP 8.5 scenarios.

Under the baseline condition, the maximum temperature during MAM season showed an upward trend that was statistically significant at the 5% level for most of the stations except for Kakamega and Kisumu. The increase in maximum temperature during the MAM season was attributed to global warming owing to increased anthropogenic greenhouse gas emissions. During the OND season, a downward and statistically significant trend at 5% level was recorded for the Garissa, Lamu, Marsabit, Mandera, Moyale, Mombasa, Voi, Lodwar and Wajir stations.

Under the RCP 4.5 condition, the maximum temperature during the MAM season displayed a rising and statistically significant trend for all stations at the 5% level. During the OND season an increasing (decreasing) and statistically significant trend was observed for the Mandera (Voi) stations at the 5% level.

Under the RCP 8.5 condition, the maximum temperature during the MAM season displayed a rising and statistically significant trend for all stations at the 5% level. The OND season

displayed an increasing and statistically significant trend at the 5% level for the Mombasa, Nakuru, Nanyuki and Narok stations, and decreasing significant trend in the Lamu station at the 5% level.

5.1.1.3 Rainfall Distribution

The rainfall pattern during MAM and OND seasons in Kenya is largely dependent on the north-south movement of the ITCZ. The presence of the Indian Ocean in the east, Lake Turkana in the north west, Lake Tanganyika in the south west, Lake Victoria in the west, and other inland lakes, and high mountains such as Mount Kilimanjaro in the south west and Mount Kenya in central Kenya influence the pattern of rainfall in Kenya such that the highest intensity of rainfall is located in the central, western, and coastal areas of Kenya. Winds play an important part in the rainfall pattern in Kenya, especially the Easterlies traversing the Indian Ocean, which transport large amounts of moisture into the country.

To study the space and time variation of rainfall in Kenya under changing climate, a collection of GCMs downscaled by the RCA4 model was first assessed for its capacity to simulate rainfall in Kenya. The different models and the ensemble simulate the annual bimodal pattern of rainfall but have notable biases where most of the models underestimate the rainfall during the MAM season and overestimate the rainfall during the OND season

During the MAM season, most of the models overestimate the spatial distribution of the observed rainfall in most parts of Kenya, except for the MOHC, NCC and NOAA models which underestimated the observed rainfall amounts. Overestimation of rainfall in the MAM season is noted in the central and western regions of Kenya, particularly around Mt. Kenya, especially by the CSIRO, IPSL, MIROC and MPI models.

The models also overestimate rainfall over the high altitude regions of Kenya during the OND season as well. It is expected that the coarse resolution of the models could lead to failure to capture the mesoscale systems which are driven by the land-water differences and orographic strain in these regions. Since the ensemble was a better depiction of rainfall when compared to the individual models, it was used to evaluate the space and time variability of rainfall in Kenya.

Under the baseline condition, the temporal trend in rainfall was not significant at a 5% level under both the MAM and OND seasons. The insignificance in trend for both seasons means

we cannot decisively state that rainfall is decreasing or increasing in these regions and this could be attributed to the variable nature of the rainfall.

Under the RCP 4.5 scenario during the MAM season, a positive 5% statistically significant trend in rainfall was noted at the Moyale, Marsabit, Mandera, Wajir, Voi, and Kitui stations. These stations are located in the eastern region of Kenya where rainfall is lesser than the western part of the country. The increased level of greenhouse emissions will favour higher temperatures to the eastern and northern parts of the country which could enhance convection and, if conditions are favourable, yield higher amounts of rainfall. During the OND season a positive 5% statistically significant trend in rainfall was recorded at the Lodwar and Kakamega stations under the RCP 4.5 scenario. These stations are on the western part of the country, which is characterised by mesoscale features such as Lake Victoria and Lake Turkana. The projected increase in greenhouse gases could lead to higher temperatures and, therefore, enhanced evaporation of moisture from the surrounding lakes. If the conditions are favourable in terms of an unstable atmosphere, availability of condensation nuclei, and a lifting mechanism, rainfall could be enhanced.

Under the RCP 8.5 scenario during the MAM season, a positive 5% statistically significant trend in rainfall was observed at the Mandera, Marsabit, Moyale, Wajir and Lodwar stations. The increase in the pattern of rainfall during the MAM season under the RCP 8.5 scenario is projected to only be concentrated towards the northern part of the country. This is in contrast to the RCP 4.5 scenario where the rainfall is projected to occur both to the eastern and northern parts of Kenya. During the OND season a positive 5% statistically significant trend was recorded at Moyale and Marsabit stations under the RCP 8.5 scenario. The increase in the projected pattern of rainfall during the OND season under the RCP 8.5 scenarios favours the north eastern part of Kenya. The increase in rainfall in the northern and eastern part of the country can be attributed to global warming due to the projected increase in greenhouse gases which could lead to higher temperatures and, therefore, enhanced evaporation of moisture from Lake Turkana and the Indian Ocean. If the conditions are favourable in terms of an unstable atmosphere, availability of condensation nuclei and a lifting mechanism, rainfall could be enhanced.

Spatially, under both the RCP 4.5 and RCP 8.5 scenarios, wetter conditions are expected over the study area. The conditions will be wetter under the RCP 8.5 in comparison to the RCP 4.5 scenario. The RCP 8.5 scenario represents higher emissions of greenhouse gases and this will

result in a higher temperature increase under the RCP 8.5 compared to the RCP 4.5 scenario. This increase in rainfall can be attributed to global warming due to the projected increase in greenhouse gases which could lead to higher temperatures and therefore enhanced convection and if conditions are favourable in terms of an unstable atmosphere, availability of condensation nuclei and a lifting mechanism rainfall will be enhanced.

5.1.2 Land Suitability Mapping for Green gram Production in Kenya

Suitability maps showing varying levels of green gram suitability in Kenya were found using a weighted overlay of past and future rainfall and temperature climate parameters, soil properties comprising pH, depth, CEC, texture, and drainage, and altitude features. Each of the parameter maps was first categorised into four classes. These classes are the Highly Suitable (S1), Moderately Suitable (S2), Marginally Suitable (S3), and Not Suitable (N) class categorised based on their suitability for green gram production.

The study showed that there are some areas in Kenya that are presently not suitable for green gram production and this limits the successful use of land for green gram production in those areas. Most areas in Kenya fall under the "Not suitable" class in terms of soil pH, depth, drainage, and altitude.

The country was found suitable for green gram production in terms of mean temperature under the baseline condition in the MAM season. In the future, during the MAM season under the RCP 4.5 and RCP 8.5 scenarios, areas in the north western and eastern regions of Kenya will not be suitable for green gram production. This is because in the future these areas are likely to experience a mean temperature greater than 30 °C which is not suitable for green gram production. A temperature range of 21 to 30 °C is the most optimal for the growth of green gram.

During the OND season under the baseline condition, some areas were found as not suitable for green gram production in terms of mean temperature. These areas are located around the counties of Nyandarua and Nyeri. This is because these regions experience a mean temperature lower than 15 °C during the OND season which is not suitable for green gram production. In the future, under the RCP 4.5 and RCP 8.5 scenarios, the country will be suitable for green gram production in terms of the mean temperature, including the counties of Nyandarua and Nyeri.

During the MAM season under the baseline condition, all areas in the country were found suitable for green gram production. The regions suitable for green gram production will remain favourable in the future under the RCP 4.5 and RCP 8.5 scenarios. An optimal rainfall of 250 to 350 mm is considered the most favourable for the sustained growth of green gram.

During the OND season under the baseline condition, some regions in the country were found not suitable for green gram production in terms of rainfall. These areas are located in the north-western region of the country during the OND season. The areas in the north-western part of the country will remain as not suitable for green gram production in the future under the RCP 4.5 and RCP 8.5 scenarios since the total seasonal rainfall are less than 75mm. Water stress reduces the rate of nutrients uptake, leaf area development, budding, flowering, and photosynthesis, which could result in yield reduction of green grams.

Overall, most of Kenya is moderately suitable for green gram production during the MAM and OND seasons under the baseline, RCP 4.5 and RCP 8.5 scenarios. Highly suitable areas are located in the counties of Kitui, Makueni, Machakos, Isiolo, Samburu, Narok, and West Pokot.

During the MAM season, the area currently highly suitable for green gram production (67842.6 km^2) is projected to increase slightly to 68600.4 km^2 by 1.1% under the RCP 4.5 scenario. The area is projected to reduce to 61307.8 km^2 by 9.6% under the RCP 8.5 scenario.

During the OND season, the area currently highly suitable for green gram production (49633.4 km^2) is projected to increase under the RCP 4.5 scenario by 22.2%. The area is projected to increase by 58.5% under the RCP 8.5 scenario. This increase is due to the projected favourable rainfall and temperature conditions in the future.

5.1.3 Effects of Change in Climate on Green gram Yield in Kenya

Kitui County, a highly suitable County for green gram production, was used for further analysis in estimating the expected yield of green gram under the baseline and future climate scenarios. The green gram model was calibrated for the *Biashara*, *Tosha*, *N26*, and *KS20* varieties. The calibrated green gram model captured the observed yield, biomass, and days to maturity of the four varieties of green gram shown by a coefficient of determination ranging between 87.0% and 99.0%; bias values between 1.3 and 25.3 and levels of normalized root mean square error ranging between 4.7% and 45.5%.

In the future, during both the RCP 4.5 and RCP 8.5 scenarios, rainfall and temperature in Kitui are projected to increase due to the projected rise in greenhouse gas emissions. The temperature change in the future will remain in the optimal range for green gram production. However, the expected increase in rainfall in the future for Kitui will be more than the range required for green gram production leading to reduced pod setting and increased biomass production.

The increase in rainfall and temperature is more during the RCP 8.5 scenario in comparison to the RCP 4.5 scenario. This is because the RCP 8.5 scenario represents higher concentrations of greenhouse gas emissions than the RCP 4.5 scenario. The increase in rainfall amount under both the RCP 4.5 and RCP 8.5 scenarios will translate to a lower yield and increased biomass. The increase in temperature will result in reduction to the days to maturity for green gram in Kitui County.

5.1.4 Overall Deductions Inferred

The study found marked variation in space in both MAM and OND seasons. This variation was attributed to the interplay of surface peculiarities, including topography, distribution of water bodies, and large scale weather controls, especially the ITCZ.

The study also found appreciable variability of rainfall in time. Temporal trends were attributed to global warming due to the projected increase in greenhouse gases which could lead to higher temperatures and therefore enhances convection and if conditions are favourable in terms of an unstable atmosphere, availability of condensation nuclei and a lifting mechanism rainfall be enhanced.

Both maximum and minimum temperatures have been increasing over time and are projected to increase significantly over the area under the RCP 4.5 and RCP 8.5 scenarios due to the projected increase in greenhouse gases.

Most of Kenya is moderately suitable for green gram production under the baseline, RCP 4.5 and RCP 8.5 scenarios during both the MAM and OND seasons. The area currently highly suitable for green production in Kenya will increase in the future under the MAM season RCP 4.5, the OND season RCP 4.5 scenario, and the OND season RCP 8.5 scenario. The area currently highly suitable for green gram production in Kenya will reduce in the future under the MAM season RCP 8.5 scenario.

The increase in rainfall amount under both the RCP 4.5 and RCP 8.5 scenarios will translate to a lower yield and increased biomass. The increase in temperature will result in reduction to the days to maturity for green gram in Kitui County. One assumption of this study is that the green gram model was only calibrated for one highly suitable region and is assumed to apply for similar areas where climate and soil patterns are similar. The drop in yield, biomass, and days to maturity is slightly larger during the RCP 8.5 scenario in comparison to the RCP 4.5 scenario for both MAM and OND seasons. This is because the RCP 8.5 scenario represents higher concentrations of greenhouse gas emissions leading to more rainfall when compared to the RCP 4.5 scenario.

The maps of green gram suitability indicate that the area suitable for green gram production will increase in the future. There is, however, a net decrease in yield of the four green gram varieties modelled. Kenya, currently, only produces 460kg/ha of green grams. The study found that despite the decrease in yield, potential production under the future climate scenarios was still above 460kg/ha. There is, thus, potential to expand on the current production of green grams. Therefore, despite the decrease in the future, green gram is still a lucrative crop since farmers still stand to increase their current production.

Policymakers can refer to the developed green gram suitability maps under past and future climate scenarios, to determine how suitable their region will be for green gram production. Policymakers should also make use of the four green gram varieties developed under the APSIM model to mitigate against the possible impacts of climate change on green gram yield. Given that the government aims to revive farming in the ASALs by promoting climate smart agriculture through planting drought resistance crops, there is need to develop green gram varieties which are more tolerant to the expected increase in rainfall and temperature to increase yield and in turn benefit farmers, the society and the country at large.

5.2 Recommendations

This section presents the recommendations of this study for the different players in the green gram value chain, namely, scientists, policymakers, and users.

5.2.1 Recommendations for Scientists

Models require initial conditions to begin a forecast. These conditions are not always accurately known. Since these initial states are not error-free they lead to errors in the model simulations. Forecasts are thus run from a range of modified initial conditions to obtain a series of possible simulations called an ensemble. This study used a multi-model ensemble

approach where all the models had equal weight. Future studies should use a weighted ensemble method depending on the rank of the models.

The scarcity of in situ data required for model initialization over the region is one of the reasons for the biases in the models. There is a need to expand the current network of upper air meteorological stations for future use in model initialization.

The coarse resolution of GCMs and RCMs mean that some systems that control the weather in Kenya are not well captured. For a forecast to be accurate, all the processes leading to cloud and rainfall formation need to be well captured. There is thus need for scientists to develop models with higher resolution so that they can capture the effects of mesoscale systems that affect weather in Kenya.

A decline in green gram yield is expected under future climate scenarios in one of the highly suitable zones for Kitui County, Kenya. There is a need to enhance research on extreme weather tolerant green gram varieties to favour the expected projected alterations in rainfall and temperature parameters.

This study only focused on green gram production during the MAM and OND seasons. An assumption was made that the seasons would remain optimal in the future. There is need to assess the likelihood of a shift in seasonal rainfall in the future since this may have an impact on crop production.

Different crop management practices have an impact on the yield of green grams. It is necessary to determine the possible impacts of different management practices on green gram production.

Green gram production is affected by the weather experienced during its growing season. This study only collected data on green gram production for three seasons. There is need to continue the collection of green gram production data under different seasons. This will help in the further validation and fine tuning of the APSIM green gram model.

There is need to quantify the possible income that could be generated in the classes that were found highly suitable class for green gram production.

There is need to conduct studies on the suitability of land to different crops, besides green gram, to make crop diversification easier. The factors that affect specific crops can be determined and overlaid in GIS environment to develop different crop suitability maps.

Although the results of this study are applicable in other ASAL areas where the climate and soil patterns are similar, future studies should carry out experiments in other highly suitable regions to assess the likely effect of climate change on green gram production.

5.2.2 Recommendations to Policymakers

Since rainfall and temperature are projected to increase under the RCP 4.5 and RCP 8.5 scenarios, there is a need for policymakers in consultation with scientists to develop climate adaptation strategies for each scenario to mitigate against the negative impacts of changing climate on green gram production.

Policymakers should encourage the use of the available technology such as mobile phones and radios to educate farmers on the effects of different weather conditions on their crops and how to mitigate these effects. The ease of access to weather information builds up the capacity of the community to make the appropriate decisions in case of climate extremes. Encouraging the use of weather products, water harvesting, giving loans to farmers for land preparation, and investing in irrigation equipment are some of the steps donors, policymakers and the government can take to cushion green gram farmers against the adverse effects of changing climate.

The government should enhance education on the importance of weather products to agriculture at the county and ward levels. This will ensure stakeholders have access to climate information to use in planning their socio-economic activities.

Global warming as a result of increased greenhouse gases emissions is one of the reasons for climate change. On a large scale landowners can help mitigate this increase in greenhouse gases by practicing agroforestry to help reduce carbon emissions.

5.2.3 Recommendations to Users

In the highly suitable areas where the climate already favourable for green gram production, players in the green gram value chain can maximise the good weather and adequately prepare their farms to plant green gram since a decent harvest is highly expected. Adequate preparation involves using the proper inputs of seeds, pesticides, and fertilizers, which will enhance a positive outcome since the environment is already appropriate for cultivation.

Players in the green gram value chain in the moderately and marginally suitable classes are encouraged to grow and invest in green gram production as well. Farmers could take advantage of the climate forecasts disseminated when planning their agricultural activities to

adequately prepare in case the weather is not favourable. One way of effecting this would be, for instance, by changing the planting dates to make maximum use of the season.

Rainfall is highly variable, hence, farmers, with help from the government, could prepare adequately by harvesting rainwater for use during dry conditions. Soil water management techniques such as conservation tillage, and building ridges and furrows can increase water infiltration, and prevent water and nutrient loss through leaching, erosion, and runoff.

REFERENCES

Adhikari, U., Nejadhashemi, A.P. and Woznicki, S.A. (2015) Climate change and eastern Africa: A review of impact on major crops. *Food and Energy Security* **4**, 110-132.

Ahamed, T. N., Rao, K. G. and Murthy, J. S. R. (2000) GIS-based fuzzy membership model for crop-land suitability analysis. *Agricultural Systems **63***, 75-95.

Akhter, J., Das, L. and Deb, A. (2017) CMIP5 ensemble-based spatial rainfall projection over homogeneous zones of India. *Climate Dynamics* **49**, 1885–1916.

Ali, M. and Gupta, S. (2012) Carrying capacity of Indian agriculture: pulse crops. *Current Science* **102**, 874-881.

Al-Mashreki, M. H., Juhari, M. A., Sahibin, A. R., Desa, K. M., Tukimat, L. and Haider, A. R. (2011) Land suitability evaluation for sorghum crop in the Ibb Governorate, Republic of Yemen using remote sensing and GIS techniques. *Australian Journal of Basic and Applied Sciences* **5**, 359-368.

Andang'o, H., Ouma, J., Muthama, N., and Opere, A. (2016) Investigating the Homogeneity of Monthly Rainfall Records in Kenya. *Journal of Meteorology and Related Sciences* **9**, 48–54

Asnani, G.C., (2005). *Tropical Meteorology* (revised edition). GC Asnani publishers, Pune, India, 1202

Ayugi, B.O., Wang, W., and Chepkemoi, D. (2016) Analysis of Spatial and Temporal Patterns of Rainfall Variations over Kenya. *Environment and Earth Science* **6**, 69–83.

Ayugi, B., Tan, G., Ruoyun, N., Babaousmail, H., Ojara, M., Wido, H., Mumo, L., Ngoma, N.H., Nooni, I.K., and Ongoma, V. (2020) Quantile mapping bias correction on rossby centre regional climate models for precipitation analysis over Kenya, East Africa. *Water (Switzerland)* **12**, 1-16.

Baldev, B. (1988). *Cropping patterns*: *Pulse crops.* Oxford and IBH Publishing Co. Pvt. Ltd, New Delhi, India, 3-51.

Akhter, J., Das, L., and Deb, A. (2017) CMIP5 ensemble-based spatial rainfall projection

over homogeneous zones of India. *Climate Dynamics*, **49**, 1885–1916.

Andang'o, H., Ouma, J., Muthama, N., and Opere, A. (2016) Investigating the Homogeneity of Monthly Rainfall Records in Kenya. *Journal of Meteorology and Related Sciences*, **9**, 48–54.

Ayugi, B., Tan, G., Ruoyun, N., Babaousmail, H., Ojara, M., Wido, H., Mumo, L., Ngoma, N.H., Nooni, I.K., and Ongoma, V. (2020) Quantile mapping bias correction on rossby centre regional climate models for precipitation analysis over Kenya, East Africa. *Water (Switzerland)*, **12**, 1–16.

Ayugi, B.O., Wang, W., and Chepkemoi, D. (2016) Analysis of Spatial and Temporal Patterns of Rainfall Variations over Kenya. *Environment and Earth Science*, **6**, 69–83.

Barron, J., Rockström, J., Gichuki, F., and Hatibu, N. (2003) Dry spell analysis and maize yields for two semi-arid locations in east Africa. *Agricultural and Forest Meteorology*, **117**, 23–37.

Buontempo, C., Mathison, C., Jones, R., Williams, K., Wang, C., and McSweeney, C. (2015) An ensemble climate projection for Africa. *Climate Dynamics*, **44**, 2097–2118.

Endris, H.S., Omondi, P., Jain, S., Lennard, C., Hewitson, B., Chang'a, L., Awange, J.L., Dosio, A., Ketiem, P., Nikulin, G., Panitz, H.J., Büchner, M., Stordal, F., and Tazalika, L. (2013) Assessment of the performance of CORDEX regional climate models in simulating East African rainfall. *Journal of Climate*, **26**, 8453–8475.

Ezéchiel, O., Eric, A.A., Josué, Z.E., Eliézer, B.I., and Amédée, C. (2016) Comparative study of seven bias correction methods applied to three Regional Climate Models in Mekrou catchment (Benin , West Africa). *International Journal of Current Engineering and Technology*, **6**, 1831–1840.

Gentry, J. and Gordon, C. (2010) *Mungbean management guide*. Queensland, 24 pp.

Gibba, P., Sylla, M.B., Okogbue, E.C., Gaye, A.T., Nikiema, M., and Kebe, I. (2019) State-of-the-art climate modeling of extreme precipitation over Africa: analysis of CORDEX added-value over CMIP5. *Theoretical and Applied Climatology*, **137**, 1041–1057. Theoretical and Applied Climatology.

Gutowski, J.W., Giorgi, F., Timbal, B., Frigon, A., Jacob, D., Kang, H.S., Raghavan, K., Lee, B., Lennard, C., Nikulin, G., O'Rourke, E., Rixen, M., Solman, S., Stephenson, T., and Tangang, F. (2016) WCRP COordinated Regional Downscaling EXperiment (CORDEX): A diagnostic MIP for CMIP6. *Geoscientific Model Development*, **9**, 4087–4095.

Islam, M.D.T. (2015) Effects of high temperature on photosynthesis and yield in mungbean. *Bangladesh Journal of Botany*, **44**, 451–454.

J. Opijah, F., N. Mutemi, J., and A. Ogallo, L. (2017) Seasonal Climate Predictability over Kenya Using the Regional Spectral Model. *Journal of Meteorology and Related Sciences*, **10**, 12–24.

Jayasinghe, S.L., Kumar, L., and Sandamali, J. (2019) Assessment of potential land suitability for tea (Camellia sinensis (L.) O. Kuntze) in Sri Lanka using a gis-based multi-criteria approach. *Agriculture (Switzerland)*, **9**, 1–25.

Kaur, R., Bains, T.S., Bindumadhava, H., and Nayyar, H. (2015) Responses of mungbean (Vigna radiata L.) genotypes to heat stress: Effects on reproductive biology, leaf function and yield traits. *Scientia Horticulturae*, **197**, 527–541. Elsevier B.V.

Kihoro, J., Bosco, N.J., and Murage, H. (2013) Suitability analysis for rice growing sites using a multicriteria evaluation and GIS approach in great Mwea region, Kenya. *SpringerPlus*, **2**, 1–9.

Kisembe, J., Favre, A., Dosio, A., Lennard, C., Sabiiti, G., and Nimusiima, A. (2019) Evaluation of rainfall simulations over Uganda in CORDEX regional climate models. *Theoretical and Applied Climatology*, **137**, 1117–1134.

Kogo, B.K., Kumar, L., Koech, R., and Kariyawasam, C.S. (2019) Modelling climate suitability for rainfed maize cultivation in Kenya using a maximum entropy (MAXENT) approach. *Agronomy*, **9**, 1–18.

EL LATEFF, E.A.B.D., EL-SALAM, M.A.B.D., SELIM, M., TAWFIK, M., Mohamad, E.-K., and FARRAG, A. (2018) Effect of climate change on mungbean growth and productivity under egyptian conditions. *International Journal of Agriculture, Forestry and Life Sciences*, **2**, 16–23.

Luo, Q. (2011) Temperature thresholds and crop production: A review. *Climatic Change*, **109**, 583–598.

Maintainer, T.P. and Pohlert, T. (2018) Non-Parametric Trend Tests and Change-Point Detection. 1–18.

Mugo, J.W., Kariuki, P.C., and Musembi, D.K. (2016) Identification of Suitable Land for Green Gram Production Using GIS Based Analytical Hierarchy Process in Kitui County, Kenya. *Journal of Remote Sensing & GIS*, **5**.

Mukhala, E., Ngaina, J.N., and Maingi, N.W. (2017) *Downscaled Climate Analysis on Historical , Current and Future Trends in the East African Community Region*. Nairobi, Kenya, 1–57 pp.

Mutayoba, E. and Kashaigili, J.J. (2017) Evaluation for the Performance of the CORDEX Regional Climate Models in Simulating Rainfall Characteristics over Mbarali River Catchment in the Rufiji Basin, Tanzania. *Journal of Geoscience and Environment Protection*, **5**, 139–151.

Ogega, O.M., Oludhe, C., Ojwang, L., and Mbugua, J. (2016) Localized Knowledge for Local Climate Change Adaptation: a Focus on Coastal Smallholder Farmers in Kenya. *International Journal of Agriculture, Environment and Biotechnology*, **1**, 67–88.

Ongoma, V., Chen, H., and Gao, C. (2019) Evaluation of CMIP5 twentieth century rainfall simulation over the equatorial East Africa. *Theoretical and Applied Climatology*, **135**, 893–910. Theoretical and Applied Climatology.

Opiyo, F., Wasonga, O., Nyangito, M., Schilling, J., and Munang, R. (2015) Drought Adaptation and Coping Strategies Among the Turkana Pastoralists of Northern Kenya. *International Journal of Disaster Risk Science*, **6**, 295–309.

Opiyo, F.E.O. (2014) Climate Variability and Change on Vulnerability and Adaptation among Turkana Pastoralists in North-Western Kenya.

Raza, M.H., Sadozai, G.U., Baloch, M.S., Khan, E.A., Din, I., and Wasim, K. (2012) Effect of irrigation levels on growth and yield of mungbean. *Pakistan Journal of Nutrition*, **11**, 876–879.

Salarijazi, M. (2012) Trend and change-point detection for the annual stream-flow series of the Karun River at the Ahvaz hydrometric station. *African Journal of Agricultural Reseearch*, **7**, 4540–4552.

SASOL Foundation. (2014) *Green Grams Hand Book*. Kitui.

Taxak, A.K., Murumkar, A.R., and Arya, D.S. (2014) Long term spatial and temporal rainfall trends and homogeneity analysis in Wainganga basin, Central India. *Weather and Climate Extremes*, **4**, 50–61.

Wanyama, D., Mighty, M., Sim, S., and Koti, F. (2019) A spatial assessment of land suitability for maize farming in Kenya. *Geocarto International*, 1–18.

Warnatzsch, E.A. and Reay, D.S. (2019) Temperature and precipitation change in Malawi: Evaluation of CORDEX-Africa climate simulations for climate change impact assessments and adaptation planning. *Science of the Total Environment*, **654**, 378–392. The Authors.

Yang, W., Seager, R., Cane, M.A., and Lyon, B. (2015) The rainfall annual cycle bias over East Africa in CMIP5 coupled climate models. *Journal of Climate*, **28**, 9789–9802.

Yvonne, M., Richard, O., Solomon, S., and George, K. (2016) Farmer Perception and Adaptation Strategies on Climate Change in Lower Eastern Kenya: A Case of Finger Millet (Eleusine coracana (L.) Gaertn) Production. *Journal of Agricultural Science*, **8**, 33–40.

Batchelor, W. D., Basso, B. and Paz, J. O. (2002) Examples of strategies to analyze spatial and temporal yield variability using crop models. *European Journal of Agronomy* **18,** 141-158.

Behera, S. K., Luo, J.J., Masson, S., Delecluse, P., Gualdi, S., Navarra, A. and Yamagata, T. (2005) Paramount impact of the Indian Ocean dipole on the East African short rains: A CGCM study. *Journal of Climate* **18**, 4514-4530.

Blake, G. R., and Hartge, K. H. (1986). Bulk Density1. *Methods of Soil Analysis: Part 1—Physical and Mineralogical Methods*. SSSA, ASA, Madison, 363-375.

Bobadoye, A. O., Ogara, W. O., Ouma, G. O. and Onono, J. O. (2016) Assessing climate change adaptation strategies among rural Maasai pastoralist in Kenya. *American Journal of Rural Development* **4**, 120-128.

Brands, S., Herrera, S., Fernández, J., Gutiérrez, J. M. (2013). How well do CMIP5 Earth System Models simulate present climate conditions in Europe and Africa? *Climate Dynamics* **41**, 803- 817.

Bremner, J. M. and Mulvaney, C. S. (1982) *Methods of soil analysis. Part 2. Chemical and microbiological properties*. SSSA, ASA, Madison, 595-624.

Buishand, T. A. (1982) Some methods for testing the homogeneity of rainfall records. *Journal of Hydrology* **58**, 11-27.

Bunruamkaew, K., and Murayam, Y. (2011) Site suitability evaluation for ecotourism using GIS and AHP: A case study of Surat Thani province, Thailand. *Procedia-Social and Behavioral Sciences* **21**, 269-278.

Buontempo, C., Mathison, C., Jones, R., Williams, K., Wang, C., and McSweeney, C. (2015) An ensemble climate projection for Africa. *Climate Dynamics* **44**, 2097–2118.

Carberry, P. (2007). *Crop development models.* In: Encyclopedia of Water Science, 2nd Edn, ed. Encyclopedia of Science. CRC Press, Boca Raton, Florida, 121-124.

Chakrabarti, B. (2013). *Crop Simulation Model.* Oxford and IBH Publishing Co. Pvt. Ltd, New Delhi, 225-229.

Challinor, A. J., Wheeler, T. R., Craufurd, P. Q., Slingo, J. M. and Grimes, D. I. F. (2004) Design and optimisation of a large-area process-based model for annual crops. *Agricultural and Forest Meteorology* **124**, 99-120.

Chauhan, Y. S., Douglas, C., Rachaputi, R. C. N., Agius, P., Martin, W., King, K., and Skerman, A. (2010). *Physiology of mungbean and development of the mungbean crop model.* Proceedings of the 1st Australian Summer Grains Conference. Gold Coast, Australia QL, 1-11.

Clarke, L., Edmonds, J., Krey, V., Richels, R., Rose, S. and Tavoni, M. (2009) International climate policy architectures: Overview of the EMF 22 International Scenarios. *Energy Economics* **31**, S64-S81.

Cooper, P. J. M., Dimes, J., Rao, K. P. C., Shapiro, B., Shiferaw, B. and Twomlow, S. (2008) Coping better with current climatic variability in the rain-fed farming systems of sub-Saharan Africa: An essential first step in adapting to future climate change. *Agriculture, Ecosystems and Environment* **126**, 24-35.

de Carvalho, J. R. P., Assad, E. D., de Oliveira, A. F. and Pinto, H. S. (2014) Annual maximum daily rainfall trends in the Midwest, southeast and southern Brazil in the last 71 years. *Weather and Climate Extremes* **5**, 7-15.

Delve, R. J., Probert, M.E., Cobo, J. G., Ricaurte, J., Rivera, M., Barrios, E. and Rao, I. M. (2009) Simulating phosphorus responses in annual crops using APSIM: model evaluation on contrasting soil types. *Nutrient cycling in agroecosystems* **84**, 293-306

Di Paola, A., Valentini, R. and Santini, M. (2016) An overview of available crop growth and yield models for studies and assessments in agriculture. *Journal of the Science of Food and Agriculture* **96**, 709-714.

El-Beltagy, A., and Madkour, M. (2012) Impact of climate change on arid lands agriculture. *Agriculture and Food Security* **1**, 3-12.

El-Lateff, E.A.B.D., El-Salam, M.A.B.D., Selim, M., Tawfik, M., Mohamad, E.K. and FARRAG, A. (2018) Effect of climate change on mungbean growth and productivity under egyptian conditions. *International Journal of Agriculture, Forestry and Life Sciences* **2**, 16–23.

Endris, H.S., Omondi, P., Jain, S., Lennard, C., Hewitson, B., Chang'a, L., Awange, J.L., Dosio, A., Ketiem, P., Nikulin, G., Panitz, H.J., Büchner, M., Stordal, F. and Tazalika, L. (2013) Assessment of the performance of CORDEX regional climate models in simulating East African rainfall. *Journal of Climate* **26**, 8453–8475.

Eriksen, S. H., Brown, K. and Kelly, P. M. (2005) The dynamics of vulnerability: locating coping strategies in Kenya and Tanzania. *The Geographical Journal* **171**, 287-305.

Ezéchiel, O., Eric, A.A., Josué, Z.E., Eliézer, B.I., and Amédée, C. (2016) Comparative study of seven bias correction methods applied to three Regional Climate Models in Mekrou catchment (Benin , West Africa). *International Journal of Current Engineering and Technology* **6**, 1831–1840.

FAO. (1976). A Framework for Land Evaluation: Soils Bulletin: 32. Food and Agriculture Organization of the United Nations, Rome, Italy.

Feng, S., Hu, Q. and Qian, W. (2004) Quality control of daily meteorological data in China, 1951–2000: a new dataset. *International Journal of Climatology* **24**, 853-870.

Flato, G., Marotzke, J., Abiodun, B., Braconnot, P., Chou, S. C., Collins, W. J., ... and Forest, C. (2013) Evaluation of climate models. In: climate change 2013: the physical science basis. Contribution of working group I to the fifth assessment report of the intergovernmental panel on climate change. *Climate Change 2013* **5**, 741-866.

Fujino, J., Nair, R., Kainuma, M., Masui, T. and Matsuoka, Y. (2006) Multi-gas Mitigation Analysis on Stabilization Scenarios Using Aim Global Model. *The Energy Journal* **27**, 343-353.

Gaiser, T., and Graef, F. (2001) Optimization of a parametric land evaluation method for cowpea and pearl millet production in semi-arid regions. *Agronomic* **21**, 705–712.

Gee, G. W., Bauder, J. W., and Klute, A. (1986) *Methods of soil analysis, part 1, physical and mineralogical methods*. Soil Science Society of America, American Society of Agronomy.

Gentry, J. and Gordon, C. (2010) *Mungbean management guide*. Australia Mungbean Association, Queensland, Australia, 1-24.

Gibba, P., Sylla, M.B., Okogbue, E.C., Gaye, A.T., Nikiema, M., and Kebe, I. (2019) State-of-the-art climate modelling of extreme precipitation over Africa: analysis of CORDEX added-value over CMIP5. *Theoretical and Applied Climatology* **137**, 1041–1057.

Gowda, P. T., Satyareddi, S. A. and Manjunath, S. B. (2013) Crop Growth Modelling: A Review. *Research and Reviews: Journal of Agriculture and Allied Sciences* **2,** 1-11.

Grealish, G. J., Ringrose-Voase, A. J., Fitzpatrick, R. W., Wong, M. T. F. and Winston, E. C. (2008). Soil Fertility Evaluation/Advisory Service in Negara Brunei Darussalam. Science Report, Brisbane, Australia, 301-309.

Gutowski, J.W., Giorgi, F., Timbal, B., Frigon, A., Jacob, D., Kang, H.S., Raghavan, K., Lee, B., Lennard, C., Nikulin, G., O'Rourke, E., Rixen, M., Solman, S., Stephenson, T. and Tangang, F. (2016) WCRP COordinated Regional Downscaling EXperiment (CORDEX): A diagnostic MIP for CMIP6. *Geoscientific Model Development* **9**, 4087–4095.

Halder, J. C. (2013) Land suitability assessment for crop cultivation by using remote sensing and GIS, *Journal of Geography and Geology* **5**, 65-74.

HanumanthaRao, B., Nair, R. M. and Nayyar, H. (2016) Salinity and High Temperature Tolerance in Mungbean [*Vigna radiata* (L.) Wilczek] from a Physiological Perspective. *Frontiers in Plant Science* **7**, 957-977.

Hatfield, J.L. and Prueger, J.H. (2015) Temperature extremes: Effect on plant growth and development. *Weather and Climate Extremes* **10**, 4–10.

Hauggaard, H., Jornsgaad, B., Kinane, J. and Jensen E. (2007) Grain legume-cereal intercropping: The practical application of diversity, competition and facilitation in arable and organic cropping systems. *Renewable Agriculture and Food Systems* **1**, 3-12.

Herrero, M., Ringler, C., van de Steeg, J., Thornton, P., Zhu, T., Bryan, E., Omolo, A., Koo, J. and Notenbaert, A. (2010) *Climate Variability and Climate Change: Impacts on Kenyan Agriculture*. Project Note for Kenya Smallholder Climate Change Adaptation Project, Washington, DC: IFPRI.

Hijioka, Y., Matsuoka, Y., Nishimoto, H., Masui, T., and Kainuma, M. (2008) Global GHG emission scenarios under GHG concentration stabilization targets. *Journal of Global Environment Engineering* **13**, 97-108.

Holzkämper, A., Calanca, P., and Fuhrer, J. (2011) Analyzing climate effects on agriculture in time and space. *Procedia Environmental Sciences* **3**, 58–62.

Indeje, M., Semazzi, F. H., Xie, L., and Ogallo, L. J. (2001) Mechanistic model simulations of the East African climate using NCAR regional climate model: Influence of large-scale orography on the Turkana low-level jet. *Journal of Climate* **14**, 2710-2724.

Indeje, M., Semazzi, F. H., and Ogallo, L. J. (2000) ENSO signals in East African rainfall seasons. *International Journal of Climatology* **20**, 19-46.

IPCC, (2007). *Climate Change 2007: The Physical Science Basis. Contribution of Working Group I to the Fourth Assessment Report of the Intergovernmental Panel on Climate Change* (Solomon, S., Qin, D., Manning, M., Chen, M., Marquis, M., Averyt, K.B., Tignor, M., and Miller, H.L. (edition.)]. Cambridge University Press, Cambridge, United Kingdom and New York, NY, USA.

Islam, M.D.T. (2015) Effects of high temperature on photosynthesis and yield in mungbean. *Bangladesh Journal of Botany* **44**, 451–454.

Jame, Y. W. and Cutforth, H. W. (1996). Crop growth models for decision support systems. *Canadian Journal of Plant Science* **76**, 9-19.

Jayasinghe, S.L., Kumar, L., and Sandamali, J. (2019) Assessment of potential land suitability for tea (Camellia sinensis (L.) O. Kuntze) in Sri Lanka using a gis-based multi-criteria approach. *Agriculture (Switzerland)* **9**, 1–25.

Jones, J. W., Hoogenboom, G., Porter, C. H., Boote, K. J., Batchelor, W. D., Hunt, L. A., ... and Ritchie, J. T. (2003) The DSSAT cropping system model. *European Journal of Agronomy* **18**, 235-265.

KALRO (2017). *Enhancing crop production and livestock keeping in arid and semi-arid lands through appropriate breeding and husbandry intervention strategies*. Agricultural Mechanisation Research Institute (AMRI), Katumani, Kenya.

Kamau, S. W., Kuria, D. and Gachari, M. K. (2015) Crop-land Suitability Analysis Using GIS and Remote Sensing in Nyandarua. *Journal of Environment and Earth Science* **5**, 121-131.

Kasampalis, D. A., Alexandridis, T. K., Deva, C., Challinor, A., Moshou, D. and Zalidis, G. (2018) Contribution of Remote Sensing on Crop Models: A Review. *Journal of Imaging* **4**, 52-71.

Kaur, R., Bains, T.S., Bindumadhava, H. and Nayyar, H. (2015) Responses of mungbean (Vigna radiata L.) genotypes to heat stress: Effects on reproductive biology, leaf function and yield traits. *Scientia Horticulturae* **197**, 527–541.

Kates, R.W. (2000) Cautionary tales: adaptation and the global poor. *Climate Change* **45,** 5-17.

Khaliq, M. N., and Ouarda, T. B. (2007) On the critical values of the standard normal homogeneity test (SNHT). *International Journal of Climatology: A Journal of the Royal Meteorological Society* **27**, 681-687.

Kihoro, J., Bosco, N.J. and Murage, H. (2013) Suitability analysis for rice growing sites using a multicriteria evaluation and GIS approach in great Mwea region, Kenya. *SpringerPlus* **2**, 1–9.

Kisaka, M.O., Mucheru-Muna, M., Ngetich, F.K., Mugwe, J.N., Mugendi, D. and Mairura, F. (2015) Rainfall variability, drought characterization, and efficacy of rainfall data reconstruction: case of eastern Kenya. *Advances in Meteorology* **2015**, 1-16.

Kisembe, J., Favre, A., Dosio, A., Lennard, C., Sabiiti, G., and Nimusiima, A. (2019) Evaluation of rainfall simulations over Uganda in CORDEX regional climate models. *Theoretical and Applied Climatology* **137**, 1117–1134.

Klute, A. (1986). *Methods of soil analysis: part 1—physical and mineralogical methods*. SSSA, ASA, Madison, 635-662.

Kogo, B.K., Kumar, L., Koech, R., and Kariyawasam, C.S. (2019) Modelling climate suitability for rainfed maize cultivation in Kenya using a maximum entropy (MAXENT) approach. *Agronomy* **9**, 1–18.

Lee, J.Y. and Wang, B. (2014) Future change of global monsoon in the CMIP5. *Climate Dynamics* **42**, 101- 119.

Li, T., Angeles, O., Marcaida III, M., Manalo, E., Manalili, M. P., Radanielson, A. and Mohanty, S. (2017) From ORYZA2000 to ORYZA (v3): An improved simulation model for rice in drought and nitrogen-deficient environments. *Agricultural and forest meteorology* **237**, 246-256.

Liebmann, B., Hoerling, M.P., Funk, C., Bladé, I., Dole, R.M., Allured, D., Quan, X., Pegion, P. and Eischeid, J.K. (2014) Understanding recent eastern horn of Africa rainfall variability and change. *Journal of Climate* **27**, 8630–8645.

Lobell, D. B. and Burke, M. B. (2010) On the use of statistical models to predict crop yield responses to climate change. *Agricultural and Forest Meteorology* **150**, 1443-1452.

Luhunga, P. M., Botai, J. O. and Kahimba, F. (2016) Evaluation of the performance of CORDEX regional climate models in simulating present climate conditions of Tanzania. *Journal of Southern Hemisphere Earth Systems Science* **66,** 32–54.

Luo, Q. (2011) Temperature thresholds and crop production: A review. *Climatic Change*, **109**, 583–598.

Malik, A., Waheed, A., Qadir, G., and Asghar, R. (2006) Interactive effects of irrigation and phosphorus on green gram (Vigna radiata L.). *Pakistan Journal of Botany* **38**, 1119-1126.

Mallya, G., Mishra, V., Niyogi, D., Tripathi, S., and Govindaraju, R. S. (2016) Trends and variability of droughts over the Indian monsoon region. *Weather and Climate Extremes* **12**, 43-68.

Mann, H. (1945) Nonparametric Tests Against Trend. *Econometrica* **13**, 245-259.

Mascaro, G., White, D. D., Westerhoff, P. and Bliss, N. (2015) Performance of the CORDEX-Africa regional climate simulations in representing the hydrological cycle of the Niger River basin. *Journal of Geophysical Research: Atmospheres* **120**, 12425-12444.

McCown, R. L., Hammer, G. L., Hargreaves, J. N. G., Holzworth, D. P. and Freebairn, D. M. (1996) APSIM: a novel software system for model development, model testing and simulation in agricultural systems research. *Agricultural Systems* **50**, 255-271.

Mohanty, M., Probert, M. E., Reddy, K. S., Dalal, R. C., Mishra, A. K., Rao, A. S., ... and Menzies, N. W. (2012) Simulating soybean–wheat cropping system: APSIM model parameterization and validation. *Agriculture, Ecosystems and Environment* **152,** 68-78.

Moore, G., and Blackwell, P. (1998) Water repellence. Soil guide: a handbook for understanding and managing agricultural soils. *Agriculture Western Australia Bulletin* **4343,** 53-63.

Mondal, A., Kundu, S., and Mukhopadhyay, A. (2012) Rainfall trend analysis by Mann-Kendall test: A case study of north-eastern part of Cuttack district, Orissa. *International Journal of Geology, Earth and Environmental Sciences* **2**, 70-78.

Mugo, J.W., Opijah, F.J., Ngaina, J., Karanja, F. and Mburu, M. (2020) Rainfall Variability under Present and Future Climate Scenarios Using the Rossby Center Bias-Corrected Regional Climate Model. *American Journal of Climate Change* **9**, 243–65.

Mugo, J. W., Kariuki, P. C. and Musembi, D. K. (2016) Identification of suitable land for green gram production using GIS based Analytical Hierarchy Process in Kitui County, Kenya. *Journal of Remote Sensing and GIS* **5,** 170-177.

Muhati, F., Ininda, J.M. and Opijah, F.J. (2007) Relationship between ENSO parameters and the trends and periodic fluctuations in East African Rainfall. *Journal of Kenya Meteorological Society*, **2**, 31-45.

Mukhala, E., Ngaina, J.N., and Maingi, N.W. (2017) *Downscaled Climate Analysis on Historical , Current and Future Trends in the East African Community Region*. Kenya Institute for Public Policy Research and Analysis, Nairobi, Kenya, 1–57

Mumo, L., Yu, J. and Ayugi, B. (2019) Evaluation of spatiotemporal variability of rainfall over Kenya from 1979 to 2017. *Journal of Atmospheric and Solar-Terrestrial Physics* **194**, 105097.

Musa, M., Grüter, E., Abbt, M., Häberli, C., Häller, E., Küng, U., Konzelmann,T., and Dössegger, R. (2003) Quality control tools for meteorological data in the meteoSwiss data warehouse system. *Proceedings ICAM/MAP*, 19-23.

Mutayoba, E., and Kashaigili, J. J. (2017) Evaluation for the Performance of the CORDEX Regional Climate Models in Simulating Rainfall Characteristics over Mbarali River

Catchment in the Rufiji Basin, Tanzania. *Journal of Geoscience and Environment Protection* **5**, 139-151.

Muthomi, J. W., Otieno, P. E., Chemining'wa, G. W. and Wagacha J.M. (2007) Effect of legume root rot pathogens and fungicide treatments on nodulation and biomass accumulation. *Journal of Biological Sciences* **7**, 1163-1170.

Nadeem, M. A., Ahmad, R., and Ahmad, M. S. (2004) The Growth and Yield of Mungbean (vigna radiata L.). *Journal of Agronomy* **3**, 40-42.

Nain, A. S., and Kersebaum, K. C. (2007) Calibration and validation of CERES model for simulating. In: Kersebaum, K.C., Hecker, J.M., Mirschel, W. and Wegehenkel. M. *Modelling water and nutrient dynamics in soil–crop systems* Springer, Dordrecht, The Netherlands, 161-181.

Nair R. M., Schafleitner R., Kenyon L., Srinivasan R., Easdown W., Ebert R. W., *et al.*,. (2012) Genetic improvement of mungbean. *SABRAO J. Breed. Genet* **44**, 177–190.

Nasher, N. R. and Uddin, M. N. (2015) Maximum and minimum temperature trends variation over northern and southern part of Bangladesh. *Journal of Environmental Science and Natural Resources* **6**, 83-88.

National Irrigation Board (NIB). (2014). *Irrigation Development in Kenya.* Government of Kenya, Nairobi, Kenya.

Nelson, D. W., and Sommers, L. E. (1996). *Methods of soil analysis part 3—chemical methods*. SSSA, ASA, Madison, 961-1010.

Nyang'au, W. O., Mati, B. M., Kalamwa, K., Wanjogu, R. K., and Kiplagat, L. K. (2014). Estimating rice yield under changing weather conditions in Kenya using CERES rice model. *International Journal of Agronomy* **5**, 292-300

Ochieng, J., Kirimi, L. and Mathenge, M. (2016) Effects of climate variability and change on agricultural production: The case of small scale farmers in Kenya. *NJAS-Wageningen Journal of Life Sciences* **77**, 71-78.

Ogega, O.M., Oludhe, C., Ojwang, L., and Mbugua, J. (2016) Localized Knowledge for Local Climate Change Adaptation: a Focus on Coastal Smallholder Farmers in Kenya. *International Journal of Agriculture, Environment and Biotechnology* **1**, 67-88.

Ogunwale, J. A., Olaniyan, J. O. and Aduloju, M. O. (2009) Suitability evaluation of the university of Ilorin farmland for cowpea. *Journal of Crop Resources* **37**, 34-39.

Okoola, R.E., Camberlin, P. and Ininda, J.M. (2008) Wet periods along the East Africa coast and the extreme wet spell event of October 1997. *Journal of Kenya Meteorological Society* **2**, 67–83.

Okoola, R.E. (1999) Midtropospheric circulation patterns associated with extreme dry and wet episodes over equatorial Eastern Africa during the Northern Hemisphere spring. *Journal of Applied Meteorology* **38**, 1161 – 1169.

Oloruntade, A. J., Mohammad, T. A., Ghazali, A. H. and Wayayok, A. (2016) Spatial and Temporal Trends in Mean, Maximum and Minimum Temperature in the Niger-South Basin, Nigeria. *Malaysian Journal of Civil Engineering* **28**, 365-381

Olsen, S. R., Sommers, L. E. and Page, A. L. (1982) Methods of soil analysis. Part 2. *Chemical and microbiological properties of Phosphorus. ASA Monograph* **9,** 403-430.

Omeny, P. A., Ogallo, L., Okoola, R. E., Hendon, H. and Wheeler, M. (2008) East African Rainfall variability associated with Madden-Julian Oscillation. *Journal of Kenya Meteorological Society* **2**, 109 – 118.

Omoyo, N.N., Wakhungu, J. and Oteng'i, S. (2015) Effects of climate variability on maize yield in the arid and semi arid lands of lower eastern Kenya. *Agriculture and Food Security* **4**, 1–13.

Ongoma, V., Guirong, T., Ogwang, B. A. and Ngarukiyimana, J. P. (2015) Diagnosis of seasonal rainfall variability over East Africa: A Case study of 2010-2011 drought over Kenya. *Pakistan Journal of Meteorology* **11**, 13-21.

Ongoma, V. and Chen, H. (2016) Temporal and spatial variability of temperature and precipitation over East Africa from 1951 to 2010. *Meteorology and Atmospheric Physics* **129,** 131-144.

Ongoma, V. and Chen, H. (2017) Temporal and spatial variability of temperature and precipitation over East Africa from 1951 to 2010. *Meteorology and Atmospheric Physics* **129**, 131–144.

Ongoma, V., Chen, H., and Gao, C. (2019) Evaluation of CMIP5 twentieth century rainfall simulation over the equatorial East Africa. *Theoretical and Applied Climatology* **135**, 893–910.

Opijah, F., Mutemi, J. and Ogallo, L. (2017) Seasonal Climate Predictability over Kenya Using the Regional Spectral Model. *Journal of Meteorology and Related Sciences* **10**, 12–24.

Opiyo, F.E.O. (2014) Climate Variability and Change on Vulnerability and Adaptation among Turkana Pastoralists in North-Western Kenya.

Opiyo, F., Wasonga, O., Nyangito, M., Schilling, J. and Munang, R. (2015) Drought Adaptation and Coping Strategies Among the Turkana Pastoralists of Northern Kenya. *International Journal of Disaster Risk Science* **6**, 295–309.

Otieno, V. O. and Anyah, R. O. (2013) CMIP5 simulated climate conditions of the Greater Horn of Africa (GHA). Part 1: contemporary climate. *Climate Dynamics* **41**, 2081-2097.

Otieno, G., Opijah, F., Mutemi, J., Ogallo, L., and Otieno, G. (2018) Evaluation of Seasonal Rainfall Pattern as Simulated by the Global Model – Europe over the Greater Horn of Africa. *Journal of Meteorology Related Sciences* **10**, 35–43.

Ouma, J. O., Olang, L. O., Ouma, G. O., Oludhe, C., Ogallo, L. and Artan, G. (2018) Magnitudes of Climate Variability and Changes over the Arid and Semi-Arid Lands of Kenya between 1961 and 2013 Period. *American Journal of Climate Change* **7**, 27-39.

Owiti, Z., and Zhu, W. (2012) Spatial distribution of rainfall seasonality over East Africa. *Journal of Geography and Regional Planning* **5**, 409-421.

Palosuo, T., Kersebaum, K. C., Angulo, C., Hlavinka, P., Moriondo, M., Olesen, J. E., ... and Trnka, M. (2011) Simulation of winter wheat yield and its variability in different climates of Europe: a comparison of eight crop growth models. *European Journal of Agronomy* **35**, 103-114

Pathak, H., Li, C., and Wassmann, R. (2005) Greenhouse gas emissions from Indian rice fields: calibration and upscaling using the DNDC model. *Biogeosciences* **2**, 113-123.

Peterson, T.C., Hoerling, M.P., Stott, P.A. and Herring, S. (2013) Explaining extreme events of 2012 from a climate perspective. *Bull American Meteorology Society* **94**, 1041–1064.

Pettitt, A. N. (1979) A non-parametric approach to the change-point problem. *Journal of the Royal Statistical Society: Series C (Applied Statistics)* **28**, 126-135.

Pohlert, T. (2018). Non-parametric trend tests and change-point detection. *CC BY-ND*, 1-4.

Raza, M.H., Sadozai, G.U., Baloch, M.S., Khan, E.A., Din, I. and Wasim, K. (2012) Effect of irrigation levels on growth and yield of mungbean. *Pakistan Journal of Nutrition* **11**, 876–879.

Riahi K, Krey V, Rao S, Chirkov V, Fischer G, Kolp P, Kindermann G, Nakicenovic N, Rafai P (2011) RCP-8.5: exploring the consequence of high emission trajectories. *Climatic Change* **109**, 1-33.

Robertson, M. J., Carberry, P. S., Huth, N. I., Turpin, J. E., Probert, M. E., Poulton, P. L., ... and Brinsmead, R. B. (2002) Simulation of growth and development of diverse legume species in APSIM. *Australian Journal of Agricultural Research* **53**, 429-446.

RoK (Republic of Kenya). (2012). *Vision 2030 Development Strategy for Northern Kenya and other Arid Lands*. Ministry of State for Development of Northern Kenya and other Arid Lands, Government of the Republic of Kenya. https://www.ndma.go.ke/index.php/resource-center/policy-documents/send/44-policy-documents/4300-vision-2030-development-strategy-for-asals/

Rowell, D.P., Booth, B.B., Nicholson, S.E. and Good, P. (2015) Reconciling past and future rainfall trends over East Africa. *Journal of Climate* **28**, 9768– 9788.

Saaty, T. L. (2008). Decision making with the analytic hierarchy process. *International Journal of Services Sciences **1***, 83-98.

Sabiiti, G., Ininda, J. M., Ogallo, L. A., Ouma, J., Artan, G., Basalirwa, C., Opijah, F., Nimusiima, A., Ddumba, S. D., Mwesigwa, J. B., and Otieno, G. (2018). Adapting Agriculture to Climate Change: Suitability of Banana Crop Production to Future Climate Change Over Uganda. In: Leal, F. W., Nalau, J. *Limits to Climate Change Adaptation*, Springer, Cham, 175-190.

Schollenberger, C. J., and Simon, R. H. (1945) Determination of exchange capacity and exchangeable bases in soil-ammonium acetate method. *Soil Science* **59**, 13-24.

Sengupta, K., Banik, N. C., Bhui, S., and Mitra, S. (2011). Effect of Brassinolide on growth and yield of summer green gram crop. *Journal of Crop Weed* **7**, 152-154.

Sen, P.K. (1968) Estimates of the Regression Coefficient Based on Kendall's Tau. *Journal of the American Statistical Association*, **63**, 1379–1389.

Shisanya, C. A., Recha, C. and Anyamba, A. (2011) Rainfall variability and its impact on normalized difference vegetation index in arid and semi-arid lands of Kenya. *International Journal of Geosciences* **2**, 36-47

Smith, S. J. and Wigley, T. M. L. (2006) Multi-gas forcing stabilization with Minicam. *The Energy Journal* **27**, 373-391.

Sombroek, W. G, Braun, H. M. H and Van der Pouw, B. J. A. (1982). *The exploratory soil map and agro-climate zone map of Kenya (1980) scale 1:1,000,000. Exploratory Soil Survey Report E1*. Kenya Soil Survey, Nairobi, Kenya.

Steduto, P., Hsiao, T. C., Raes, D. and Fereres, E. (2009) AquaCrop—The FAO crop model to simulate yield response to water: I. Concepts and underlying principles. *Agronomy Journal* **101**, 426-437.

Steinacker, R., Mayer, D. and Steiner, A. (2011) Data quality control based on self-consistency. *Monthly Weather Review* **139**, 3974-3991.

Stöckle, C. O., Donatelli, M. and Nelson, R. (2003) CropSyst, a cropping systems simulation model. *European Journal of Agronomy* **18**, 289-307.

Taxak, A. K., Murumkar, A. R. and Arya, D. S. (2014) Long term spatial and temporal rainfall trends and homogeneity analysis in Wainganga basin, Central India. *Weather and Climate Extremes* **4,** 50-61.

Tharanathan, R. N. and Mahadevamma, S. (2003) Grain legumes- a boon to human nutrition. Trends. *Food Science and Technology*, **14**, 507-518.

Thornton, P. K., Jones, P.G., Owiyo, T., Kruska, R. L., Herrero, M., Kristjanson, P., Notenbaert, A., Bekele, N., Omolo, A., Orindi, V., Otiende, B., Ochieng, A., Bhadwal, S., Anantram, K., Nair, S., Kumar, V. and Kulka, U. (2006) *Mapping climate vulnerability and poverty in Africa*. Department for International Development, International livestock Research Institute, Nairobi, Kenya.

Tierney, J. E., Ummenhofer, C. C. and deMenocal, P. B. (2015) Past and future rainfall in the Horn of Africa. *Science advances* **1**, e1500682.

Van Vuuren, D. P., Edmonds, J., Kainuma, M., Riahi, K., Thomson, A., Hibbard, K., ... and Masui, T. (2011) The representative concentration pathways: an overview. *Climatic change* **105,** 5-31.

Wanyama, D., Mighty, M., Sim, S., and Koti, F. (2019) A spatial assessment of land suitability for maize farming in Kenya. *Geocarto International* **0**, 1–18.

Warnatzsch, E.A. and Reay, D.S. (2019) Temperature and precipitation change in Malawi: Evaluation of CORDEX-Africa climate simulations for climate change impact assessments and adaptation planning. *Science of the Total Environment* **654**, 378–392.

Wetterhall, F., Pappenberger, F., He, Y., Freer, J. and Cloke, H. (2012) Conditioning model output statistics of regional climate model precipitation on circulation patterns. *Nonlinear Process Geophysics* **19,** 623–633.

Wise, M., Calvin, K., Thomson, A., Clarke, L., Bond-Lamberty, B., Sands, R., Smith, S., Janetos, A. and Edmonds, J. (2009) Implications of limiting CO2 concentrations for land use and energy. *Science* **324**, 1183-1186.

Yang, W., Seager, R., Cane, M.A. and Lyon B. (2014) The east African long rains in observations and models. *Journal of Climate* **27**, 7185–7202.

Yang, W., Seager, R., Cane, M. A., Lyon, B. (2015) The rainfall annual cycle bias over East Africa in CMIP5 coupled climate models. *Journal of Climate* **28**, 9789-9802.

Yin, X., Struik, P. C. and Kropff, M. J. (2004) Role of crop physiology in predicting gene-to-phenotype relationships. *Trends in Plant Science* **9**, 426-432.

Yohannes, H. and Soromessa, T. (2018) Land suitability assessment for major crops by using GIS-based multi-criteria approach in Andit Tid watershed, Ethiopia. *Cogent Food & Agriculture* **4**, 1-28.

Yvonne, M., Richard, O., Solomon, S., and George, K. (2016) Farmer Perception and Adaptation Strategies on Climate Change in Lower Eastern Kenya: A Case of Finger Millet (Eleusine coracana (L.) Gaertn) Production. *Journal of Agricultural Science* **8**, 35-40.

Internet references

Agesa, L.B. (2014). Evaluation of Land Cover and Crop Type Change: Building Evidence on the Effect of Cropping Systems And Organic Inputs On Sorghum Yield And Enhancing Farmers Climate Change Adaptive Capacity (Msc Thesis). http://erepository.uonbi.ac.ke/handle/11295/76617 (Accessed 8th April, 2018).

Cornell University Cooperative Extension (CUCE). (2007). *Cation Exchange Capacity (CEC)*. [Agronomy Fact Sheet Series # 22]. Department of Crop and Soil Sciences, College of Agriculture and Life Sciences, Cornell University. www.nmsp.cals.**cornell**.edu/publi**cations**/factsheets/factsheet22.pdf/ (Accessed 10th June, 2016).

Economic Review of Agriculture (ERA). (2013). *Central Planning and project Monitoring unit Ministry of Agriculture, Livestock and Fisheries*. http://www.asdsp.co.ke/index.php/kitui-County/ (Accessed 12th January, 2018).

Hansen, L.J., Biringer, J.L., and Hoffman, J.R. (2003). *Buying time: A user's manual for building resistance and resilience to climate variability and change in natural systems*. Washington D.C: World Wildlife Fund. www://ecoadapt.org/ (Accessed 8th July, 2018).

Infonet, (2018). (2018). *Green gram*. http://www.Infonet-biovision.org/PlantHealth/Crops/Green-gram/ (Accessed 18th February, 2018).

Kilimo Trust (2017). *Characteristics of green gram markets in the East Africa Community*. Regional East African Trade in Staples (REACTS) Project. https://www.kilimotrust.org/reacts/files/GreenGrams_markets_X-tisation.pdf (Accessed 18th February, 2018).

Meena, M. K. (2013). *Effect of sulphur and phosphorus on growth and yield of greengram [vigna radiata (l.) wilczek] varieties under bael [aegle marmelos (l.) corr.] based agri-horti system* (Doctoral dissertation, Institute of Agricultural Sciences, Banaras Hindu University, Varanasi). http://krishikosh.egranth.ac.in/handle/1/90805 (Accessed 18th July, 2018).

Mogotsi, K. K. (2006). *Vigna radiata* (L.) R.Wilczek. [Internet] Record from Protabase. Brink, M. and Belay, G. (Editors). PROTA (Plant Resources of Tropical Africa/Ressources végétales de l'Afrique tropicale), Wageningen, Netherlands. http://database.prota.org/search.htm

Morton, F., Smith, R. E., and Poehlman, J. M. (1982). *The Mungbean*. http://eprints.icrisat.ac.in/13284/ (Accessed 18th March, 2018).

Njoka, J. T., Yanda, P., Maganga, F., Liwenga, E., Kateka, A., Henku, A., Mabhuye, E., Malik, N., and Bavo, C. (2016). *Kenya: Country situation assessment*. http://prise.odi.org/wp-content/uploads/2016/01/Low-Res_Kenya-CSA (Accessed 19th May, 2018).

Opiyo, E. O. (2014). *Climate variability and change on vulnerability and adaptation among turkana pastoralist in north-western Kenya* (PhD thesis submitted to the Department of Rangeland management, University of Nairobi). http://erepository.uonbi.ac.ke/handle/11295/77661 (Accessed 16th May, 2018).

Oplinger, E., Hardman, L., Kaminski, A., Combs, S., and Doll1, J. (1990). Alternative fields crop manual. Center for New Crops and Plant Products: https://hort.purdue.edu/newcrop/afcm/mungbean.html/ (Accessed 12th February, 2016).

SASOL (Sahelian Solution Foundation). (2015). *Green grams Hand Book: A guide to farmers within project enhancing food security with Diversified Dry land Farming Techniques in Kitui County*. http://www.SASOLfoundation.co.ke/2013/wp-content/uploads/2015/02/Green-Grams-Manual.pdf (Accessed 8th March, 2018).

UN (United Nations). (2015). *Sustainable Development Goals*. http://www.un.org/sustainabledevelopment/sustainable-development-goals/ (Accessed 8th March, 2018).